

**LOCAL LEVEL FLOOD FORECASTING SYSTEM USING  
MATHEMATICAL MODEL INCORPORATING WRF  
MODEL PREDICTED RAINFALL**

**Md. Shahadat Hossain  
Student ID: 0411162013 P**



**Department of Water Resources Engineering,  
Bangladesh University of Engineering & Technology,  
BUET, DHAKA**

**April 2015**

**LOCAL LEVEL FLOOD FORECASTING SYSTEM USING  
MATHEMETICAL MODEL INCORPORATING WRF  
MODEL PREDICTED RAINFALL**

**Md. Shahadat Hossain**  
**Student ID: 0411162013 P**

A thesis Submitted to The Department of Water Resources Engineering of Bangladesh University  
of Engineering and Technology in partial fulfillment of the requirement for the degree of  
**MASTER OF SCIENCE IN WATER RESOURCES ENGINEERING**

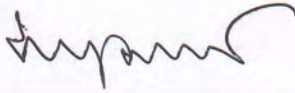


**Department of Water Resources Engineering,  
Bangladesh University of Engineering & Technology,  
BUET, DHAKA**

**April 2015**

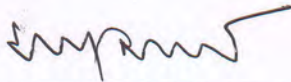
## CERTIFICATION OF APPROVAL

The thesis titled "Local Level Flood Forecasting System Using Mathematical Model Incorporating WRF Model Predicted Rainfall", submitted by Md. Shahadat Hossain, Roll No. 0411162013P, Session April 2011, has been accepted as satisfactory in partial fulfillment of the requirement for the degree of **Master of Science in Water Resources Engineering** on 27 April, 2015.



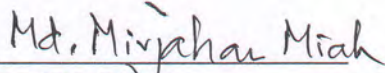
**Dr. Md. Sabbir Mostafa Khan**  
Professor  
Department of WRE, BUET, Dhaka.

**Chairman  
(Supervisor)**



**Dr. Md. Sabbir Mostafa Khan**  
Head  
Department of WRE, BUET, Dhaka.

**Member  
(Ex-Officio)**



**Dr. M. Mirjahan**  
Professor  
Department of WRE, BUET, Dhaka.

**Member**



**Dr. Umme Kulsum Navera**  
Professor  
Department of WRE, BUET, Dhaka.

**Member**



**Md. Abu Saleh Khan (M. Sc.)**  
Deputy Executive Director (Opn.)  
Institute of Water Modelling (IWM), Dhaka.

**Member  
(External)**

## **DECLARATION**

It is hereby declared that this thesis work or any part of it has not been submitted elsewhere for the award of any degree or diploma.

Signature of the Author

.....  
Md. Shahadat Hossain  
Student No: 0411162013P

# Table of Contents

	Page No
Certification of Approval	i
Declaration	ii
Table of Contents	iii
List of Figures	v
List of Tables	viii
List of Abbreviation	ix
Acknowledgement	x
Abstract	xi
<b>CHAPTER 1 INTRODUCTION</b>	<b>1</b>
1.1 General	1
1.2 Background of the Study	1
1.2 Objectives of the Study	2
1.3 Structure of the thesis	3
<b>CHAPTER 2 LITERATURE REVIEW</b>	<b>4</b>
2.1 General	4
2.2 Flood in Bangladesh	4
2.3 Flood Management In Bangladesh	7
2.3.1 Flood Management by Structural Measures	8
2.3.2 Flood Management by Non-Structural Measures	8
2.3.3 Flood Forecasting and Warning in Bangladesh	9
2.4 Flood Forecasting and Warning in Rowmari	10
2.5 Flood Forecasting and Warning In Different Countries	11
2.6 The Brahmaputra - Jamuna River System	12
2.7 Application of HEC-HMS Model	13
2.8 Application of HEC-RAS Model and Development of Flood Map	16
2.9 Application of WRF Model	18
<b>CHAPTER 3 THEORY AND MODEL DESCRIPTION</b>	<b>20</b>
3.1 General	20
3.2 WRF Model	20
3.2.1 The WRF Modeling System	21
3.2.2 WRF Preprocessing System	22
3.2.3 ARW solver	24
3.3 Hydrologic Modeling System : HEC-HMS	28
3.3.1 Model Component	29
3.3.2 Catchment Delineation	31
3.3.3 Computing Runoff Volumes	31
3.3.4 Soil Moisture Accounting Loss Model	33
3.3.5 Clark Unit Hydrograph Model	38
3.4 Hydrodynamic Modeling System : HEC-RAS	39

3.5	HEC-GeoRAS Mapping	42
<b>CHAPTER 4 METHODOLOGY AND MODEL SETUP</b>		<b>43</b>
4.1	General	43
4.2	Selection of Study Area	43
4.3	Methodology	45
4.4	Data Collection	46
4.4.1	Digital Elevation Model	46
4.4.2	Meteorological Data	46
4.4.3	Water Level	47
4.4.4	Discharge	47
4.4.5	Cross Section	48
4.5	Model Setup	49
4.5.1	Rainfall–runoff model: HEC-HMS	49
4.5.1.1	Sketching of the river system	49
4.5.1.2	Delineation of sub-catchment	49
4.5.1.3	Computation of mean area rainfall and evaporation	50
4.5.1.4	Set up rainfall runoff model	51
4.5.2	Hydrodynamic model: HEC-RAS	52
4.5.2.1	Precipitation-Runoff Model	52
4.5.2.2	Hydrodynamic Model	53
4.5.2.3	Boundary Condition	55
4.6	WRF Model Simulation	55
4.7	Forecast Methodology	56
4.8	Inundation Mapping	58
<b>CHAPTER 6 RESULTS AND DISCUSSION</b>		<b>60</b>
5.1	Calibration of HEC-HMS Model	60
5.2	Validation of HEC-HMS Model	63
5.3	Sensitivity Analysis of HEC-HMS Model	64
5.4	Calibration of HEC-RAS Model	65
5.5	Validation of HEC-RAS Model	68
5.6	Flood Forecast System	70
5.7	Forecast Hydrograph	71
5.8	Forecast Inundation Map	72
5.9	Forecast Performance	79
<b>CHAPTER 7 CONCLUSION AND RECOMMENDATION</b>		<b>92</b>
6.1	General	92
6.2	Conclusion	92
6.3	Recommendations	95
<b>REFERENCES</b>		<b>97</b>

## List of Figures

	Page No	
Figure 2.1	Brahmaputra river basin in different countries	13
Figure 3.1	WRF Modeling System Program Components	21
Figure 3.2	WRF Preprocessing System	22
Figure 3.3	ARW $\eta$ coordinate	24
Figure 3.4	Physical Processes involved in Runoff Generation.	30
Figure 3.5	Typical representation of watershed runoff	31
Figure 3.6	Conceptual schematic of the continuous soil moisture accounting algorithm	33
Figure 3.7	Channel and floodplain flows	40
Figure 4.1	Location map of the study area	44
Figure 4.2	Flow chart of methodology applied in the study	45
Figure 4.3	Location of discharge and water level station near the study area	48
Figure 4.4	River network, sub-catchments and catchment nodes of the HEC-HMS model of Brahmaputra basin	50
Figure 4.5	Rainfall station and its weightage area each sub-basin.	51
Figure 4.6	Evaporation station and its weightage area each sub-basin.	51
Figure 4.7	HEC-HMS schematic description of Brahmaputra basin	52
Figure 4.8	HEC-RAS model schematic description of study area	53
Figure 4.9	HEC-RAS schematic description of local catchment distribution and boundary of the study area	54
Figure 4.10	Extent of WRF model for GBM Basin	55
Figure 4.11	Sequence of activities for flood forecast system in study area	56
Figure 4.12	Forecast WL generation at Jamalpur with respect to Bahadurabad	58
Figure 4.13	Developed Arc-GIS model builder layout for forecasting inundation mapping.	59
Figure 5.1	Observed and Simulated discharge at the outlet of the Brahmaputra basin	61

Figure 5.2	Scatter plots for Observed and simulated data comparison	62
Figure 5.3	Observed and Simulated discharge at the outlet of the Brahmaputra basin for validation period.	63
Figure 5.4	Scatter plots for Observed and simulated data comparison for validation period	64
Figure 5.5	Sensitivity scenarios of the change in the continuous model parameters.	65
Figure 5.6	Sensitivity analysis of n-value at Brahmaputra river with respect to observed and simulated water data data.	66
Figure 5.7	Observed and Simulated WL at Chilmari and Noonkhwa on the Brahmaputra River.	67
Figure 5.8	Observed and Simulated WL at Chilmari, Dhonarchar and Noonkhwa on the Brahmaputra river and Lalkura on the Jinjiram river.	69
Figure 5.9	Flood Forecasting System	70
Figure 5.10	Sample plot of flood forecast as hydrographs, Forecast date: 19 Sep, 2014	71
Figure 5.11	Real time inundation map prepared on 19 September, 2014	73
Figure 5.12	1st day (20 Sep, 2014) forecast inundation map prepared on 19 September, 2014	74
Figure 5.13	2st day (21 Sep, 2014) forecast inundation map prepared on 19 September, 2014	75
Figure 5.14	3st day (22 Sep, 2014) forecast inundation map prepared on 19 September, 2014	76
Figure 5.15	4st day (23 Sep, 2014) forecast inundation map prepared on 19 September, 2014	77
Figure 5.16	5st day (24 Sep, 2014) forecast inundation map prepared on 19 September, 2014	78
Figure 5.17	1 <sup>st</sup> day forecast water level and observed WL comparison at Dhonarchar	80
Figure 5.18	Scatter plots for 1 <sup>st</sup> day forecast WL and observed comparison at Dhonarchar	80
Figure 5.19	2 <sup>nd</sup> day forecast water level and observed WL comparison at Dhonarchar	81



Figure 5.20	Scatter plots for 2 <sup>nd</sup> day forecast WL and observed comparison at Dhonarchar	81
Figure 5.21	3 <sup>rd</sup> day forecast water level and observed WL comparison at Dhonarchar	82
Figure 5.22	Scatter plots for 3 <sup>rd</sup> day forecast WL and observed comparison at Dhonarchar	82
Figure 5.23	4 <sup>th</sup> day forecast water level and observed WL comparison at Dhonarchar	83
Figure 5.24	Scatter plots for 4 <sup>th</sup> day forecast WL and observed comparison at Dhonarchar	83
Figure 5.25	5 <sup>th</sup> day forecast water level and observed WL comparison at Dhonarchar	84
Figure 5.26	Scatter plots for 5 <sup>th</sup> day forecast WL and observed comparison at Dhonarchar	84
Figure 5.27	1st day forecast water level and observed WL comparison at Lalkura	86
Figure 5.28	Scatter plots for 1 <sup>st</sup> day forecast WL and observed comparison at Lalkura	86
Figure 5.29	2 <sup>nd</sup> day forecast water level and observed WL comparison at Lalkura	87
Figure 5.30	Scatter plots for 2 <sup>nd</sup> day forecast WL and observed comparison at Lalkura	87
Figure 5.31	3 <sup>rd</sup> day forecast water level and observed WL comparison at Lalkura	88
Figure 5.32	Scatter plots for 3 <sup>rd</sup> day forecast WL and observed comparison at Lalkura	88
Figure 5.33	4 <sup>th</sup> day forecast water level and observed WL comparison at Lalkura	89
Figure 5.34	Scatter plots for 4 <sup>th</sup> day forecast WL and observed comparison at Lalkura	89
Figure 5.35	5 <sup>st</sup> day forecast water level and observed WL comparison at Lalkura	90
Figure 5.36	Scatter plots for 5 <sup>th</sup> day forecast WL and observed comparison	90

## List of Tables

		Page No
Table 2.1	Year-wise flood affected area in Bangladesh (BWDB, 2013)	6
Table 2.2	Flood damages loss occurred in recent floods (WB, 2010)	7
Table 2.3	Event and Continuous modeling Methodology	14
Table 2.4	Event and Continuous modeling Methodology	15
Table 4.1	Summary of the rainfall data	46
Table 4.2	Summary of the water level data	47
Table 4.3	Summary of the discharge data	47
Table 4.4	Summary of the cross-section data	49
Table 4.5	Summary of Forecast Boundary generation	58
Table 5.1	SMA parameters for Brahmaputra Basin simulation	60
Table 5.2	Statistical analysis for calibration period at Bahadurabad	62
Table 5.3	Statistical analysis for Validation period at Bahadurabad	63
Table 5.4	Calibrated Manning's n-value for schematized rivers in HEC RAS.	66
Table 5.5	Statistical analysis for calibration period at Noonkhwa and Chilmari station on Brahmaputra River.	67
Table 5.6	Statistical analysis for validation period at different station on Brahmaputra river Brahmaputra river.	68
Table 5.7	Model forecast performance based on statistical parameter (FFWC, 2013)	79
Table 5.8	Statistical analysis for five days forecast flood water level at Dhonarchar, Rowmari	79
Table 5.9	Statistical analysis for five days forecast flood water level at lalkura, Rowmari	85

## List of Abbreviation

AFWA	Air Force Weather Agency
BDT	Bangladesh Time
BM	Bench Mark
BMD	Bangladesh Meteorological Department
BTM	Bangladesh Transverse Marketor
BWDB	Bangladesh Water Development Board
CEGIS	Center for Environmental and Geographic Information Services
CFAB	Climate Forecast Application in Bangladesh
CPC	Climate Prediction Center
DEM	Digital Elevation Model
DSM	Digital Surface Model
DTM	Digital Terrain Model
EMC	Environmental Modeling Center
FAP	Flood Action Plan
FCD/I	Flood Control Drainage/Irrigation
FF	Flood Forecasting
FFWC	Flood Forecasting and Warning Centre
FFWS	Flood Forecasting and Warning Services
GIS	Geographical Information System
GBM	Ganges Brahmaputra Meghna
GCM	Global Climate Model
GoB	Government of Bangladesh
GPS	Global Positioning System
GSMaP	Global Rainfall Map
HD	Hydrodynamic
HEC-HMS	Hydraulic Engineering Center- Hydrologic Modeling System
HEC-RAS	Hydraulic Engineering Center- River Analysis System
IWM	Institute of Water Modelling
JAXA	Japan Aerospace Exploration Agency
MIKE BASIN	Water Management Software of DHI
MIKE 11	One-dimensional One Layer Model Develop by MIKE ABBOTT
MMM	Mesoscale and Microscale Meteorology
NCEP	National Centers for Environmental Prediction
NOAA	National Oceanic and Atmospheric Administration
NRL	Naval Research Laboratory
RIMES	Regional Integrated Multi-Hazard Early Warning System for Africa and Asia
UTC	Coordinate Universal Time
WPS	WRF Preprocessing System
WRF	Weather Research Forecasting

## ACKNOWLEDGEMENT

I am using this opportunity to express my gratitude to everyone who supported me throughout the Thesis work. I am thankful for their aspiring guidance, invaluable constructive criticism and friendly advice during the thesis work. I am sincerely grateful to them for sharing their truthful and illuminating views on a number of issues related to the work.

I express my warm thanks to my thesis supervisor and Head, Dr. Md. Sabbir Mostafa Khan Professor, Department of Water Resources Engineering, BUET for his constant guidance, inspiration and valuable advice at all stages of the study.

I would also like to thank Dr. M. Mirjahan Miah, Professor, Department of Water Resources Engineering, BUET, Dr. Umme Kulsum Navera, Professor, Department of Water Resources Engineering, BUET and Mr. Abu Saleh Khan, Deputy Executive Director, IWM, who were the members of the board of Examiners. Their valuable comments on this thesis are duly acknowledged.

I am also grateful to Institute of Water Modelling (IWM), for providing necessary data, information and modelling tools to carry out this research work.

## ABSTRACT

Bangladesh is one of the most flood prone countries in the world. To mitigate the recurrent flood damage, flood forecasting is used as an efficient non-structural flood induced disaster management system in the country. National level flood forecasting system is forecasted mainly for river station water level hydrograph and very coarse level inundation map whereas this study objective is to develop 5 days forecasted flood inundation map and hydrograph at house level flood information at Rowmari Upazilla of Kurigram district. This study area is surrounded by the mighty Brahmaputra River and flashy Jinjiram River. As a result flood occurs every year and destroys agricultural products of large areas, causes death, damage to property, environmental pollution and destruction to roads and bridges. A reliable forecast with longer lead time is a way of reducing the damages.

In this study a weather prediction model (WRF) was coupled with a hydrologic model and a hydrodynamic model for predicting floods at Rowmari upazilla of Kurigram district. At first a HEC-HMS continuous hydrologic simulation model is developed for the Brahmaputra basin based on Soil Moisture Accounting (SMA) algorithm and excess rainfall was transformed to direct runoff using the Clark unit hydrograph technique. At the same time, Hydrodynamic Model HEC-RAS 4.1 is setup with geometry data and observed boundary data. This hydrodynamic model is simulated with unsteady condition and calibrated and validated with observed water level. WRF 3.2 weather model was configured and used to predict rainfall over the basin 120 hours into future. Output of the weather model is incorporated with calibrated and validated hydrologic model HEC-HMS 4.0 and simulated every day during monsoon to forecast discharge at Bahadurabd. This study has developed three mathematical relations between Bahadurabad station to other boundary of hydrodynamic model for forecast boundary generation. Then hydrodynamic model is simulated every day using forecast boundary to generate flood inundation map and forecast hydrograph at Rowmari Upazilla of Kurigram.

The HEC-HMS application produced satisfactory performance taking into consideration lumped parameters. Also, among the optimized parameters; Maximum Soil Infiltration Rate, Surface Storage Capacity, Initial Surface Storage and Tension Zone Storage Capacity show the higher sensitive. The estimated NSE value for the calibration and validation period is 0.85 and 0.82. Hydrodynamic Model (HEC-RAS) performance

during calibration and validation period in terms of  $R^2$  and NSE against observed water level data is found to nearly 1. The Manning's roughness coefficient (n) and the coefficient of expansion/contraction (k) are key parameters to calibrate of HEC-RAS model. Analysis of forecast performance indicates that the forecast for the first 3 days are good and next 2 days are average to poor according to BWDB guideline. This developed flood forecasting system is capable of predicting the inundated area of Rowmari Upazilla during a monsoon season.

# **CHAPTER 1**

## **INTRODUCTION**

### **1.1 GENERAL**

Bangladesh is one of the most flood prone countries in the world. Due to its location in the low-lying deltaic floodplains at the convergence of three Himalayan Rivers, heavy monsoon rainfall concomitant with poor drainage often results in annual flooding. The river systems drain a catchment area of about 1.72 million sq. km. The floodplains of the rivers are home to a large population, most of which is rural and poor, whose life is intricately linked to the flooding regime. Thus, any significant flood causes widespread damage in rural and urban areas and set back the country's efforts to alleviate poverty. A major portion of flood damages is due to damage or destruction of infrastructure, and infrastructure managers could not efficiently use the flood forecast information available to plan emergency damage prevention measures in flood-affected areas.

### **1.2 BACKGROUND OF THE STUDY**

Of all the natural hazards capable of producing a disaster, floods are the most common phenomenon that causes human suffering, inconvenience and widespread damage to buildings, structures, crops and infrastructures (Moges, 2007; Hossain, 2006). Floods have been observed to disrupt personal, economic and social activities and set back a nation's security and development by destroying roads, buildings and other assets (Moges, 2007). Bangladesh is one of the most flood prone countries in the world. Due to its location in the low-lying deltaic floodplains at the convergence of three Himalayan Rivers (Hossain, 2006), heavy monsoon rainfall and extensive alluvial river network concomitant with poor drainage; which often results in annual flooding (Bhuiyan, M.S., 2006). These river systems drain a catchment area of about 1.72 million sq. km (Hopson, et al, 2009). Flood occurs in Bangladesh almost every year and the devastating ones in every 5 to 10 years (Bhuiyan, 2006). The floodplains are home to a large population, most of which are rural and poor, whose life is intricately linked to the flooding regime. Floods in 1987, 1988, 1998, 2004 and 2007 caused widespread damage to rural and urban areas and set back the country's efforts to alleviate poverty (IWM, 2006).

For managing floods, Bangladesh has taken many structural and non-structural measures. One of the main non-structural measures is the flood forecasting and warning system (Bhuiyan, M.S., 2006). Flood Forecasting and Warning Centre (FFWC) of Bangladesh Water Development Board (BWDB) provides 24, 48 and 72 hours flood forecasts at 54 gauge stations situated in the major rivers of the country. FFWC uses a mathematical model-based forecasting system for the generation of flood forecasts. The flood forecasting model of FFWC is called "Super Model" is simulated providing boundary conditions subjectively estimated on the basis of previous day's data, upstream water level (if available), and rainfall. The accuracy of this procedure is quite dependent on the personal skill of the engaged modeler. Nevertheless, there is no scope of further increasing of lead time of forecast over 3 days in this present system (IWM, 2006). Last year FFWC has started 5 days flood forecast at 54 gauge station situated in major rivers of the country with incorporating WRF predicted rainfall data using GBM Basin model and supper model, its developed flood forecasting system with the "MIKE11" hydrodynamic and "NAM" rainfall run-off model (IWM, 2006, Sammany, M.S., 2010). In 2014, BWDB has developed local level flood forecasting and warning system for Rowmari Upazilla of Kurigram district and kulkandi union of Jamalur district. This flood forecasting and warning system is comprised with three models: i) MIKE BASIN (GBM Basin Model), ii) Supper Model (MIKE 11) and iii) Local Flood Model (MIKE 11). MIKE BASIN model is setup for whole GBM basin using GSMaP satellite estimate data as a nearly real-time data, and forecast part is used WRF predicted data. This system also is showed GSMaP estimate data is under estimate with respect to real data. As a result, this model is always under simulated the boundary forecast. Other drawback of this system, supper model is used in intermediate part for generating boundary forecast for local flood model. Supper model is comprised with all major river in Bangladesh, so this model take few longer time to generate forecast boundary for local flood model. And generated forecast boundary is also under simulated as a basin output is under simulated.

The fundamental hurdle to improving the flood forecasting capability of a downstream and highly flood-prone country like Bangladesh is well-known (Hossain, et al., 2013). Bangladesh, which receives more than 90% of its surface water from upstream nations during the Monsoon season of June-Sept due to heavy rainfall and snow melting in the Himalayas (Hossain, M.A., 2006), has been able to maintain a fairly comprehensive in-situ network within its boundary for flood monitoring since the 1990s (Hossain, F. et al.,



2013). In addition, MIKE11 is very expensive modelling software; on the other hand HEC-package is freeware and open source code modelling software (Zhang, 2013). This study will incorporate upstream WRF forecasted rainfall (during monsoon season) with HEC-HMS hydrological module (Wardah, et al. 2011) and generated upstream flow boundary for one dimensional HEC-RAS (Adams, T. et al. 2008), which gives forecasted water surface profile and HEC-GEORAS gives the forecasted inundation map forecast.

### **1.3 OBJECTIVES OF THE STUDY**

Objectives of the researches are as follows:

1. To calibrate and validate of hydrological model (HEC-HMS) by observed rainfall
2. To calibrate and validate of hydrodynamic model (HEC-RAS) by observed water level
3. To simulate Weather Research and Forecasting (WRF) model for predicting rainfall
4. To simulate calibrated HEC-HMS and HEC-RAS model with WRF predicted rainfall
5. To generate flood inundation map using HEC-GEORAS

### **1.4 STRUCTURE OF THE THESIS**

The thesis has been organized under seven chapters. Chapter 1 describes the background and objectives of the study. Chapter 2 describes different definition of relevant topics, literatures, previous studies related to this study. Theories regarding this thesis work and a brief description of model have been described in Chapter 3. Chapter 4 describes methodology of the study, data collection from various sources and its processing. The hydrological and hydrodynamic model setup and discuss about forecast methodology is also represented in this chapter. Chapter 5 describes about hydrodynamic and hydrological model calibration as well as validation and sensitivity analysis. Chapter 6 demonstrates the results in terms of forecast performance and inundation map and forecast hydrograph. Conclusion and recommendations for further study are outlined in Chapter 7.

## CHAPTER 2

### LITERATURE REVIEW

#### 2.1 General

The South Asian country Bangladesh located next to India is prone to flooding due to being situated on the Ganges-Brahmaputra Delta and the many tributaries flowing into the Bay of Bengal. The local flooding is mainly occurred the bursting of Bangladesh's river banks and its small branch banks. It is common and severely affects the landscape and society of Bangladesh but most of the studies and research is focused on river station flood like Ganges, Jamuna, Padma, Meghna and other important location. The present study will be directed towards local level forecasting. In addition, previous studies and researches relevant to current study is discussed in the following articles.

#### 2.2 Flood in Bangladesh

Bangladesh is the largest delta in the world created by the three mighty rivers: the Ganges, the Brahmaputra and the Meghna. The country has an area of 147,570 sq. km. while the total basin area of its river system is 1,726,300 sq. km. Thus, only 8.5 % of the river basin lies within the country, and the rest 91.5 % lies in four different countries: India, China, Nepal, and Bhutan. Annual average renewable fresh water resources in the country is around 1210.6  $\text{km}^3$  out of which only 105  $\text{km}^3$  (8.7%) is locally generated and the rest 1,105.6  $\text{km}^3$  (91.3%) is externally added (IWR, 2014). Due to high external flows, Bangladesh is one of the most flood prone countries in the world. Floods of different magnitudes and types occur recurrently. The country experiences four types of flood (Hossain, 2004):

**Flash flood:** it is characterized by rapid rise and fall in water levels with duration ranging from a few minutes to few hours. Occurs mostly in some of the northernmost, north-central, northeastern and southeastern part of the country. In northeastern and north-central part, it prevails in April-May and September-November. In other parts, flash flood starts with the onset of the southwesterly monsoon.

**Rain-fed flood:** Occurs generally in the moribund Gangetic deltas in the southwestern part of the country, and in the flood plains. This type of flood is caused by drainage congestion and heavy rains.

**River flood:** The word flood is generally synonymous with river flood. River flood is a common phenomenon in the country caused by bank overflow. Of the total flow, around 80% occurs in the 5 months of monsoon from June to October (WARPO, 2004). A similar pattern is observed in case of rainfall also. As a consequence to these skewed temporal distribution of river flow and rainfall, Bangladesh suffers from abundance of water in monsoon, frequently resulting into floods and water scarcity in other parts of the year, developing drought conditions (IEB, 1998). Climatologically, the discharge into Bangladesh, from upper catchments, occurs at different time of the monsoon. In the Brahmaputra maximum discharge occurs in early monsoon in June and July whereas in the Ganga maximum discharge occurs in August and September. Synchronization of the peaks of these rivers results in devastating floods. Such incidents aren't uncommon in Bangladesh. The rivers of Bangladesh drain about 1.72 million sq.km area of which 93% lies outside its territory in India, Nepal, Bhutan and China. The annual average runoff of the cross boundary rivers is around 1200 cubic kilometers (WARPO, 2004)

**Storm Surge flood:** This kind of flood mostly occurs along the coastal areas of Bangladesh over a coastline of about 800 km along the southern part. Continental shelves in this part of the Bay of Bengal are shallow and extend to about 20-50 km. Moreover, the coastline in the eastern portion is conical and funnel like in shape. Because of these two factors, storm surges generated due to any cyclonic storm is comparatively high compared to the same kind of storm in several other parts of the world. In case of super-cyclones maximum height of the surges were found to be 10-15 m, which causes flooding in the entire coastal belt. The worst kind of such flooding was on 12 Nov 1970 and 29 April 1991 which caused loss of 300,000 and 138,000 human lives respectively (FFWC, 2005). Coastal areas are also subjected to tidal flooding during the months from June to September when the sea is in spate due to the southwest monsoon wind

Normally, 20-25% of the country is flooded increasing up to 35-70% in extreme years. Approximately 37%, 43%, 52% and 68% of the country is inundated with floods of return periods of 10, 20, 50 and 100 years respectively. In the 19th century, 13 major floods were recorded among which two severe floods in 1822 and 1876 were seriously

catastrophic. Fifteen major floods occurred in the 20th century among which four severe floods in 1955, 1987, 1988, 1998 were catastrophic. In the first 14 years of this 21st century, two major floods have been observed in 2004 and 2007 (IWM, 2014).

A flood with inundation area exceeding 21% of the total land area of Bangladesh is classified as above normal. Above normal floods are further decomposed into four categories: moderate, severe, exceptional and catastrophic depending on the extent of inundation area being 21%-26%, 26% - 34%, 34%-38.5% and greater than 38.5% of the total land area respectively (IWM, 2014). Flood affected areas since 1954 are shown in Table 2.1. Flood damages occurred in different major flood years are shown in Table 2.2. A historical overview of floods since 1954 indicates that the frequency, magnitude, and duration of floods have increased substantially, probably due to climate change.

**Table 2.1** Year-wise flood affected area in Bangladesh

Year	Flood Affected		Year	Flood Affected		Year	Flood Affected	
	sq. km	%		sq. km	%		sq. km	%
1954	36,800	25	1974	52,600	36	1993	28,742	20
1955	50,500	34	1975	16,600	11	1994	419	0.2
1956	35,400	24	1976	28,300	19	1995	32,000	22
1960	28,400	19	1977	12,500	8	1996	35,800	24
1961	28,800	20	1978	10,800	7	1998	1,00,250	68
1962	37,200	25	1980	33,000	22	1999	32,000	22
1963	43,100	29	1982	3,140	2	2000	35,700	24
1964	31,000	21	1983	11,100	7.5	2001	4,000	2.8
1965	28,400	19	1984	28,200	19	2002	15,000	10
1966	33,400	23	1985	11,400	8	2003	21,500	14
1967	25,700	17	1986	6,600	4	2004	55,000	38
1968	37,200	25	1987	57,300	39	2005	17,850	12
1969	41,400	28	1988	89,970	61	2006	16,175	11
1970	42,400	29	1989	6,100	4	2007	62,300	42
1971	36,300	25	1990	3,500	2.4	2008	33,655	23
1972	20,800	14	1991	28,600	19	2009	28,593	19
1973	29,800	20	1992	2,000	1.4	2010	26,530	18

Source: BWDB, 2013

The Ganges–Brahmaputra–Meghna (GBM) river system is the third largest freshwater outlet to the world’s oceans; it is exceeded only by the Amazon and the Congo rivers. The average annual flow of the Ganges-Brahmaputra-Megna river is around 41570 m<sup>3</sup>/s (16650 m<sup>3</sup>/s in Ganges, 19820 m<sup>3</sup>/s in Brahmaputra and 5100 m<sup>3</sup>/s in Meghna) while the average peak flow is around 141,000 m<sup>3</sup>/s at its estuary. The recorded peak flood

discharges of the three rivers are:76,000 m<sup>3</sup>/s (at Hardinge Bridge, 1987), 102,534m<sup>3</sup>/s (at Bahadurabad, 1998), and 19500 m<sup>3</sup>/s (Bhairabbazar, 1988), respectively (Mirza, 2013).

**Table 2.2** Flood damages loss occurred in recent floods

<b>Item</b>	<b>1974</b>	<b>1987</b>	<b>1988</b>	<b>1998</b>	<b>2004</b>	<b>2007</b>
Inundated area (%)	37	40	63	69	39	42
People affected (million)	30	40	47	31	33	14
Total deaths (no of people)	28700	1657	2,379	918	285	1,110
House damaged ('000s)	na	989	2880	2647	895	1000
Road damaged (km)	na	na	13000	15927	27970	31533
Crops damaged (million	na	na	2.12	1.7	1.3	2.1
Assetlosses(million US\$)	936	1167	1424	2128	1860	1100
GDP current (million US\$)	12459	23969	26034	44092	55900	68400
Asset losses as % GDP	7.5	4.9	5.5	4.8	3.3	1.6
Return Period (years)	9	13	55	90	12	14

Source: WB, 2010

### **2.3 Flood Management In Bangladesh**

Bangladesh tries to deal with flood and disaster with structural and non-structural measures. Systematic structural measures began by implementing flood control projects in sixties after the colossal flood of 1963. Non-structural measures have introduced in seventies. Flooding is a natural phenomenon, which cannot be prevented. Complete flood control is not in the interests of most Bangladeshi farmers. The flood control measures and policies should be directed to mitigation of flood damage, rather than flood prevention. Resources should be allocated to help people adopt a life style that is conformable to their natural environment. Indigenous solutions such as changing the housing structures and crop patterns can help reduce flood damage. Moreover, good governance, appropriate environmental laws, acts and ordinances will be necessary to achieve sustainable economic development and to reduce any environmental degradation. In addition, implementation of an improved real-time flood and drought control warning system can reduce the damage caused by floods. In recent years, improved forecasting & early warning system and preparedness measures have helped to reduce the number of lives lost by natural disasters (Rahman, et. al. 2014).

### **2.3.1 Flood Management by Structural Measures**

Structural option provided some benefits specially increase in agricultural production (BWDB, 2005 & BBS, 2002) at earlier period but some adverse effects were observed later on (Rahman, et. al. 2014). Notably, the construction of high embankment along the both banks of the rivers in some cases resulted in rise in bed levels due to siltation causing obstruction to drainage. In the coastal areas, although the construction of polders prevented salinity intrusion, but resulted in restriction of the movement of the tidal prism, sedimentation of tidal rivers and obstruction to the gravity drainage. Another important impact on agriculture was found that the farmers in most cases opted for production of cereal crops, especially HYV rice enjoying a flood free situation rather than going for crop diversification. Structural measure caused many adverse effects on the aquatic lives especially on open water fisheries.

National and regional highways and railways: to the extent feasible, have been raised above flood level. Raising feeder and rural roads will be determined in the context of disaster management plans.

River maintenance and erosion control: River maintenance through dredging are also going on in a limited case due to the high cost. Efforts are continued for erosion control on medium and small rivers.

Flood control and drainage project: Where possible Flood Control, Drainage and/or Irrigation (FCD/I) projects have been constructed. FCD/I project are of two types, namely (i) full flood control facilities; and (ii) partial flood control. Till date FCD/I projects provide facilities in about 5.38 million ha which is about 59% of the country's net cultivated land (BWDB, 2000-01). Flood control and drainage structures have also been provided in major cities to make the cities flood free.

### **2.3.2 Flood Management by Non-Structural Measures**

Introduction of non-structural option i.e. Flood Forecasting and Warning System, Bangladesh started from early '70s and contributed to the improvement of the capacity for flood preparedness and mitigation/minimization of flood losses. Other non-structural measures are discussed in the following.

**Flood cum Cyclone Shelter:** School buildings are so constructed that they can be used as flood-cum cyclone shelter especially in the coastal zone with highest risk of flood and storm surge. These structures are not intended to change the flood regime, and therefore, considered as no-structural measures of flood management.

**Flood proofing:** Efforts have been made to provide vulnerable communities with mitigation by raising homesteads, schools and marketplaces in low-lying areas (rather than flood control) and in the char lands so that peasants can save their livestock and food stuff.

**Concept of flood zoning and flood insurance:** already are practiced in the country. Flood zoning will facilitate development in a co-coordinated way to avoid expensive investments in vulnerable areas. Proper land development rules need to be developed based on the flood-zoning map. Other non-structural measures practiced are:

- Working with communities to improve disaster awareness.
- Develop disaster management plans.
- Relief and evacuation.

### **2.3.3 Flood Forecasting and Warning in Bangladesh**

Flood Forecasting and Warning is also non-structural flood management. Flood warning is concerned to reduce sufferings to human life and damages of economy and environment. Flood forecasting and Warning Service of Bangladesh was established in 1972 as a permanent entity under Bangladesh Water Development Board (BWDB). Initially co-axial correlation, gauge to gauge relationship and Muskingum-Cunge Routing Model were used for forecasting. From early nineties a numerical modeling based approach has been applied for flood forecasting and warning. Using the principal concept of mass transfer based on the continuity and momentum equations, dynamic computation has been used in this method. Very briefly, it comprises of estimating water levels using hydrodynamic simulation model (MIKE 11). Research on Modelling System and capacity building in the forecasting is currently emphasized. During the mohaplalon (the severest flood) of the country in 1998, loss of lives and damage of FCD/I projects were minimum mainly because of flood forecasting and early warning (Islam and Dhar, 2000).

## 2.4 Flood Forecasting and Warning in Rowmari

IWM (2014), in this study is developed flood forecasting and warning system for Rowmari Upazilla, Kurigram. This flood forecasting and warning system is comprised with three models: i) MIKE BASIN (GBM Basin Model), ii) Supper Model (MIKE 11) and iii) Local Flood Model (MIKE 11). MIKE BASIN model is setup for whole GBM basin using GSMaP satellite estimate data as a nearly real-time data, and forecast part is used WRF predicted data. This study also is showed GSMap estimate data is under estimate with respect to real data. As a result, this model is always under simulated the boundary forecast. Other drawback of this study, supper model is used in intermediate part for generating boundary forecast for local flood model. Supper model is comprised with all major river in Bangladesh, so this model take few longer time to generate forecast boundary for local flood model. And generated forecast boundary is also under simulated as a basin output is under simulated. In addition, MIKE11 is very expensive modelling software; on the other hand HEC-package is freeware and open source code modelling software (Zhang, et al, 2013).

RIMES, (2014), This study is present current ensemble discharge forecasts; for the Ganges River, at Hardinge Bridge and for Brahmaputra River, at Bahadurabad station. The study present forecasts of up to 10 days for the river discharge at the respective gauging stations. Shown in these plots are 51 individual ensemble member (colored lines) forecasts. The variance of the ensemble members represent an estimate of the range of uncertainty we expect in our forecasts. The ensemble members were derived by incorporating both the uncertainty in the precipitation forecasts, as represented by the European Center for Medium Scale Weather Forecast (ECMWF) ensemble dispersion, along with all other aspects of uncertainty in hydrological forecasts models. Main drawback of this study is its only gives the water level hydrograph at river station. Another part of this study, its forecast 10 days water level forecast in Bandeber Union at Rowmari. This study methodology is gauge to gauge relation and this relation based on only datum difference, not hydraulic routing. Rowmari's Western side is flooded by mighty Brahmaputra and Eastern side is flood by Jinjiram river. This study is forecast only Western part of Rowmari Upazill.



## **2.5 Flood Forecasting and Warning In Different Countries**

Practical Action (2007), this study paper is published by Practical action which contains the early warning system setup in different part of the country including the research area. The literature of early warning uses a 13 number of different terminologies and classifications for the stages necessary to establish early warning system (EWS). Broadly speaking however they can be summarized as, risk awareness, monitoring and warning, dissemination of warning, community response. Basically early warning system comprises of awaring vulnerable people about the risk, monitoring of the hazard at community level or country level dissemination of the information at the right time to the people or concerned authorities so that they can response and minimize their loss. This research shows the SWOT analysis of the early warning initiatives in Nepal but undermine issues how people take actions and respond to the messages of early warning also study regarding the perception of the EWS which will be addressed by the research.

Vera Thiemig et al, (2014), In this study the early warning and flood forecasting system in Africa is reviewed by sending the questionnaires to the institutions who are basically seeing the forecasting and issues of early warning but research lack on the how end users perceive the warning messages before the event is not clearly mentioned. The vulnerability of the flood and its possible catastrophic effect is rising due to Climatic change and the increase in population density. Hence, many institutions are evolved to improve the knowledge and their dissemination to public and concerned authorities; however different institution working with the same objective due to poor coordination is complicating the dissemination and forecasting. The main aim of this particular survey was to identify the need of flood forecasting and warning for African countries and also identify the shortcomings of the ongoing approach or system so, as to improve them in future. Basically most of the concerned bodies working in this field are using an international system EFAS (European flood alert system) which is an advanced prototype of "continental flood alert system. The system uses various determinants (not mentioned in the article) and helps to predict flooding at least 15 days prior to actual flooding. No any traditional means of warning and forecasting methods are not mentioned in the paper and this all proceedings are carried out by the administrative body with low participation of the community which may have impact on the sustainability of the facility. The paper gives an overview of modern and scientific early warning practices in the country but

lacks to convey how these practices are disseminated among the people and how people respond to those.

Erich plate et al (2007), Erich J Plate, in the keynote lecture on "Early Warning Systems for the Mekong River", has focused on an approach for improving Early Warning Systems via introducing different stages of early warning processes which would help the Mekong River countries and the Mekong River Commission to obtain an effective warning system. The approach focuses on improving data base along the river, by installing more stations along the main river. It also discusses about the modern technologies and use of more refined and more detailed models in order to improve the early warning as well as Forecasting systems. The writer has also shown the need of identification of best feasible ways of improving the existing system and making it an ideal system. However, the document lacks to give an emphasis to recognize the traditional strategies existing in the area. Understanding of traditional practices in the area would help to recognize what is needed and accepted locally. Although traditional practices are not based on scientific facts, they are formulated on the basis of past observation and have been proven to be effective enough for people to adapt even in harsh conditions. Further, in this paper people's perception on the present EWS in the Mekong delta has not been studied. Lastly paper suggests that for the sustainability of the prevailing system community involvement from the beginning of the project is very important.

## **2.6 The Brahmaputra - Jamuna River System**

The Brahmaputra flows through a narrow valley, which is known as the Brahmaputra valley in about east west direction for 640 km with a very low gradient. In this valley it is joined by several tributaries from both sides. On the west, the valley is open and beyond Assam it widens into a broad low lying deltaic plain of Bangladesh. The Brahmaputra, after traversing the spurs of the Meghalaya plateau, turns south and enters Bangladesh with the name of Jamuna. The total length of the river from its source in south-western Tibet to the mouth in the Bay of Bengal is about 2,850 km (including Padma and Meghna up to the mouth). Within Bangladesh territory, Jamuna is 240 km long (upto Aricha). The Jamuna enters Bangladesh east of Bhabanipur (India) and northeast of Kurigram district. Originally, the Jamuna (Brahmaputra) flowed southeast across Mymensingh district where it received the Surma River and united with the Meghna, as shown in Rennell's

Atlas (1785). By the beginning of the 19th century its bed had risen due to tectonic movement of the Madhupur Tract and it found an outlet farther west along its present course (Coleman, 1969). It has four major tributaries: the Dudhkumar, Dharla, Teesta and the Baral-Gumani-Hurasagar system. The first three rivers are flashy in nature, rising from the steep catchment on the southern side of the Himalayas. The main distributaries of the Jamuna River are the Old Brahmaputra River, which leaves the left bank of the Brahmaputra River 20 km north of Bahadurabad, and the New Dholeswari River just south of the Bangabandhu Bridge. The Brahmaputra-Jamuna drains the northern and eastern slopes of the Himalayas, and has a catchment area of 5, 83,000 sq.km. 50.5 percent of which lie in China, 33.6 percent in India, 8.1 percent in Bangladesh and 7.8 percent in Bhutan (Figure 2.1).

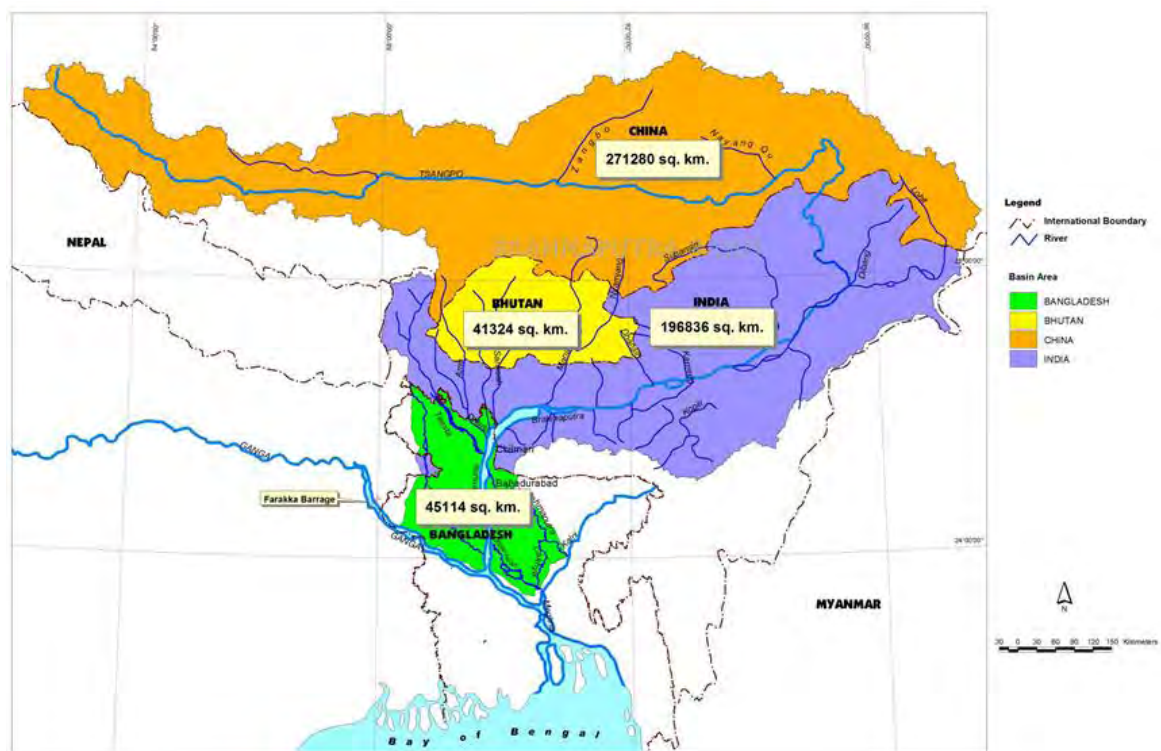


**Figure 2.1** Brahmaputra river basin in different countries (Source: IWM, 2014)

## 2.7 Application of HEC-HMS Model

The program is a generalized modeling system capable of representing many different watersheds. A model of the watershed is constructed by separating the hydrologic cycle into manageable pieces and constructing boundaries around the watershed of interest. Any mass or energy flux in the cycle can then be represented with a mathematical model.

In most cases, several model choices are available for representing each flux. Each mathematical model included in the program is suitable in different environments and under different conditions. Making the correct choice requires knowledge of the watershed, the goals of the hydrologic study, and engineering judgment. The program features a completely integrated work environment including a database, data entry utilities, computation engine, and results reporting tools. A graphical user interface allows the seamless movement between the different parts of the program. Program functionality and appearance are the same across all supported platforms. Among various literature found some of most appropriate literature is presented over here.

Silva et al (2012), this study describes a Modeling of event and continuous flow hydrographs with HEC-HMS; a case study in the Kelani River basin Sri-Lanka. An extremely high rainfall event in November 2005 was used for calibration of model parameters and extremely high rainfall events in April– May 2008, May – June 2008, and May 2010 were used for validation of the event model. Two consecutive extreme flood events occurred during April to June 2008 were selected for model calibration under continuous simulations. The time series data from January 2005 to December 2007 and January 2009 to December 2010 were used for validation. The calibrated, direct runoff and base flow parameters were then used in the continuous hydrologic model. For event and continuous modeling Methodology used for study is as described in below table 2.3:

**Table 2.3** Event and Continuous modeling Methodology

PARAMETERS	METHODS FOR EVENT MODELLING	METHODS FOR CONTINUOUS MODELLING
Base flow parameters	Recession baseflow	Recession baseflow
Loss parameters	Green and ampt	Soil moisture accounting
Runoff transform parameters	Clark unit hydrograph	Clark unit hydrograph

Xuefeng Chu et al (2009), this study describes a case study of Event and Continuous Hydrologic Modeling with HEC-HMS on Mona Lake watershed. Joint event and continuous hydrologic modeling with the Hydrologic Engineering Center’s Hydrologic Modeling System HEC-HMS is discussed in this technical note and an application to the Mona Lake Watershed in west Michigan is presented. Specifically, four rainfall events

were selected for calibrating/verifying the event model and identifying model parameters. The calibrated parameters were then used in the continuous hydrologic model. The Soil Conservation Service curve number and soil moisture accounting methods in HEC-HMS were used for simulating surface runoff in the event and continuous models, respectively, and the relationship between the two rainfall-runoff models was analyzed. The simulations provided hydrologic details about quantity, variability, and sources of runoff in the watershed. The model output suggests that the fine-scale (5 min time step) event hydrologic modeling, supported by intensive field data, is useful for improving the coarse-scale (hourly time step) continuous modeling by providing more accurate and well calibrated parameters. For event and continuous modeling Methodology used for this study is as described in below table 2.4.

**Table 2.4** Event and Continuous modeling Methodology

PARAMETERS	METHODS FOR EVENT MODELLING	METHODS FOR CONTINUOUS MODELLING
Base flow parameters	Recession baseflow	Recession baseflow
Loss parameters	SCS-CN	Soil moisture accounting
Runoff transform parameters	Clark transform	Clark unit hydrograph

Using Watershed Modeling System (WMS), overland flow directions and accumulations were computed and the drainage network and sub-basin boundaries were determined.

Reshma (2013), this study describes Simulation of Event Based Runoff Using HEC-HMS Model for an Experimental Watershed. In this study, Hydrologic Engineering Center – Hydrologic Modeling System (HEC-HMS) hydrological model has been used to simulate runoff process in Walnut Gulch watershed located in Arizona, USA. Estimation of accurate runoff for a given rainfall event is a difficult task due to various influencing factors. Several computer based hydrological model have been developed for simulation of runoff in watershed and water resource studies. The HEC-HMS model has been applied for 7 rainfall events of sub watershed of Walnut Gulch watershed. The model has been calibrated for four rainfall events and validated for three rainfall events. Methodology is use in this study

- Digital Elevation Model (DEM), Land Use/Land Cover (LU/LC) data was used for watershed delineation.

- To compute infiltration, rainfall excess conversion to runoff and flow routing, methods like Green-Ampt, Clark's Unit hydrograph and Kinematic wave routing were chosen.
- The model has been calibrated and validated for the seven rainfall events.

From the results, it is observed that HEC-HMS model has performed satisfactorily for the simulation runoff for the different rainfall events.

Rabi Gyawali et al (2013), This study describes Continuous Hydrologic Modeling of Snow-Affected Watersheds in the Great Lakes Basin Using HEC-HMS. Watershed and sub watershed models are calibrated and validated on a daily time step using gauge precipitation measurements, observed snow water equivalent data, and physically based parameters estimated using geospatial databases. Methodology is used in this study.

- The watersheds were disaggregated into a number of sub-basins, with each sub-basin featuring a USGS stream gauge at its outlet.
- Meteorological data inputs, required for each sub-basin, were summarized.
- Thiessen polygons were used to compute areal average precipitation based on available gage measurements.
- Parameter estimation of SMA in HMS was discussed. Unlike the seasonal parameterization approach used in that study, a single parameter estimate was used for different variables throughout the calibration and validation periods in this study, spanning 2004–2009.
- Geographic information system (GIS) and State Soil Geographic (STATSGO) databases have been used for parameter estimation in this hydrologic study.

The results show modest improvements resulting from the increased spatial resolution of the HEC-HMS models, in addition to the benefits of the more process based snow algorithm in HEC-HMS, particularly for the snow dominated St. Louis watershed. However, both LBRM and HEC-HMS models had difficulty reproducing peaks in late winter and early spring runoff, and discrepancies could not be attributed to any systematic errors in the snowmelt models.

## **2.8 Application of HEC-RAS Model and Development of Flood Map**

Bedient et al (2008), in this study is described HEC-RAS is a hydraulic model for rivers and channels that was released in 1995 by the US Army Corps of Engineers. The main functionality of the model is to simulate water surface elevation given inputs of river geometry and channel flows. HEC-RAS is a one dimensional model, which means it does not model the bends or shape changes in a channel directly. When combined with hydrologic software such as HEC-HMS, applications for HEC-RAS include floodplain delineation, channel modification studies, and dam breach analysis. HEC-RAS has sophisticated capabilities such as being able to model complex structures like bridges, weirs, and culverts, as well as subcritical, supercritical and mixed flow regimes. HEC-RAS is used in this study for the software's steady state and unsteady state flow simulation capability. The steady flow analysis involves inputting peak flows into the model geometry in order to generate a maximum water surface profile for the entire river. HEC-RAS uses the 1D energy and momentum equations and calculates energy losses through Manning's roughness coefficient and contraction/expansion coefficients. Unsteady flow simulations require the input of entire hydrographs instead of just peak flows. This allows the software to model water surface profiles through time. The code within HEC-RAS that solves the unsteady flow equations is based on a solver called UNET (Barkau 1996). The program solves the 1D St. Venant Equations using an implicit finite difference scheme. Unlike the steady state simulation, the unsteady state model requires experienced users to insure stable and accurate solutions.

Yang J et al (2006,) The goal of this paper was to develop a direct-processing approach to river system floodplain delineation. Floodplain zones of part of the South Nation River system, located just east of Ottawa, Ontario, were mapped in two dimensions and three dimensions by integrating the hydraulic model of the choice with geographic information systems (GIS). The first objective was to construct and validate a Hydrologic Engineering Center's River Analysis System (HEC-RAS) river network model of the system using existing HEC-2 model-generated data. Next, HECRAS simulations were performed to generate water surface profiles throughout the system for six different design storm events. The in-channel spatial data of HECRAS were then geo-referenced and mapped in the GIS domain and integrated with digital elevation model (DEM) over-bank data to build a triangular irregular network (TIN) terrain model. In the final step, floodplain

zones for the six design storms were reproduced in three dimensions by overlaying the integrated terrain model for the region with the corresponding water surface TIN.

Alho, et al (2007), in this paper Alho et al. investigated Jökulhlaups that are the consequence of a sudden and significant release of melt water from the edge of a glacier. Such floods are sourced commonly from ice-dammed lakes, but occasional volcanic eruptions beneath ice can produce intense jökulhlaups due to prodigious rates of melt water release. In this study it was presented the results of one-dimensional hydraulic modeling of the inundation area of a massive, hypothetical jökulhlaup on the Jökulsá á Fjöllum River in northeast Iceland. Remotely sensed data were used to derive a digital elevation model and to assign surface-roughness parameters. Also it was used a HEC-RAS/HEC-GeoRAS system to host the hydraulic model; to calculate the steady water-surface elevation; to visualize the flooded area; and to assess flood hazards.

River flood extent mapping is the process of determining inundation extents and depth by comparing river water levels with ground surface elevation. The process requires the understanding of flow dynamics over the flood plain, topographic relationships and the sound judgments of the modeller (Noman et al., 2001; Sinnakaudan et al., 2003). Flood hazard maps produced may include water depth, flood extent, flow velocity and flood duration. This is a basic and important indicator for the flood plain land use development planning and regulations (Walesh, 1989).

## **2.9 Application of WRF Model**

Moustafa, (2010), this study described applicability of WRF model to forecast flash flood. The results of the study show that the WRF model is a reliable short term forecasting tool for flash flood events over Sinai Peninsula. The calibration shows significant consistency between real rainfall measurements and WRF model results. The prediction of small or mesoscale hazards such as tornadoes, severe thunderstorms, squall lines and flash floods requires the early detection of signatures, a near instantaneous assessment of the threat and a rapid dissemination of alerts to the end users. The WRF model succeeded to simulate flash floods events; hence, it can be used as a component of an early warning system. Useful forecasts of the behavior of the larger scale weather systems such as tropical storms, cyclones, intense depressions and severe flash floods can be prepared several days in advance using WRF model.



Ismail Yucel et al (2015), A fully-distributed, multi-physics, multi-scale hydrologic and hydraulic modeling system, WRF-Hydro, is used to assess the potential for skillful flood forecasting based on precipitation inputs derived from the Weather Research and Forecasting (WRF) model and the EUMETSAT Multi-sensor Precipitation Estimates (MPEs). The study then undertook a comparative evaluation of the impact of MPE versus WRF precipitation estimates, both with and without data assimilation, in driving WRF-Hydro simulated stream flow. Several flood events that occurred in the Black Sea region were used for testing and evaluation. Following model calibration, the WRF-Hydro system was capable of skillfully reproducing observed flood hydrographs in terms of the volume of the runoff produced and the overall shape of the hydrograph. Stream flow simulation skill was significantly improved for those WRF model simulations where storm precipitation was accurately depicted with respect to timing, location and amount. Accurate stream flow simulations were more evident in WRF model simulations where the 3DVAR scheme was used compared to when it was not used. Because of substantial dry bias feature of MPE, stream flow derived using this precipitation product is in general very poor. Overall, root mean squared errors for runoff were reduced by 22.2% when hydrological model calibration is performed with WRF precipitation. Errors were reduced by 36.9% (above uncalibrated model performance) when both WRF model data assimilation and hydrological model calibration was utilized. This study also indicated that when assimilated precipitation and model calibration is performed jointly, the calibrated parameters at the gauged sites could be transferred to ungaged neighboring basins where WRF-Hydro reduced mean root mean squared error from 8.31 m<sup>3</sup>/s to 6.51 m<sup>3</sup>/s.

## **CHAPTER 3**

### **THEORY AND MODEL DESCRIPTION**

#### **3.1 General**

Flood forecasting is the use of real-time precipitation and stream flow data in rainfall-runoff and stream flow routing models to forecast flow rates and water levels for periods ranging from a few hours to days ahead, depending on the size of the watershed or river basin. Flood forecasting can also make use of forecasts of precipitation in an attempt to extend the lead-time available. But precipitation prediction is the most uncertain part that mainly influences the forecasting lead-time. The purpose of this chapter is to give a brief description of the related theories regarding precipitation forecast and using forecasted precipitation data in mathematical model for flood forecast. Moreover, various mathematical equations and formulas of HEC-HMS and HEC-RAS are also explained in the following section.

#### **3.2 WRF Model**

The development of the Weather Research and Forecasting (WRF) modeling system is a multiagency effort intended to provide a next-generation mesoscale forecast model and data assimilation system that will advance both the understanding and prediction of mesoscale weather and accelerate the transfer of research advances into operations. The model is being developed as a collaborative effort among the NCAR Mesoscale and Microscale Meteorology (MMM) Division, the National Oceanic and Atmospheric Administration's (NOAA) National Centers for Environmental Prediction (NCEP) and Forecast System Laboratory (FSL), the Department of Defense's Air Force Weather Agency (AFWA) and Naval Research Laboratory (NRL), the Center for Analysis and Prediction of Storms (CAPS) at the University of Oklahoma, and the Federal Aviation Administration (FAA), along with the participation of a number of university scientists. The WRF model is designed to be a flexible, state-of-the-art, portable code that is efficient in a massively parallel computing environment. A modular single-source code is maintained that can be configured for both research and operations. It offers numerous physics options, thus tapping into the experience of the broad modeling community. The

Advanced Research WRF (ARW) is suitable for use in a broad range of applications across scales ranging from meters to thousands of kilometers, including:

- Idealized simulations (e.g. LES, convection, baroclinic waves)
- Parameterization research
- Data assimilation research
- Forecast research
- Real-time NWP
- Hurricane research
- Regional climate research
- Coupled-model applications

### 3.2.1 The WRF Modeling System

The following figure shows the flowchart for the WRF Modeling System Version 3.

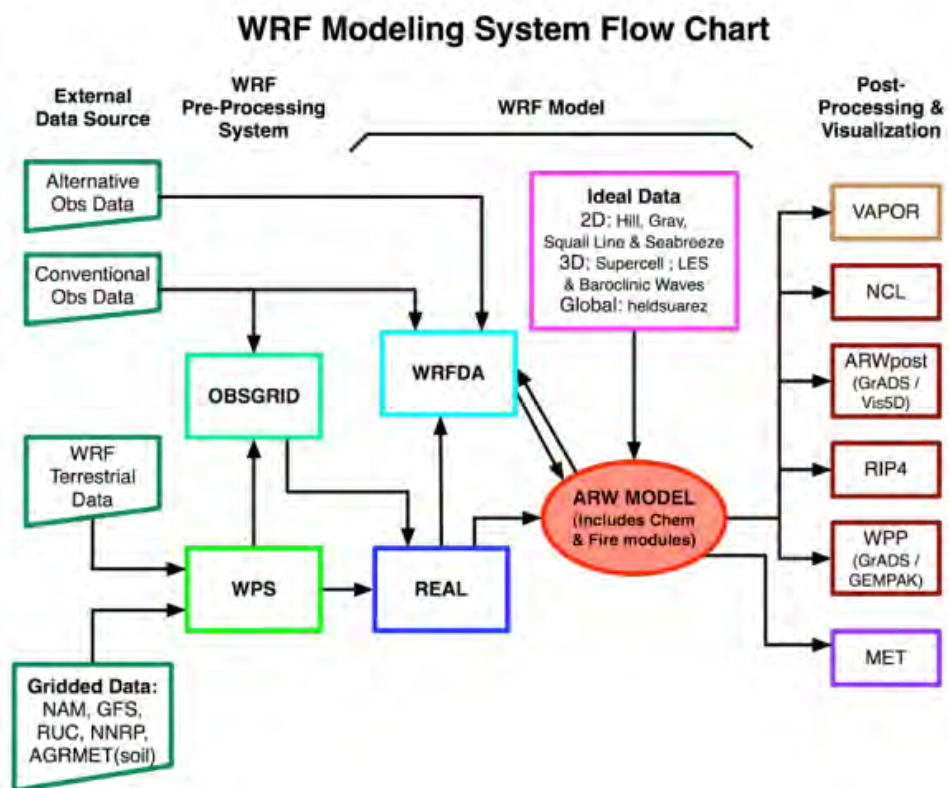


**Figure 3.1** WRF Modeling System Program Components (Source: WRF, 2012)

As shown in the diagram, the WRF Modeling System consists of these major programs:

- The WRF Preprocessing System (WPS)
- ARW solver

- Post-processing & Visualization tools

### 3.2.2 WRF Preprocessing System (WPS)

The WRF Preprocessing System (WPS) is a set of three programs whose collective role is to prepare input to the real program for real-data simulations. Each of the programs performs one stage of the preparation: geogrid defines model domains and interpolates static geographical data to the grids; ungrib extracts meteorological fields from GRIBformatted files; and metgrid horizontally interpolates the meteorological fields extracted by ungrib to the model grids defined by geogrid. The work of vertically interpolating meteorological fields to WRF eta levels is performed within the real program.

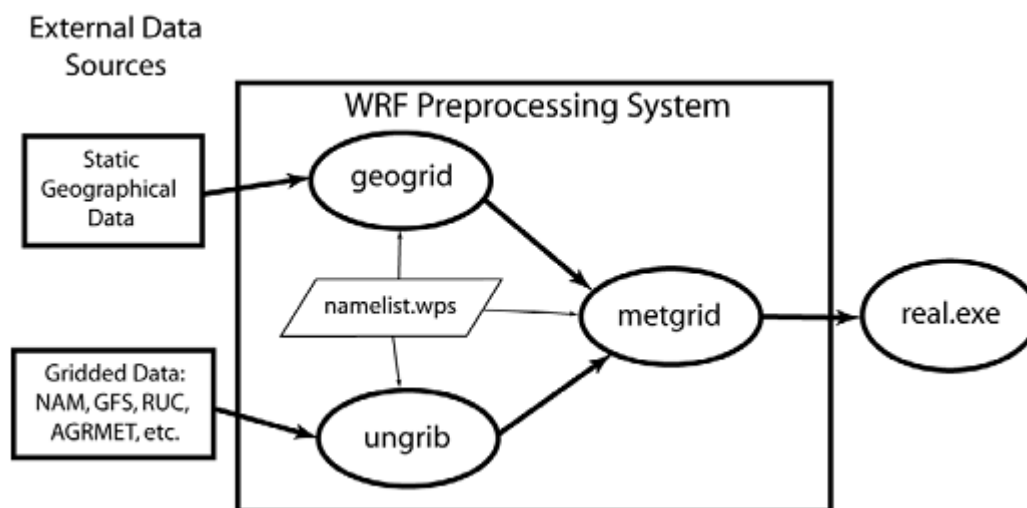


**Figure 3.2** WRF Preprocessing System (Source: WRF, 2012)

This program is used primarily for real-data simulations. Its main features include:

- GRIB 1/2 meteorological data from various centers around the world
- USGS 24 category and MODIS 20 category land datasets
- Map projections for 1) polar stereographic, 2) Lambert-Conformal, 3) Mercator and 4) latitude-longitude
- Nesting

**Geogrid:** The purpose of geogrid is to define the simulation domains, and interpolate various terrestrial data sets to the model grids. The simulation domains are defined using

information specified by the user in the `—geogrid`". In addition to computing the latitude, longitude, and map scale factors at every grid point, geogrid will interpolate soil categories, land use category, terrain height, annual mean deep soil temperature, monthly vegetation fraction, monthly albedo, maximum snow albedo, and slope category to the model grids by default. Global data sets for each of these fields are time-invariant. Besides interpolating the default terrestrial fields, the geogrid program is general enough to be able to interpolate most continuous and categorical fields to the simulation domains. New or additional data sets may be interpolated to the simulation domain through the use of the table file, GEOGRID.TBL.

**Ungrib:** The ungrib program reads GRIB files, "degrib" the data, and writes the data in a simple format, called the intermediate format. The GRIB files contain time-varying meteorological fields and are typically from another regional or global model, such as NCEP's NAM or GFS models. GRIB files typically contain more fields than are needed to initialize WRF. Ungrib uses tables of these codes – called Vtables, for "variable tables" – to define which fields to extract

Table 3.1: Time-varying meteorological fields and are typically from another or global (Source: WRF, 2012)

GRIB1 Param	Level Type	From Level1	To Level2	metgrid Name	metgrid Units	metgrid Description	GRIB2 Discp	GRIB2 Catgy	GRIB2 Param	GRIB2 Level
11	100	*		TT	K	Temperature	0	0	0	100
33	100	*		UU	m s-1	U	0	2	2	100
34	100	*		VV	m s-1	V	0	2	3	100
52	100	*		RH	%	Relative Humidity	0	1	1	100
7	100	*		HGT	m	Height	0	3	5	100
11	105	2		TT	K	Temperature at 2 m	0	0	0	103
52	105	2		RH	%	Relative Humidity at 2 m	0	1	1	103
33	105	10		UU	m s-1	U at 10 m	0	2	2	103
34	105	10		VV	m s-1	V at 10 m	0	2	3	103
1	1	0		PSFC	Pa	Surface Pressure	0	3	0	1
2	102	0		PMSL	Pa	Sea-level Pressure	0	3	1	101
144	112	0	10	SM000010	fraction	Soil Moist 0-10 cm below grn layer (Up)	2	0	192	106
144	112	10	40	SM010040	fraction	Soil Moist 10-40 cm below grn layer	2	0	192	106
144	112	40	100	SM040100	fraction	Soil Moist 40-100 cm below grn layer	2	0	192	106
144	112	100	200	SM100200	fraction	Soil Moist 100-200 cm below gr layer	2	0	192	106
144	112	10	200	SM010200	fraction	Soil Moist 10-200 cm below gr layer	2	0	192	106
11	112	0	10	ST000010	K	T 0-10 cm below ground layer (Upper)	0	0	0	106
11	112	10	40	ST010040	K	T 10-40 cm below ground layer (Upper)	0	0	0	106
11	112	40	100	ST040100	K	T 40-100 cm below ground layer (Upper)	0	0	0	106
11	112	100	200	ST100200	K	T 100-200 cm below ground layer (Bottom)	0	0	0	106
	112	0	10	ST000010	K	T 0-10 cm below ground layer (Upper)	2	0	2	106
	112	10	40	ST010040	K	T 10-40 cm below ground layer (Upper)	2	0	2	106
	112	40	100	ST040100	K	T 40-100 cm below ground layer (Upper)	2	0	2	106
	112	100	200	ST100200	K	T 100-200 cm below ground layer (Bottom)	2	0	2	106
11	112	10	200	ST010200	K	T 10-200 cm below ground layer (Bottom)	0	0	0	106
91	1	0		SEAICE	proprtn	Ice flag	10	2	0	1
81	1	0		LANDSEA	proprtn	Land/Sea flag (1=land, 0 or 2=sea)	2	0	0	1
7	1	0		SOILHGT	m	Terrain field of source analysis	0	3	5	1
11	1	0		SKINTEMP	K	Skin temperature	0	0	0	1
65	1	0		SNOW	kg m-2	Water equivalent snow depth	0	1	13	1
	1	0		SNOWH	m	Physical Snow Depth	0	1		1

From the GRIB file and write to the intermediate format. Ungrib can write intermediate data files in any one of three user-selectable formats: WPS – a new format containing additional information useful for the downstream programs; SI – the previous intermediate format of the WRF system; and MM5 format, which is included here so that ungrib can be used to provide GRIB2 input to the MM5 modeling system.

**Metgrid:** The metgrid program horizontally interpolates the intermediate-format meteorological data that are extracted by the ungrib program onto the simulation domains defined by the geogrid program. The interpolated metgrid output can then be ingested by the WRF real program. The range of dates that will be interpolated by metgrid are defined in the `–share` namelist record of the WPS namelist file, and date ranges must be specified individually in the namelist for each simulation domain.

### 3.2.3 ARW solver

This is the key component of the modeling system, which is composed of several initialization programs for idealized, and real-data simulations, and the numerical integration program. The ARW dynamics solver integrates the compressible, non-hydrostatic Euler equations. The equations are cast in flux form using variables that have conservation properties, following the philosophy of Ooyama (1990). The equations are formulated using a terrain-following mass vertical coordinate (Laprise, 1992). In this section defined the vertical coordinate and present the flux form equations in Cartesian space, extend the equations to include the effects of moisture in the atmosphere, further augment the equations to include projections to the sphere.

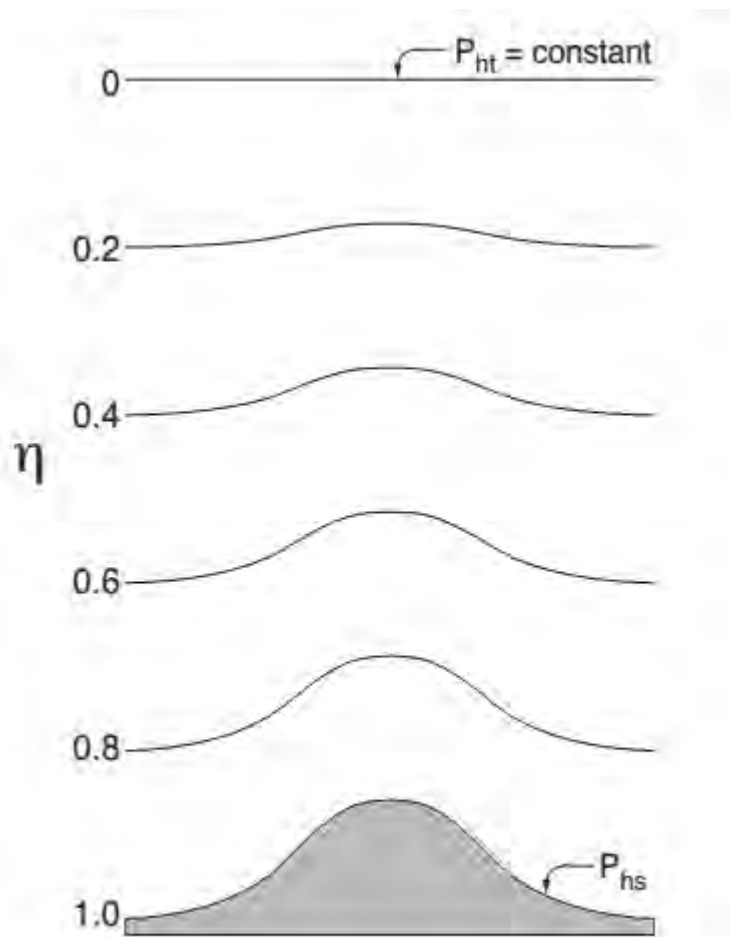


Figure 3.3 ARW  $\eta$  coordinate

### Vertical Coordinate and Variables:

The ARW equations are formulated using a terrain-following hydrostatic-pressure vertical coordinate denoted by  $\eta$  and defined as

$$\eta = (p_h - p_{ht})/\mu \text{ where } \mu = p_{hs} - p_{ht} \quad (3.1)$$

$p_h$  is the hydrostatic component of the pressure, and  $p_{hs}$  and  $p_{ht}$  refer to values along the surface and top boundaries, respectively. The coordinate definition (3.1), proposed by Laprise (1992), is the traditional  $\sigma$  coordinate used in many hydrostatic atmospheric models.  $\eta$  varies from a value of 1 at the surface to 0 at the upper boundary of the model domain (Figure 3.3). This vertical coordinate is also called a mass vertical coordinate. Since  $\mu(x, y)$  represents the mass per unit area within the column in the model domain at  $(x, y)$ , the appropriate flux form variables are

$$\mathbf{V} = \mu \mathbf{v} = (U, V, W), \Omega = \mu^{-1} \eta, \Theta = \mu \theta \quad (3.2)$$

$\mathbf{v} = (u, v, w)$  are the covariant velocities in the two horizontal and vertical directions, respectively, while  $\omega = -\eta$  is the contra variant ‘vertical’ velocity.  $\theta$  is the potential temperature. Also appearing in the governing equations of the ARW are the non-conserved variables  $\phi = g_z$  (the geo-potential),  $p$  (pressure), and  $\alpha = 1/\rho$  (the inverse density).

### Flux-Form Euler Equations:

Using the variables defined above, the flux-form Euler equations can be written as

$$\partial_t U + (\nabla \cdot \mathbf{V}u) - \partial_x(p\phi\eta) + \partial_x(p\phi x) = FU \quad (3.3)$$

$$\partial_t V + (\nabla \cdot \mathbf{V}v) - \partial_y(p\phi\eta) + \partial_y(p\phi y) = FV \quad (3.4)$$

$$\partial_t W + (\nabla \cdot \mathbf{V}w) - g(\partial_\eta p - \mu) = FW \quad (3.5)$$

$$\partial_t \Theta + (\nabla \cdot \mathbf{V}\theta) = F\Theta \quad (3.6)$$

$$\partial_t \mu + (\nabla \cdot \mathbf{V}) = 0 \quad (3.7)$$

$$\partial_t \phi + \mu^{-1}[(\mathbf{V} \cdot \nabla \phi) - gW] = 0 \quad (3.8)$$

along with the diagnostic relation for the inverse density

$$\partial_\eta \phi = -\alpha \mu \quad (2.9)$$

and the equation of state

$$p = p_0(R_d\theta/p_0\alpha)^\gamma \quad (2.10)$$

In (3.3) – (3.10), the subscripts  $x, y$  and  $\eta$  denote differentiation,

$$\nabla \cdot \mathbf{V}a = \partial_x(Ua) + \partial_y(Va) + \partial_\eta(\Omega a),$$

and

$$V \cdot \nabla a = U \partial_x a + V \partial_y a + \Omega \partial_\eta a,$$

where  $a$  represents a generic variable.  $\gamma = c_p/c_v = 1.4$  is the ratio of the heat capacities for dry air,  $R_d$  is the gas constant for dry air, and  $p_0$  is a reference pressure (typically 105 Pascals). The right-hand-side (RHS) terms  $F_U$ ,  $F_V$ ,  $F_W$ , and  $F_\Theta$  represent forcing terms arising from model physics, turbulent mixing, spherical projections, and the earth's rotation. The prognostic equations (3.3) – (3.8) are cast in conservative form except for (3.8) which is the material derivative of the definition of the geo-potential. (3.8) could be cast in flux form but we find no advantage in doing so since  $\mu\phi$  is not a conserved quantity. We could also use a prognostic pressure equation in place of (3.8) (Laprise, 1992), but pressure is not a conserved variable and we could not use a pressure equation and the conservation equation for  $\Theta$  (3.6) because they are linearly dependent. Additionally, prognostic pressure equations have the disadvantage of possessing a mass divergence term multiplied by a large coefficient (proportional to the sound speed) which makes spatial and temporal discretization problematic. It should be noted that the relation for the hydrostatic balance (3.9) does not represent a constraint on the solution, rather it is a diagnostic relation that formally is part of the coordinate definition. In the hydrostatic counterpart to the nonhydrostatic equations, (3.9) replaces the vertical momentum equation (3.5) and it becomes a constraint on the solution.

### **Inclusion of Moisture:**

In formulating the moist Euler equations, we retain the coupling of dry air mass to the prognostic variables, and we retain the conservation equation for dry air (3.7), as opposed to coupling the variables to the full (moist) air mass and hence introducing source terms in the mass conservation equation (3.7). Additionally, we define the coordinate with respect to the dry-air mass. Based on these principles, the vertical coordinate can be written as

$$\eta = (p_{dh} - p_{dht})/\mu_d \quad (3.11)$$

Where  $\mu_d$  represents the mass of the dry air in the column and  $p_{dh}$  and  $p_{dht}$  represent the hydrostatic pressure of the dry atmosphere and the hydrostatic pressure at the top of the dry atmosphere. The coupled variables are defined as



$$\mathbf{V} = \mu_d \mathbf{v}, \quad \Omega = \mu_d \eta, \quad \Theta = \mu_d \theta. \quad (3.12)$$

With these definitions, the moist Euler equations can be written as

$$\partial_t U + (\nabla \cdot \mathbf{V}u)_\eta + \mu_d \alpha \partial_x p + (\alpha/\alpha_d) \partial_\eta p \partial_x \phi = F_U \quad (3.13)$$

$$\partial_t V + (\nabla \cdot \mathbf{V}v)_\eta + \mu_d \alpha \partial_y p + (\alpha/\alpha_d) \partial_\eta p \partial_y \phi = F_V \quad (3.14)$$

$$\partial_t W + (\nabla \cdot \mathbf{V}w)_\eta - g[(\alpha/\alpha_d) \partial_\eta p - \mu_d] = F_W \quad (3.15)$$

$$\partial_t \Theta + (\nabla \cdot \mathbf{V}\theta)_\eta = F_\Theta \quad (3.16)$$

$$\partial_t \mu_d + (\nabla \cdot \mathbf{V})_\eta = 0 \quad (3.17)$$

$$\partial_t \phi + \mu_d^{-1} [(\mathbf{V} \cdot \nabla \phi)_\eta - gW] = 0 \quad (3.18)$$

$$\partial_t Q_m + (\mathbf{V} \cdot \nabla Q_m)_\eta = F_{Q_m} \quad (3.19)$$

with the diagnostic equation for dry inverse density

$$\partial_\eta \phi = -\alpha_d \mu_d \quad (3.20)$$

and the diagnostic relation for the full pressure (vapor plus dry air)

$$p = p_0 (R_d \theta_m / p_0 \alpha_d)^\gamma \quad (3.21)$$

In these equations,  $\alpha_d$  is the inverse density of the dry air ( $1/\rho_d$ ) and  $\alpha$  is the inverse density taking into account the full parcel density  $\alpha = \alpha_d(1 + q_v + q_c + q_r + q_i + \dots) - 1$  where  $q^*$  are the mixing ratios (mass per mass of dry air) for water vapor, cloud, rain, ice, etc. Additionally,  $\theta_m = \theta(1 + (R_v/R_d)q_v) \approx \theta(1 + 1.61q_v)$ , and  $Q_m = \mu_d q_m$ ;  $q_m = q_v, q_c, q_i, \dots$

### **Perturbation Form of the Governing Equations:**

Before constructing the discrete solver, it is advantageous to recast the governing equations using perturbation variables so as to reduce truncation errors in the horizontal pressure gradient calculations in the discrete solver, in addition to reducing machine rounding errors in the vertical pressure gradient and buoyancy calculations. For this purpose, new variables are defined as perturbations from a hydrostatically-balanced reference state, and we define reference state variables (denoted by overbars) that are a function of height only and that satisfy the governing equations for an atmosphere at rest. That is, the reference state is in hydrostatic balance and is strictly only a function of  $z$ . In this manner,  $p = \bar{p}(z) + p_0$ ,  $\phi = \bar{\phi}(z) + \phi_0$ ,  $\alpha = \bar{\alpha}(z) + \alpha_0$ , and  $\mu_d = \bar{\mu}_d(x, y) + \mu_{0d}$ . Because the  $\eta$  coordinate surfaces are generally not horizontal, the reference profiles  $\bar{p}$ ,  $\bar{\phi}$ , and  $\bar{\alpha}$  are functions of  $(x, y, \eta)$ . The hydrostatically balanced portion of the pressure

gradients in the reference sounding can be removed without approximation to the equations using these perturbation variables. The momentum equations are written as

$$\partial_t U + m[\partial_x(Uu) + \partial_y(Vu)] + \partial_\eta(\Omega u) + (\mu_d \alpha \partial_x p_0 + \mu_d \alpha_0 \partial_x p^-) + (\alpha/\alpha_d)(\mu_d \partial_x \phi_0 + \partial_\eta p_0 \partial_x \phi - \mu_{0d} \partial_x \phi) = F_U \quad (3.22)$$

$$\partial_t V + m[\partial_x(Uv) + \partial_y(Vv)] + \partial_\eta(\Omega v) + (\mu_d \alpha \partial_y p_0 + \mu_d \alpha_0 \partial_y p^-) + (\alpha/\alpha_d)(\mu_d \partial_y \phi_0 + \partial_\eta p_0 \partial_y \phi - \mu_{0d} \partial_y \phi) = F_V \quad (3.23)$$

$$\partial_t W + m[\partial_x(Uw) + \partial_y(Vw)] + \partial_\eta(\Omega w) - m_{-1} g (\alpha/\alpha_d) [\partial_\eta p_0 - \mu_{-d} (q_v + q_c + q_r)] + m_{-1} \mu_{0d} g = F_W, \quad (3.24)$$

and the mass conservation equation and geo-potential equation become

$$\partial_t \mu_{0d} + m_2 [\partial_x U + \partial_y V] + m \partial_\eta \Omega = 0 \quad (3.25)$$

$$\partial_t \phi_0 + \mu_{-d} [m_2 (U \phi_x + V \phi_y) + m \Omega \phi_\eta - gW] = 0. \quad (3.26)$$

Remaining unchanged are the conservation equations for the potential temperature and scalars

$$\partial_t \Theta + m_2 [\partial_x (U\theta) + \partial_y (V\theta)] + m \partial_\eta (\Omega \theta) = F_\Theta \quad (3.27)$$

$$\partial_t Q_m + m_2 [\partial_x (U_{qm}) + \partial_y (V_{qm})] + m \partial_\eta (\Omega_{qm}) = F_{Q_m}. \quad (3.28)$$

In the perturbation system the hydrostatic relation (2.30) becomes

$$\partial_\eta \phi_0 = -\mu_{-d} \alpha \alpha_0 - \alpha \mu_{0d}. \quad (3.29)$$

Equations (3.22) – (3.29), together with the equation of state (3.21), represent the equations solved in the ARW. The RHS terms in these equations include the Coriolis terms, mixing terms, and parameterized physics. Also note that the equation of state (3.21) cannot be written in perturbation form because of the exponent in the expression. For small perturbation simulations, accuracy for perturbation variables can be maintained by linearizing (3.21) for the perturbation variables.

### 3.3 Hydrologic Modeling System (HEC-HMS)

The Hydrologic Modeling System (HEC-HMS) is designed to simulate the precipitation-runoff processes of dendritic drainage basins. It is designed to be applicable in a wide range of geographic areas for solving the widest possible range of problems. This includes large river basin water supply and flood hydrology, and small urban or natural watershed runoff. Hydrographs produced by the program are used directly or in conjunction with other software for studies of water availability, urban drainage,

flow forecasting, future urbanization impact, reservoir spillway design, flood damage reduction, floodplain regulation, and systems operation. The program is a generalized modeling system capable of representing many different watersheds. A model of the watershed is constructed by separating the water cycle into manageable pieces and constructing boundaries around the watershed of interest. Each mathematical model included in the program is suitable in different environments and under different conditions. HEC-HMS is a product of the Hydrologic Engineering Center within the U.S. Army Corps of Engineers. The program was developed beginning in 1992 as a replacement for HEC-1 which has long been considered a standard for hydrologic simulation. Now, HEC-HMS provides almost all of the same simulation capabilities, but has modernized them with advances in numerical analysis that take advantage of the significantly faster desktop computers available today. It also includes a number of features that were not included in HEC-1, such as continuous simulation and grid cell surface hydrology. The program is now widely used and accepted for many official purposes, such as floodway determinations, water availability, urban drainage, flow forecasting, future urbanization impact, reservoir spillway design, flood damage reduction, floodplain regulation, and systems operation.

### **3.3.1 Model Component**

The paths water can take in moving to a stream are illustrated in Figure 1. Precipitation may be in the form of rain or snow. Vegetation may intercept some fraction of precipitation. Precipitation that penetrates the vegetation is referred to as through fall and may consist of both precipitation that does not contact the vegetation, or that drops or drains off the vegetation after being intercepted. A large fraction of intercepted water is commonly evaporated back to the atmosphere. There is also flux of water to the atmosphere through transpiration of the vegetation and evaporation from soil and water bodies. The surface water input available for the generation of runoff consists of through fall and snowmelt. This surface water input may accumulate on the surface in depression storage, or flow overland towards the streams as overland flow, or infiltrate into the soil, where it may flow laterally towards the stream contributing to interflow. Infiltrated water may also percolate through deeper soil and rock layers into the groundwater. The water table is the surface below which the soil and rock is saturated and at pressure greater than atmospheric. This serves as the boundary between the saturated zone containing

groundwater and unsaturated zone. Water added to the groundwater is referred to as groundwater recharge.

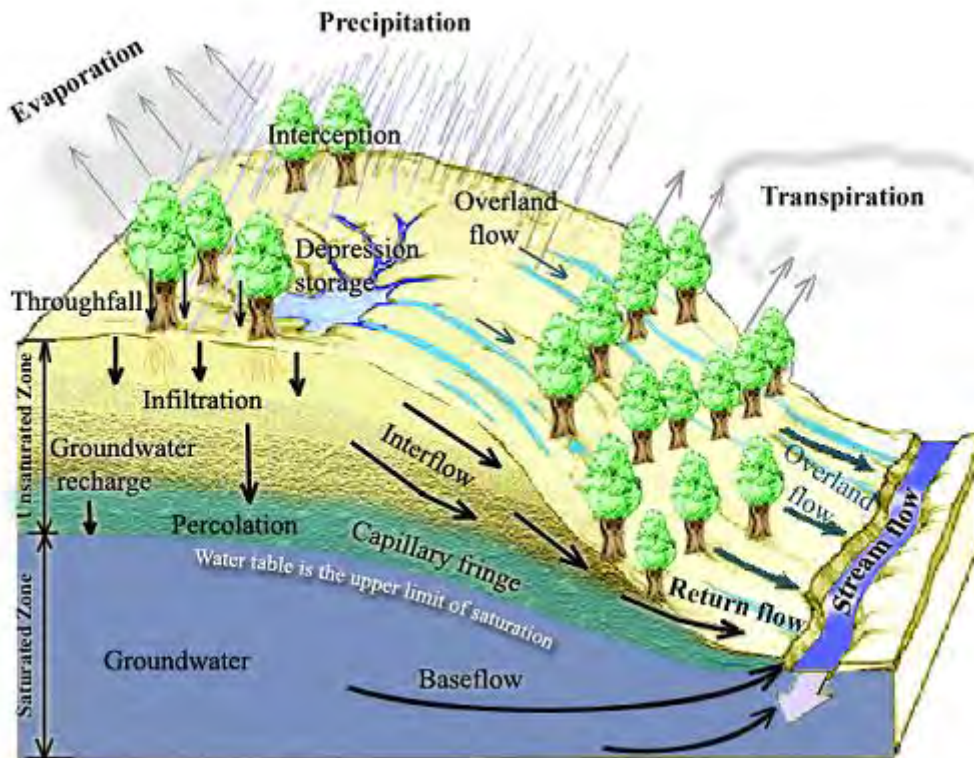


**Figure 3.4** Physical Processes involved in Runoff Generation (Source: HEC, 2000)

Immediately above the water table is a region of soil that is close to saturation, due to water being held by capillary forces. This is referred to as the capillary fringe. Lateral drainage of the groundwater into streams is referred to as base flow, because it sustains stream flow during rainless periods. Subsurface water, either from interflow or from groundwater may flow back across the land surface to add to overland flow. This is referred to as return flow. Overland flow and shallower interflow processes that transport water to the stream within the time scale of approximately a day or so are classified as runoff. Water that percolates to the groundwater moves at much lower velocities and reaches the stream over longer periods of time such as weeks, months or even years. The terms quick flow and delayed flow are also used to describe and distinguish between runoff and base flow. Runoff includes surface runoff (overland flow) and subsurface runoff or subsurface storm flow (interflow).

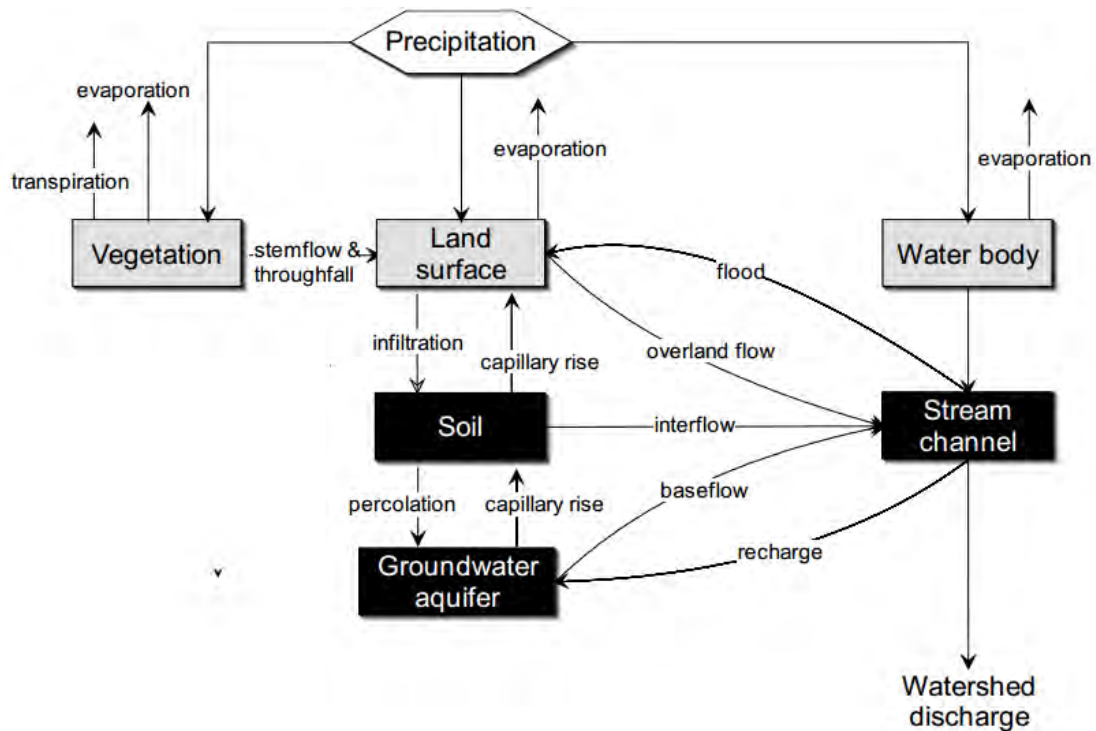


**Figure 3.5** Typical representation of watershed runoff (Source: HEC, 2000)

### 3.3.2 Catchment Delineation

River basins are local open systems. A river basin is an area of land drained by a river and its tributaries (river system). It includes water found in the water table and surface runoff. There is an imaginary line separating drainage basins called a watershed. Usually, this is a ridge of high land. The blue line in Figure 4.4 shows the watershed for a river basin. Any precipitation that falls on the other side of the watershed will flow into a river in the adjacent river basin.

### 3.3.3 Computing Runoff Volumes

HEC-HMS computes runoff volume by computing the volume of water that is intercepted, infiltrated, stored, evaporated, or transpired and subtracting it from the precipitation. Interception and surface storage are intended to represent the surface storage of water by trees or grass, local depressions in the ground surface, cracks and crevices in parking lots or roofs, or a surface area where water is not free to move as overland flow. Infiltration represents the movement of water to areas beneath the land surface. Interception, infiltration, storage, evaporation, and transpiration collectively are referred to in the program and documentation as losses. This chapter describes the loss models and how to use them to compute runoff volumes.

HEC-HMS considers that all land and water in a watershed can be categorized as either

- Directly-connected impervious surface.
- Pervious surface.

Directly-connected impervious surface in a watershed is that portion of the watershed for which all contributing precipitation runs off, with no infiltration, evaporation, or other volume losses. Precipitation on the pervious surfaces is subject to losses. The following alternative models are included to account for the cumulative losses:

- The initial and constant-rate loss model.
- The deficit and constant-rate model.
- The SCS curve number (CN) loss model.
- The Green and Ampt loss model.
- Soil Moisture Accounting Loss Model

With each model, precipitation loss is found for each computation time interval, and is subtracted from the MAP depth for that interval. The remaining depth is referred to as precipitation excess. This depth is considered uniformly distributed over a watershed area, so it represents a volume of runoff.

Direct runoff describes the models that simulate the process excess precipitation on a watershed. This process refers to the "transformation" of precipitation excess into point runoff. The program provides two options for these transform methods:

- a) Empirical models (also referred to as system theoretic models):

These are the traditional unit hydrograph (UH) models. The system theoretic models attempt to establish a causal linkage between runoff and excess precipitation without detailed consideration of the internal processes. The equations and the parameters of the model have limited physical significance. Instead, they are selected through optimization of some goodness-of-fit criterion.

- b) Conceptual model:

The conceptual model included in the program is a kinematic-wave model of overland flow. It represents, to the extent possible, all physical mechanisms that govern the

movement of the excess precipitation over the watershed land surface and in small collector channels in the watershed

Other two options for direct runoff hydrograph computations: the unit hydrograph (UH) model and the kinematic-wave model. With a UH model, the excess on pervious portions of the watershed is added to the precipitation on directly connected impervious area, and the sum is used in runoff computations. With the kinematic-wave model, directly connected impervious areas may be modeled separately from pervious areas if two overland flow planes are defined.

### 3.3.4 Soil Moisture Accounting Loss Model

The model simulates the movement of water through and storage of water on vegetation, on the soil surface, in the soil profile, and in groundwater layers. Given precipitation and potential evapotranspiration (ET), the model computes basin surface runoff, groundwater flow, losses due to ET, and deep percolation over the entire basin

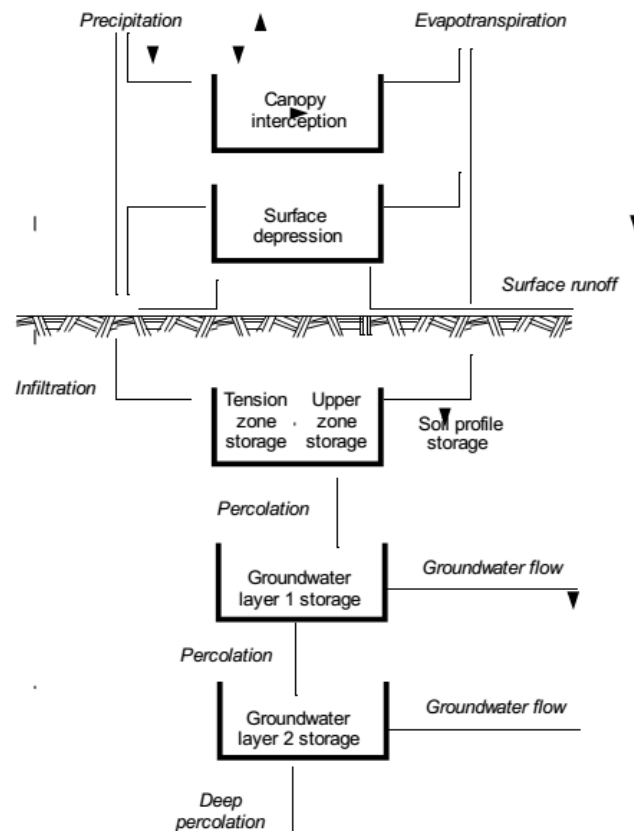


**Figure 3.6** Conceptual schematic of the continuous soil moisture accounting algorithm (Source: HEC, 2000)

**Storage Component:**

The SMA model represents the watershed with a series of storage layers, as illustrated by Figure 3.6. Rates of inflow to, outflow from, and capacities of the layers control the volume of water lost or added to each of these storage components. Current storage contents are calculated during the simulation and vary continuously both during and between storms. The different storage layers in the SMA model are:

**Canopy-interception storage:** Canopy interception represents precipitation that is captured on trees, shrubs, and grasses, and does not reach the soil surface. Precipitation is the only inflow into this layer. When precipitation occurs, it first fills canopy storage. Only after this storage is filled does precipitation become available for filling other storage volumes. Water in canopy interception storage is held until it is removed by evaporation.

**Surface-interception storage:** Surface depression storage is the volume of water held in shallow surface depressions. Inflows to this storage come from precipitation not captured by canopy interception and in excess of the infiltration rate. Outflows from this storage can be due to infiltration and to ET. Any contents in surface depression storage at the beginning of the time step are available for infiltration. If the water available for infiltration exceeds the infiltration rate, surface interception storage is filled. Once the volume of surface interception is exceeded, this excess water contributes to surface runoff.

**Soil-profile storage:** The soil profile storage represents water stored in the top layer of the soil. Inflow is infiltration from the surface. Outflows include percolation to a groundwater layer and ET. The soil profile zone is divided into two regions, the upper zone and the tension zone. The upper zone is defined as the portion of the soil profile that will lose water to ET and/or percolation. The tension zone is defined as the area that will lose water to ET only. The upper zone represents water held in the pores of the soil. The tension zone represents water attached to soil particles. ET occurs from the upper zone first and tension zone last. Furthermore, ET is reduced below the potential rate occurring from the tension zone, as shown in Figure 15. This represents the natural increasing resistance in removing water



**Groundwater storage:** Groundwater layers in the SMA represent horizontal interflow processes. The SMA model can include either one or two such layers. Water percolates into groundwater storage from the soil profile. The percolation rate is a function of a user-specified maximum percolation rate and the current storage in the layers between which the water flows. Losses from a groundwater storage layer are due to groundwater flow or to percolation from one layer to another. Percolation from the soil profile enters the first layer. Stored water can then percolate from layer 1 to groundwater layer 2 or from groundwater layer 2 to deep percolation. In the latter case, this water is considered lost from the system; aquifer flow is not modeled in the SMA attached to soil particles. ET can also be limited to the volume available in the upper zone during specified winter months, depicting the end of transpiration by annual plants.

**Flow Component:**

The SMA model computes flow into, out of, and between the storage volumes. This flow can take the form of:

**Precipitation:** Precipitation is an input to the system of storages. Precipitation first contributes to the canopy interception storage. If the canopy storage fills, the excess amount is then available for infiltration.

**Infiltration:** Infiltration is water that enters the soil profile from the ground surface. Water available for infiltration during a time step comes from precipitation that passes through canopy interception, plus water already in surface storage. The volume of infiltration during a time interval is a function of the volume of water available for infiltration, the state (fraction of capacity) of the soil profile, and the maximum infiltration rate specified by the model user. For each interval in the analysis, the SMA model computes the potential infiltration volume, PotSoilInfl, as:

$$\text{PotSoilInfil} = \text{MaxSoilInfil} - \frac{\text{CurSoilStore}}{\text{MaxSoilStore}} \text{MaxSoilInfil} \quad 3.30$$

where MaxSoilInfl = the maximum infiltration rate; CurSoilStore = the volume in the soil storage at the beginning of the time step; and MaxSoilStore = the maximum volume of the soil storage. The actual infiltration rate, ActInfil, is the minimum of PotSoilInfil and the volume of water available for infiltration. If the water available for infiltration exceeds this calculated infiltration rate, the excess then contributes to surface interception storage

**Percolation:** Percolation is the movement of water downward from the soil profile, through the groundwater layers, and into a deep aquifer. In the SMA model, the rate of percolation between the soil-profile storage and a groundwater layer or between two groundwater layers depends on the volume in the source and receiving layers. The rate is greatest when the source layer is nearly full and the receiving layer is nearly empty. Conversely, when the receiving layer is nearly full and the source layer is nearly empty, the percolation rate is less. In the SMA model, the percolation rate from the soil profile into groundwater layer 1 is computed as:

$$\text{PotSoilPerc} = \text{MaxSoilPerc} \left( \frac{\text{CurSoilStore}}{\text{MaxSoilStore}} \right) 1 - \left( \frac{\text{CurGwStore}}{\text{MaxGwStore}} \right) \quad 3.31$$

where PotSoilPerc = the potential soil percolation rate; MaxSoilPerc = a user-specified maximum percolation rate; CurSoilStore = the calculated soil storage at the beginning of the time step; MaxSoilStore = a user specified maximum storage for the soil profile; CurGwStore = the calculated groundwater storage for the upper groundwater layer at the beginning of the time step; and MaxGwStore = a user-specified maximum groundwater storage for groundwater layer 1. The potential percolation rate computed with Equation 22 is multiplied by the time step to compute a potential percolation volume. The available water for percolation is equal the initial soil storage plus infiltration. The minimum of the potential volume and the available volume percolates to groundwater layer 1. A similar equation is used to compute PotGwPerc, the potential percolation from groundwater layer 1 to layer 2:

$$\text{PotGwPerc} = \text{MaxPercGw} \left( \frac{\text{CurGwStore}}{\text{MaxGwStore}} \right) 1 - \left( \frac{\text{CurGwStore}}{\text{MaxGwStore}} \right) \quad 3.32$$

where MaxPercGw = a user-specified maximum percolation rate; CurGwStore = the calculated groundwater storage for the groundwater layer 2; and MaxGwStore = a user-specified maximum groundwater storage for layer 2. The actual volume of percolation is computed as described above. For percolation directly from the soil profile to the deep aquifer in the absence of groundwater layers, for percolation from layer 1 when layer 2 is not used, or percolation from layer 2, the rate depends only on the storage volume in the source layer. In those cases, percolation rates are computed as

$$\text{PotSoilPerc} = \text{MaxSoilPerc} \left( \frac{\text{CurSoilStore}}{\text{MaxSoilStore}} \right) \quad 3.33$$

and

$$\text{PotGwPerc} = \text{MaxPercGw} \left( \frac{\text{CurGwStore}}{\text{MaxGwStore}} \right) \quad 3.34$$

respectively, and actual percolation volumes are computed as described above.

**Surface runoff and groundwater flow:** Surface runoff is the water that exceeds the infiltration rate and overflows the surface storage. Groundwater flow is the sum of the volumes of groundwater flow from each groundwater layer at the end of the time interval.

$$G_w\text{Flow}_{t+1} = \frac{\text{ActSoilPerc} + \text{CurGwtSrore} - \text{PotGwPerc} - \left(\frac{1}{2}\right)G_w\text{Flow}_t \cdot \text{TimeStep}}{\text{RoutGwtStore} + (1/2)\text{TimeStep}} \quad 3.35$$

where  $G_w\text{Flow}_t$  and  $G_w\text{Flow}_{t+1}$  = groundwater flow rate at beginning of the time interval  $t$  and  $t+1$ , respectively;  $\text{ActSoilPerc}$  = actual percolation from the soil profile to the groundwater layer;  $\text{PotGwiPerc}$  = potential percolation from groundwater layer  $i$ ;  $\text{RoutGwiStore}$  = groundwater flow routing coefficient from groundwater storage  $i$ ;  $\text{TimeStep}$  = the simulation time step; and other terms are as defined previously. The volume of groundwater flow that the watershed releases,  $G_w\text{Volume}$ , is the integral of the rate over the model time interval. This is computed as

$$G_w\text{Volume} = (1/2)(G_w\text{Flow}_{t+1} + G_w\text{Flow}_t) \cdot \text{TimeStep} \quad 3.36$$

**Evapotranspiration (ET):** ET is the loss of water from the canopy interception, surface depression, and soil profile storages. In the SMA model, potential ET demand currently is computed from monthly pan evaporation depths, multiplied by monthly-varying pan correction coefficients, and scaled to the time interval. The potential ET volume is satisfied first from canopy interception, then from surface interception, and finally from the soil profile. Within the soil profile, potential ET is first fulfilled from the upper zone, then the tension zone. If potential ET is not completely satisfied from one storage in a time interval, the unsatisfied potential ET volume is filled from the next available storage.

### 3.3.5 Clark Unit Hydrograph Model

Clark's model derives a watershed UH by explicitly representing two critical processes in the transformation of excess precipitation to runoff:

**Translation** or movement of the excess from its origin throughout the drainage to the watershed outlet.

**Attenuation** or reduction of the magnitude of the discharge as the excess is stored throughout the watershed.

**Basic Concepts and Equations** Short-term storage of water throughout a watershed—in the soil, on the surface, and in the channels—plays an important role in the transformation of precipitation excess to runoff. The linear reservoir model is a common representation of the effects of this storage. That model begins with the continuity equation:

$$dS/dt = I_t - O_t \quad 3.37$$

in which  $dS/dt$  = time rate of change of water in storage at time  $t$ ;  $I_t$  = average inflow to storage at time  $t$ ; and  $O_t$  = outflow from storage at time  $t$ . With the linear reservoir model, storage at time  $t$  is related to outflow as:  $S_t = RO_t$

Where,  $R$  = a constant linear reservoir parameter. Combining and solving the equations using a simple finite difference approximation yields:

$$O_t = C_A I_t + C_B O_{t-1} \quad 3.38$$

Where,  $C_A, C_B$  = routing coefficients. The coefficients are calculated from:

$$C_A = \Delta t / (R + 0.5\Delta t) \quad 3.39$$

$$C_B = 1 - C_A \quad 3.40$$

The average outflow during period  $t$  is:

$$\bar{O} = \frac{O_{t-1} + O_t}{2} \quad 3.41$$

With Clark's model, the linear reservoir represents the aggregated impacts of all watershed storage. Thus, conceptually, the reservoir may be considered to be located at the watershed outlet. In addition to this lumped model of storage, the Clark model

accounts for the time required for water to move to the watershed outlet. It does that with a linear channel model (Dooge, 1959), in which water is "routed" from remote points to the linear reservoir at the outlet with delay (translation), but without attenuation. This delay is represented implicitly with a so-called time-area histogram. That specifies the watershed area contributing to flow at the outlet as a function of time. If the area is multiplied by unit depth and divided by  $\Delta t$ , the computation time step, the result is inflow,  $I_t$ , to the linear reservoir. Solving Equation 46 and Equation 49 recursively, with the inflow thus defined, yields values of  $O_t$ . However, if the inflow ordinates in Equation 46 are runoff from a unit of excess, these reservoir outflow ordinates are, in fact,  $U_t$ , the UH.

### **3.4 Hydrodynamic Modeling System (HEC-RAS)**

HEC-RAS is a computer program that models the hydraulics of water flow through natural rivers and other channels. The program is one-dimensional, meaning that there is no direct modeling of the hydraulic effect of cross section shape changes, bends, and other two- and three-dimensional aspects of flow. The program was developed by the US Department of Defense, Army Corps of Engineers in order to manage the rivers, harbors, and other public works under their jurisdiction; it has found wide acceptance by many others since its public release in 1995. It includes numerous data entry capabilities, hydraulic analysis components, data storage and management capabilities, and graphing and reporting capabilities. The following is a description of the major hydraulic capabilities of HEC-RAS.

#### **Steady Flow Water Surface Profiles:**

This component of the modeling system is intended for calculating water surface profiles for steady gradually varied flow. The system can handle a single river reach, a dendritic system, or a full network of channels. The steady flow component is capable of modeling subcritical, supercritical, and mixed flow regime water surface profiles. The basic computational procedure is based on the solution of the one dimensional energy equation. Energy losses are evaluated by friction (Manning's equation) and contraction/expansion (coefficient multiplied by the change in velocity head). The momentum equation is utilized in situations where the water surface profile is rapidly varied. These situations include mixed flow regime calculations (i.e., hydraulic jumps), hydraulics of bridges, and evaluating profiles at river confluences (stream junctions). The effects of various obstructions such as bridges, culverts, weirs, spillways and other structures in the flood

plain may be considered in the computations. The steady flow system is designed for application in flood plain management and flood insurance studies to evaluate floodway encroachments. Also, capabilities are available for assessing the change in water surface profiles due to channel improvements, and levees. Special features of the steady flow component include: multiple plan analyses; multiple profile computations; multiple bridge and/or culvert opening analysis, and split flow optimization at stream junctions and lateral weirs and spillways.

**Unsteady Flow Simulation:**

This component of the HEC-RAS modeling system is capable of simulating one-dimensional unsteady flow through a full network of open channels. The unsteady flow equation solver was adapted from Dr. Robert L. Barkau's UNET model (Barkau, 1992 and HEC, 1997). This unsteady flow component was developed primarily for subcritical flow regime calculations. The hydraulic calculations for cross-sections, bridges, culverts, and other hydraulic structures that were developed for the steady flow component were incorporated into the unsteady flow module. Additionally, the unsteady flow component has the ability to model storage areas and hydraulic connections between storage areas, as well as between stream reaches.

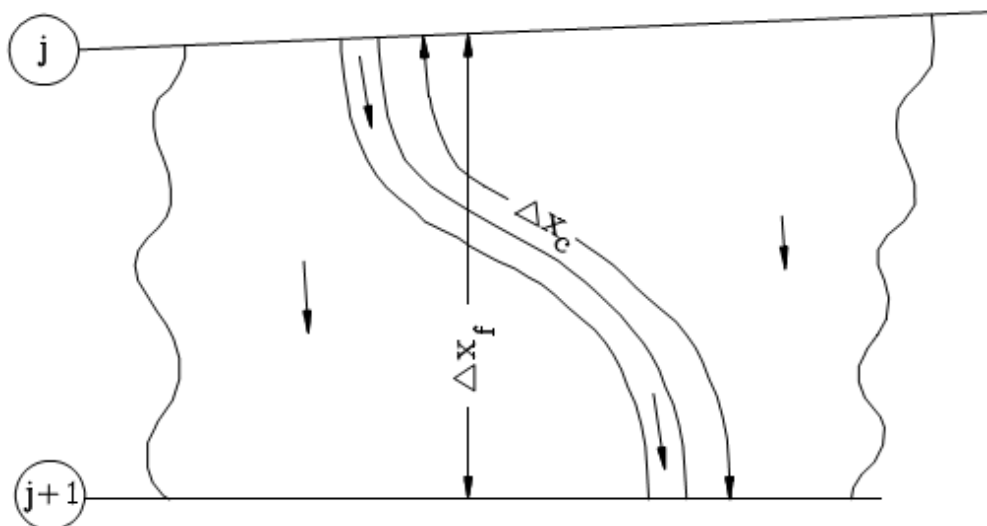


**Figure 3.7** Channel and floodplain flows (Source: HEC, 2005)

Figure 3.7 illustrates the two-dimensional characteristics of the interaction between the channel and floodplain flows. When the river is rising water moves laterally away from

the channel, inundating the floodplain and filling available storage areas. As the depth increases, the floodplain begins to convey water downstream generally along a shorter path than that of the main channel. When the river stage is falling, water moves toward the channel from the overbank supplementing the flow in the main channel.

The computation engine of HEC-RAS is based on the solution of the one-dimensional energy equation. Energy losses are evaluated by friction (Manning's formula), contraction, and expansion. In cases where the water surface profile varies rapidly, use of the momentum equation is necessary. These cases include: mixed flow regime calculations, bridge hydraulic calculations and evaluation of profiles at river confluence. The governing equations for open-channel flows are the Saint-Venant equations,

$$\frac{dz}{dt} + \frac{1}{B} \frac{dQ}{dx} = \frac{q}{B} \quad 3.42$$

$$\frac{dz}{dt} + \left( gA - \frac{BQ^2}{A^2} \right) \frac{dz}{dx} + \frac{2Q}{A} \frac{dQ}{dx} = \frac{Q^2}{A^2} \frac{dA}{dx} \Big|_z - \frac{gQ|Q|}{Ac^2R} \quad 3.43$$

Where A = cross-sectional area perpendicular to the flow; Q = discharge;  $q_l$  = lateral inflow due to tributary; g = acceleration due to gravity; H = elevation of the water surface above a specified datum, also called stage;  $S_f$  = longitudinal boundary friction slope; t = temporal coordinate; and x = longitudinal coordinate. The equations are solved using the well-known four-point implicit box finite difference scheme, also employed in models such as the U.S. National Weather Service's FLDWAV model and its predecessor, the DAMBRK model (Fread, 1988). This numerical scheme has been shown to be completely non-dissipative but marginally stable when run in a semi-implicit form, which corresponds to a  $\theta$  weighting factor of 0.5 for the unsteady solution (Hicks and Steffler, 1990). This value represents a half weighting explicit to the previous time step's known solution, and a half weighting implicit to the current time step's unknown solution. However, practically speaking, due to its marginal stability for the semi-implicit formulation, a  $\theta$  weighting factor of 0.6 or more is necessary, since the scheme is diffusive only at values of  $\theta$  greater than 0.5. This increases solution stability, but at the expense of solution accuracy. The diffusive nature of the scheme increases as  $\theta$  is increased; furthermore, this effect is more pronounced as the length of the wave disturbance is decreased. For long flat flood waves the effect is negligible, while for flow discontinuities (e.g., the surges resulting from dam break events or ice jam release surges)

the effect can be quite significant in terms of its detrimental effect on solution accuracy. HEC-RAS defaults to a value of  $\theta = 1.0$  (fully implicit, highly stable and highly diffusive) but does allow the user to specify any value between 0.6 and 1.0. Generally, the box finite difference scheme is limited in its ability to handle transitions between subcritical and supercritical flow, since a different solution algorithm is required for each. An attempt has been made to overcome this limitation in HEC-RAS by employing a mixed-flow routine to patch solutions in sub-reaches. This option was not tested in this investigation.

### **3.5 HEC-GeoRAS Mapping**

HEC-GeoRAS is an ArcView GIS extension specifically designed to process geospatial data for use with the Hydrologic Engineering Center's River Analysis System (HEC-RAS). The extension allows users to create a HEC-RAS import file containing geometric attribute data from an existing Digital Elevation Model (DEM) and complementary data sets. The channel shape, principle dimension of channel cross section and channel roughness is extracted for implementing the hydrodynamic model in HEC-RAS. In order to access such physical characteristics of the natural channel the extension software of ArcMap 10.1 developed by USACE, HEC-GEORAS can be used.



## CHAPTER 4

### METHODOLOGY AND MODEL SETUP

#### 4.1 General

In order to develop the mathematical flood model, various kinds of data, recent and previous years have been collected and compiled. These data also form the basis for further analysis and interpretation of the model results leading to accurate assessment of hydrological condition of the study area. According to the Modelling requirements, a significant amount of data includes water level, discharge, cross-section; WRF predicted rainfall data etc. have been collected. And setup flood forecast model using this data. This chapter describes a brief discussion about the collected data and model setup.

#### 4.2 Selection of Study Area

Bangladesh is the largest delta in the world created by the three mighty rivers: the Ganges, the Brahmaputra and the Meghna, while the total basin area of its river system is 1,726,300 sq. km. Thus, only 8.5 % of the river basin lies within the country, and the rest 91.5 % lies outside of the countries. Annual average renewable fresh water resources in the country are around 1210.6  $\text{km}^3$  out of which only 105  $\text{km}^3$  (8.7%) is locally generated. Due to high external flows, Bangladesh is one of the most flood prone countries in the world. Floods of different magnitudes and types occur recurrently. The country experiences four types of flood: Flash flood, Rain-fed flood, River flood and Storm surge flood (IWM, 2014).

The study area is located in Roumari Upazilla of Kurigram district. It includes complete administrative areas of five Unions are Raumar, Jadurchar, Bandaber and Saulmari. The area is located on the left side of the mighty Brahmaputra River and right side of the Jijiram River. The area extends from  $25.42^{\circ}$  to  $25.60^{\circ}$  North Latitudes and  $89.77^{\circ}$  to  $89.87^{\circ}$  East Longitudes. Figure 4.1 shows the study area. The main cause of flooding in the area is the Trans-boundary inflow from upstream catchment carried by the Brahmaputra River and Jinjiram River.

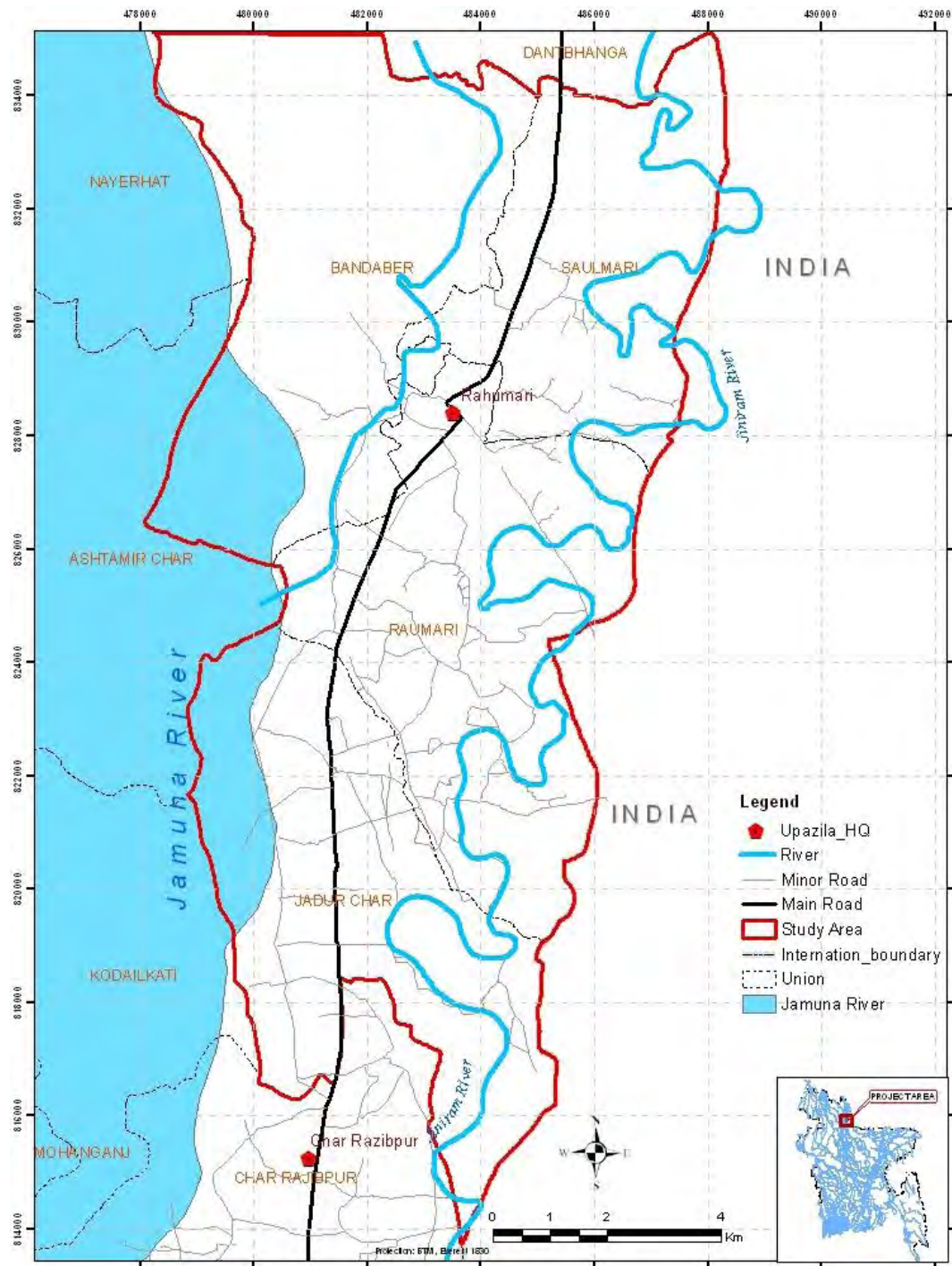


**Figure 4.1** Location map of the study area

Here, the Brahmaputra River which dominates Western part Rowmari flooding, which originates from Kailas Range of the Himalays and flows across China, India and Bangladesh and Eastern part of Rowmari is dominated by Jinjiram river, this river is originated form Indian Tura hilly region. The location and the catchment area of Brahmaputra are shown in Figure 4.4. Due to the geographic location of the study area have been facing big flood almost every year. Floods have been observed to disrupt

personal, economic & social activities and set back a nation's security and development by destroying roads, buildings and other assets of this study area. For managing floods, mitigate the impact of flood and early warning system of this study is main concern using non-structural measures is the flood forecasting and warning system.

### 4.3 Methodology

Modeling of any physical phenomenon is an iterative development of a process. Model refinements are based on the availability and quality of data, hydrological understanding and scopes of the study. The general approach that has been followed in the current study can be summarized in the flowchart given in Figure 4.2. A brief description of the methodology and approaches are provided in this section to achieve the study objectives. It includes-

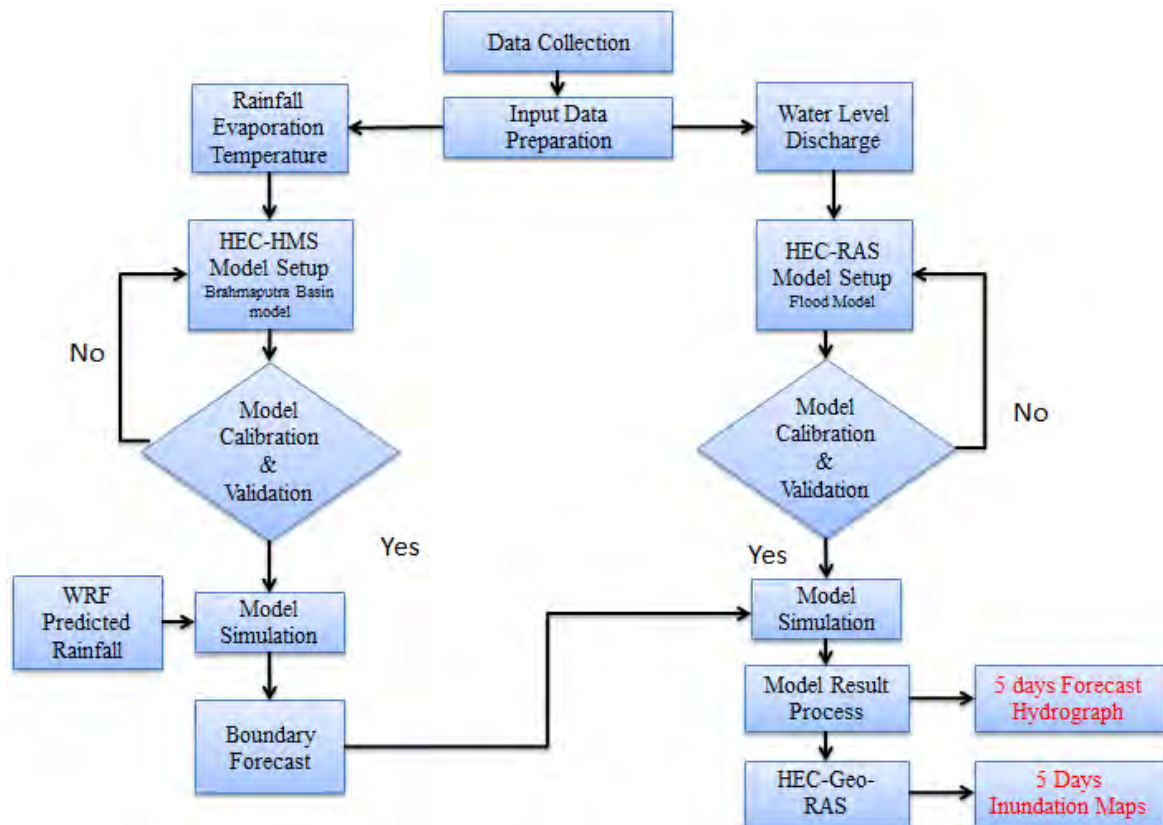


**Figure 4.2** Flow chart of methodology applied in the study

#### 4.4 Data Collection

Quality data are prerequisite for reliable model setup, model results and to have understanding on the existing physical processes. To determine the present hydrologic, hydrodynamic, present flood situation, quality flood forecasting and to develop a hydrological model of Brahmaputra basin and local flood model for Rowmari Upazilla, various data have been collected from different sources. A brief description of data is given below:

##### 4.4.1 Digital Elevation Model

A digital elevation model (DEM) is a digital model or 3D representation of a terrain's surface, created from terrain elevation data. This data is required to formulate mathematical models for the study area. DEM data identifies the elevations of the earth surface and to locate natural and relevant features on it. The Shuttle Radar Topography Mission (SRTM) data has emerged as a global elevation data in the past one decade because of its free availability, homogeneity and consistent accuracy compared to other global elevation dataset. This study explores the hydrological modeling of Brahmaputra basin with the help of the SRTM digital elevation model (DEM). In this study DEM image in raster format has been collected from SRTM website. Also collect high regulation (5m x 5m) DEM for Rowmari Upazilla from IWM to generate forecast inundation map precisely.

##### 4.4.2 Meteorological Data

Historical real-time rainfall daily data, evaporation data and temperature data of at Brahmaputra Basin have been collected from IWM. IWM all this data have been collecting from public website everyday

**Table 4.1** Summary of the rainfall data

Type	No of Stations	Data Type	Years	Source
Rainfall	50	Daily Rainfall	2009-2014	IWM
Evaporation	9	Monthly	2009-2014	IWM
Temperature	2	Monthly	2009-2014	IWM

#### 4.4.3 Water Level

Water level data at different locations are required for defining water level of different flood events as well as providing boundary of one-dimensional hydrodynamic model and to calibrate the model. Therefore, historical water level data at Bahadurabad, Chilmari, Dhonarchar and Noonkhawa station of Jamuna River, Lalkura station of Jinjiram River and Jamalpur station of Old Brahmaputra River have been collected and analyzed to get an idea about the amount of water is flowing at this location. The duration of collected data are listed in Table 4.2.

**Table 4.2** Summary of the water level data

Station Name	River Name	Easting(BTM)	Northing(BTM)	Duration	Source
Bahadurabad	Brahmaputra	470050.2	782401.8	2013-2014	BWDB
Chilmari	Brahmaputra	465302.9	825375.5	2013-2014	BWDB
Dhonarchar	Brahmaputra	480382	820853	2014	IWM
Noonkhawa	Brahmaputra	488190.18	862002.83	2013-2014	BWDB
Lalkura	Jijiram	482345	819387	2014	IWM
Jamalpur	Old Brahmaputra	499081.24	753394.77	2013-2014	BWDB

#### 4.4.4 Discharge

Discharge data are needed to investigate the hydrological characteristics of the river and to provide boundary for the one-dimensional hydrodynamic model and need for hydrological model calibration. Available discharge data for the Brahmaputra River is listed below (Table 4.3):

**Table 4.3** Summary of the discharge data

Station Name	River Name	Easting(BTM)	Northing(BTM)	Duration	Source
Bahadurabad	Brahmaputra	470050.2	782401.8	2010-2014	BWDB
Noonkhawa	Brahmaputra	488190.18	862002.83	2013-2014	BWDB

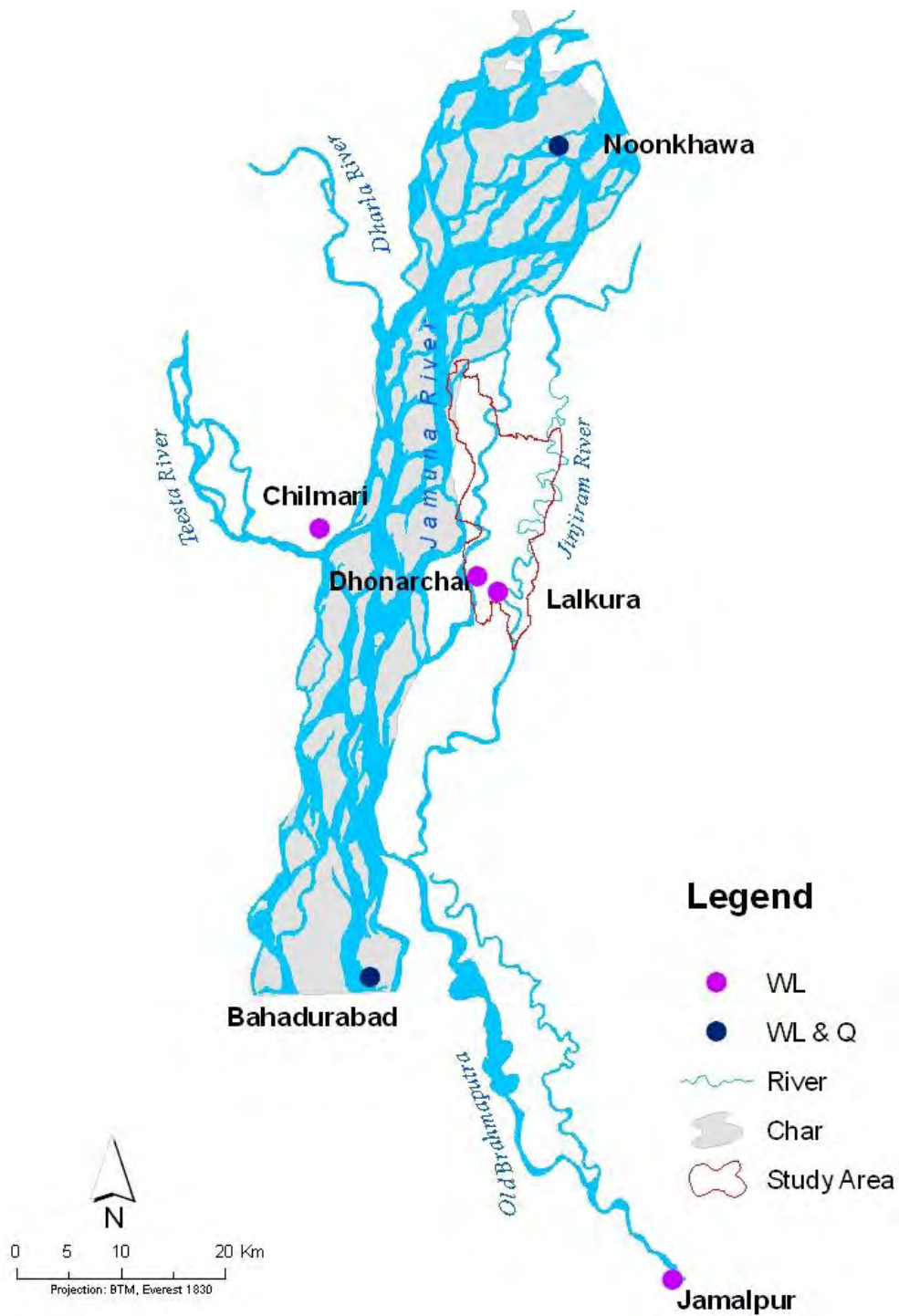


**Figure 4.3** Location of discharge and water level station near the study area

#### 4.4.5 Cross Section

River cross-sections of Brahmaputra, Old Brahmaputra and Jinjiram River are collected for the years of 2005, 2008 and 2014 respectively, from Morphology Department of Bangladesh Water Development Board (BWDB) and IWM.



**Table 4.4** Summary of the cross-section data

River Name	No of Cross- Section	Surveyed year	Source
Brahmaputra	17	2008-09	BWDB
Old Brahmaputra	13	2001-02	BWDB
Jinjiram	16	2013-14	IWM

## **4.5 Model Setup**

Mathematical modeling is an advance technology in engineering practice for predicting flood water level. A hydrological and one dimensional hydrodynamic model have setup using HEC-package to forecast flood inundation map and hydrograph. Using this modeling software, a mathematical model for flood forecasting system has been developed. The various key steps during processing the model are described below.

### **4.5.1 Rainfall–runoff model: HEC-HMS**

Development of model using HEC-HMS includes several steps: (i) sketching of the river system, (ii) delineation of sub-catchments, (iii) computation of mean rainfall and evaporation for each sub-catchment, (iv) setup hydrological / rainfall runoff model and (v) simulation as well as calibration of the model.

#### **4.5.1.1 Sketching of the river system**

At the start of HEC-HMS version 4.1 modelling, flow direction has been calculated using land terrain data of SRTM. Subsequently, main stream and tributaries of the Brahmaputra river have been sketched using the HEC-GEORAS. Rivers sketched in the basin are: Brahmaputra River, Dibang, Lohit, Buri Dihing, Dhansiri, Kopili, Subansiri, Kameng, Manas, Sunkosh, Dudkumar, Dharala, and Teesta are shown figure 4.4.

#### **4.5.1.2 Delineation of sub-catchment**

Placing catchment nodes on the sketched river reaches, sub-catchments in the basin have been delineated using the available tool of HEC-GEORAS. Total delineated sub-catchments in the basin are 49 nos. (Figure 4.4). Total basin area under the model is 521144 sq. km. It is to be noted that the Brahmaputra River accumulates flow up to

Bahadurabad point of Bangladesh. After Bahadurabad, the Brahmaputra River has several distributaries in the left bank which are not possible to model using hydrological modelling concept. Thus, the downstream boundary of the HEC-HMS model has been taken at Bahadurabad.

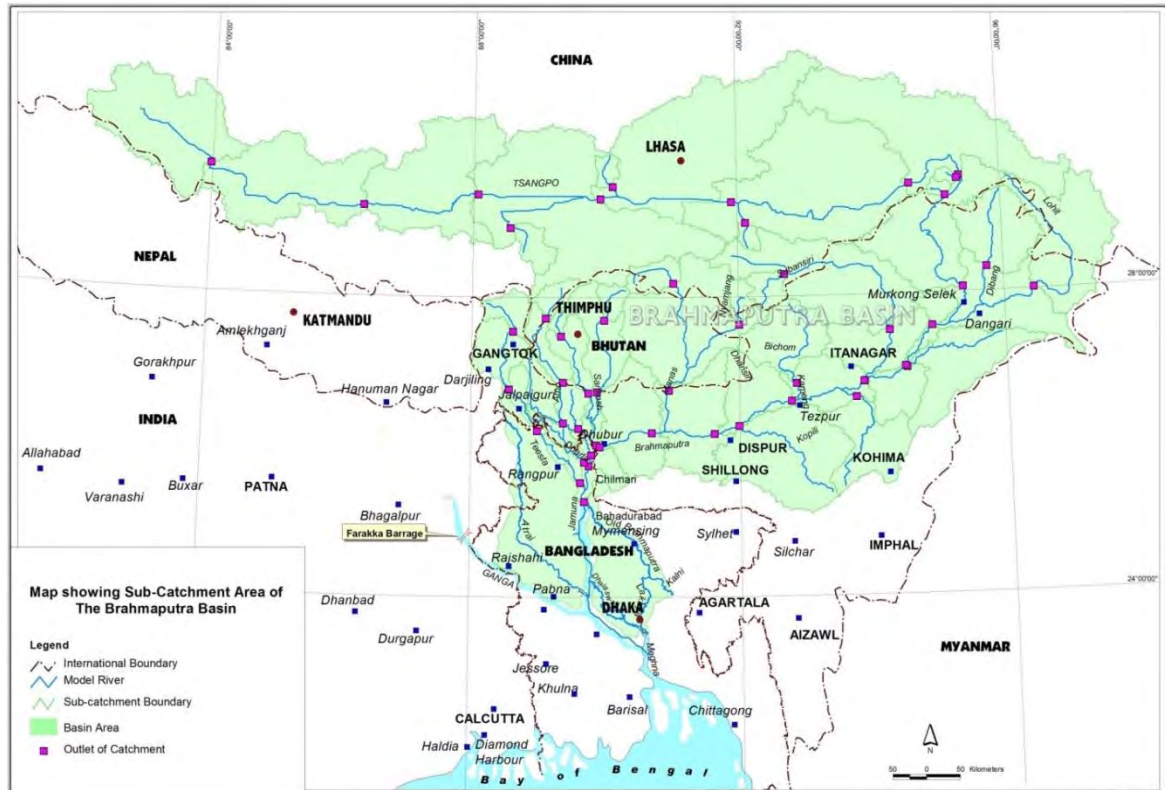


**Figure 4.4** River network, sub-catchments and catchment nodes of the HEC-HMS model of Brahmaputra basin

#### 4.5.1.3 Computation of mean area rainfall and evaporation

Mean area rainfall for each sub-catchment has been computed by using the weightage of rainfall stations to the sub-catchment. The weightage factors of rainfall stations to a sub-catchment have been computed by Thiessen Polygon Analysis using Arc-GIS. Since, the distribution of rainfall stations in the basin is quite uneven, some manual adjustment has been applied on the computed weightage factors. Same procedure has been applied for mean area evaporation computation.



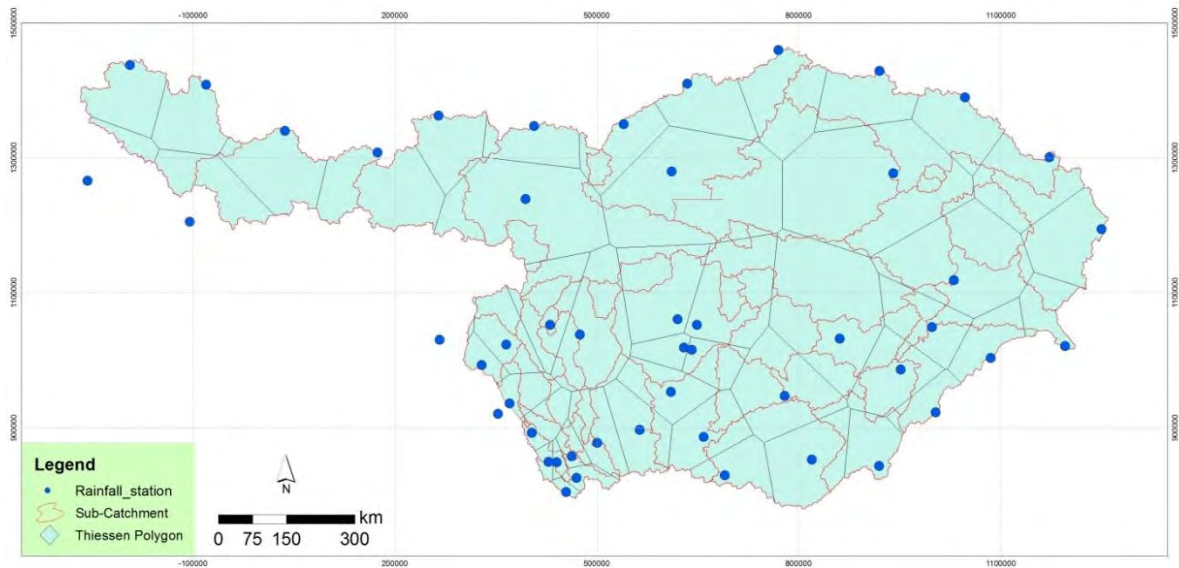


**Figure 4.5** Rainfall station and its weightage area each sub-basin.

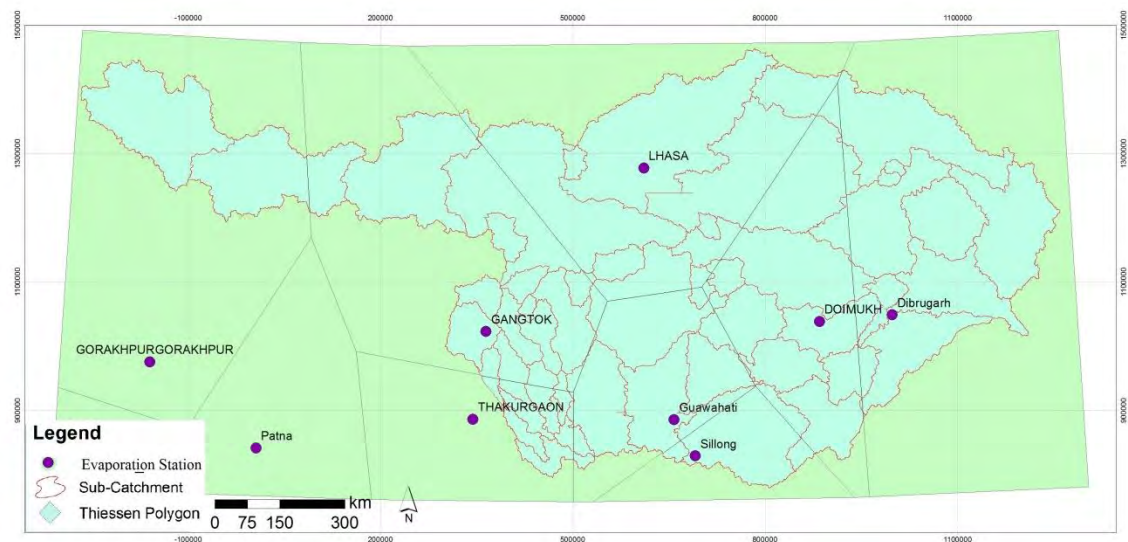


**Figure 4.6** Evaporation station and its weightage area each sub-basin.

#### 4.5.1.4 Set up rainfall runoff model

A rainfall runoff model has been developed using HEC-HMS model of US Army. The rainfall runoff model comprises 49 sub-catchments, rainfall stations of 50 nos., evaporation stations of 6 nos., and temperature stations of 2 nos. Potential evapotranspiration required in the model has been computed from available evaporation records multiplying by the factors ranging from 0.30 to 0.80 depending on the soil condition, vegetation coverage: 0.3 used for bare hilly catchments and 0.8 used for densely vegetated plane lands (IWM, 2104). For snow fed catchments, the areas under different

elevations have been computed by accumulating areas calculated for each incremental elevation using SRTM DEM.

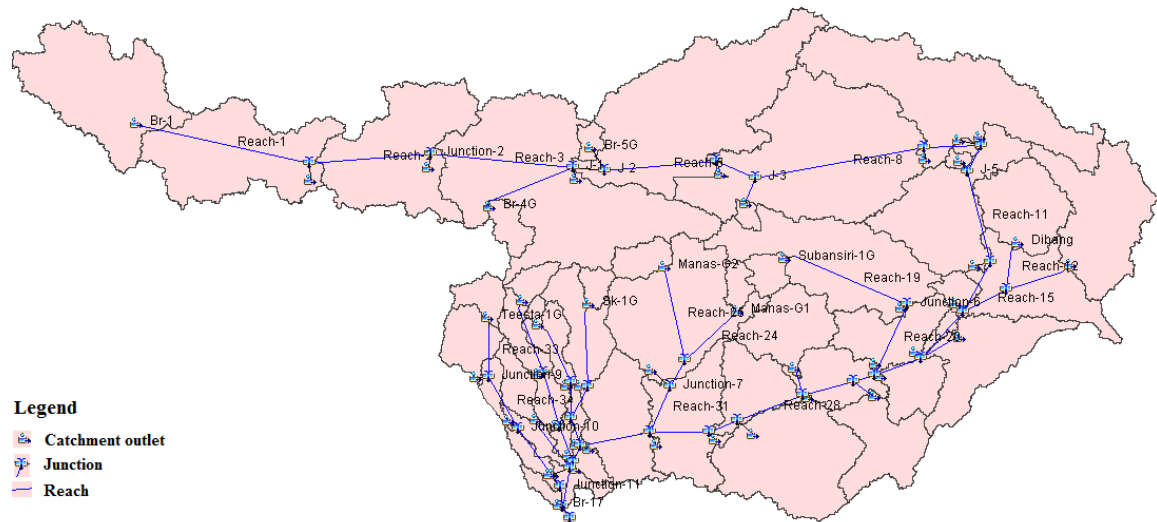


**Figure 4.7** HEC-HMS schematic description of Brahmaputra basin

It is to be noted that the rainfall runoff model (HEC-HMS) comprises four conceptual storages: snow storage, surface storage, sub-surface/root zone storage, and ground water storages. At the beginning of setting up the model, default values of parameters were included. The parameters were then updated considering size, slope, vegetation, undulation, soil characteristics, human intervention, etc. of catchment.

#### **4.5.2 Hydrodynamic model: HEC-RAS**

A local flood model of the study area has been developed. The model is based on three modules: HEC-HMS, HEC-RAS and HEC-GeoRAS of HEC software package of The Hydrologic Engineering Center, U.S. Army Corps of Engineers. The local flood model basically comprises two components: a Hydrologic Modeling System (HEC-HMS), it contributes local rainfall runoff and lateral inflow to river in the study area and a hydrodynamic model (HEC-RAS) for major river of the study area.

##### **4.5.2.1 Precipitation-Runoff Model**

The rainfall runoff model comprises 2 nos. of sub-catchments having a total area of 1476 sq. km. There are 3 nos. of real time rainfall stations in and around the model area, which have been used. A constant value of evapo-transpiration 4 mm/day is used for round the

year. The parameters of the sub-catchment have been kept similar as that in the Brahmaputra basin model. The sub-catchments of the hydrodynamic Model are shown in Figure 4.9. The sub-catchments of the model could not be calibrated or validated individually due to unavailability of measured discharges at their outlets. However, the model has been calibrated and validated together with the hydrodynamic model for the hydrological event of 2013 and validated for the hydrological event 2014 based on real time data made available from sources and measured under the study.

#### 4.5.2.2 Hydrodynamic Model

The hydrodynamic model of the study areas has been developed along with the mighty Brahmaputra River and Jinjiram River. The total length of river/khals in the model is around 328 km.

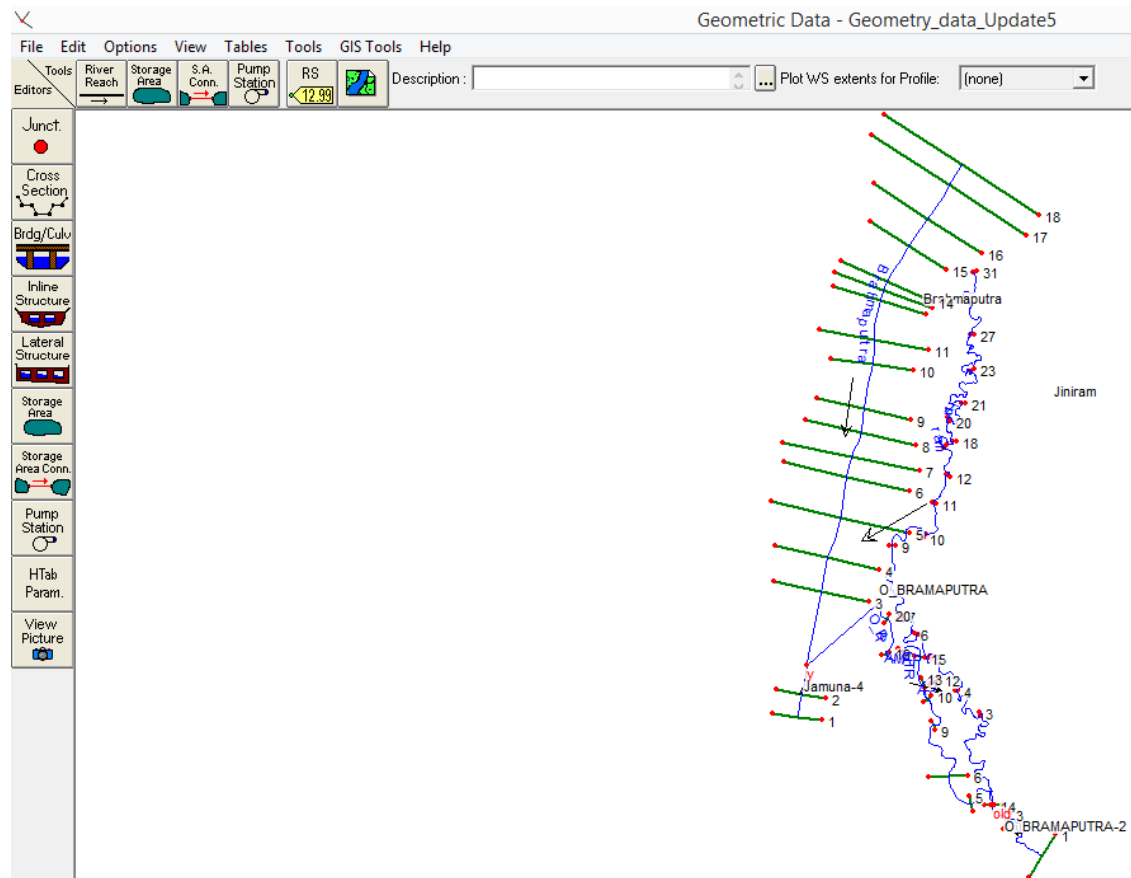


**Figure 4.8** HEC-RAS model schematic description of study area

The model comprises around 45 nos. of cross-sections of the river/khals. There are 6 nos. of open boundaries in the model, where boundary input data are collected from BWDB and IWM and some are generated through simulation of Brahmaputra basin model.

Figure 4.9 shows the schematized rivers/khals in the model. The HEC-RAS Model has been calibrated for hydrological event of 2013 and validated for hydrological event of 2014.

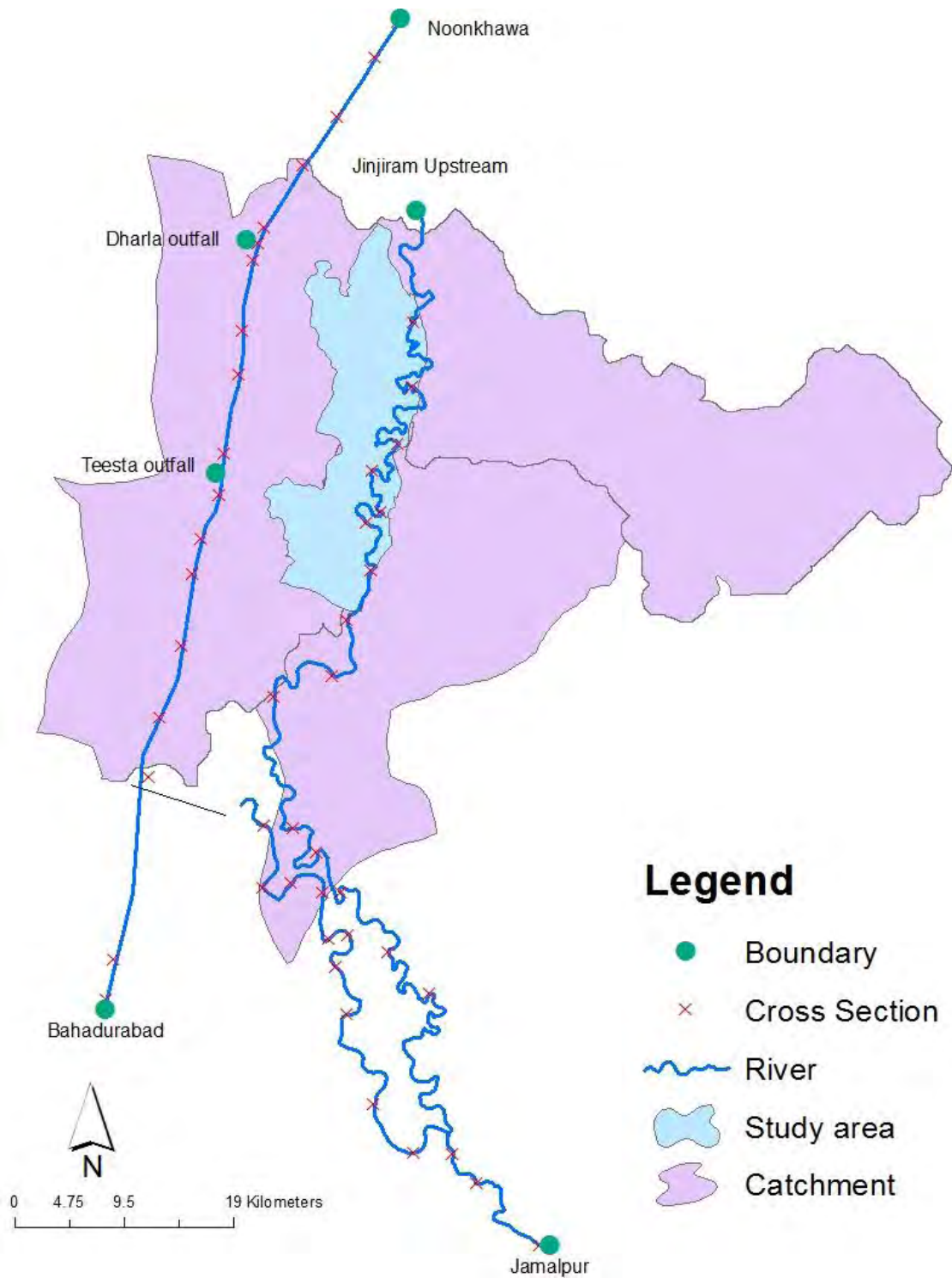


**Figure 4.9** HEC-RAS schematic description of local catchment distribution and boundary of the study area

#### 4.5.2.3 Boundary Condition

To simulate hydrodynamic model, it is necessary to use the following hydrological data at the model boundaries.

- Discharge at the upstream boundary
- Water level at the downstream boundary

There are six peripheral boundaries in the hydrodynamic model (HEC-RAS) of the study area out of which four are inflow boundaries, and the two are outflow boundaries. Catchment runoff has been used as boundary in Jinjiram River upstream boundary. Also catchment runoff has been used in Dharla River and Teesta River inflow discharge as in flow boundary of Brahmaputra river. The channels and corresponding catchment-runoff-boundaries incorporated in the hydrodynamic model have been shown in the figure 4.9.

#### 4.6 WRF Model Simulation

A customized WRF model comprising the Ganges Brahmaputra Meghna (GBM) Basin including the Bay of Bengal is available at IWM.



**Figure 4.10** Extent of WRF model for GBM Basin



The model has been simulated once in everyday during 1<sup>st</sup> June to 15<sup>th</sup> October, 2014 for producing rainfall forecast with lead time of five days for this study. Globally available WRF model has been customized for the GBM basin area extending 406'28.8'' to 46037'4.8'' Latitude and 65013'50'' to 107041'45.6'' Longitude (Figure 4.10). The model is simulated once in every day starting from 00 UTC of the day for next 5 days for generating weather forecast with lead time of 5 days.

#### 4.7 Forecast Methodology

The HEC-RAS Model of the study area generates flood forecast with lead time of five days in the study area at the desired locations or objects. It needs boundary inputs both for real time and forecast period. Two different models: WRF model and Brahmaputra basin (HEC-HMS) model work together to produce boundary inputs of the hydrodynamic model (HEC-RAS). The details of activities for generation of local level flood forecast are described as below, and the sequence of the works done is shown in Flow figure 4.11.

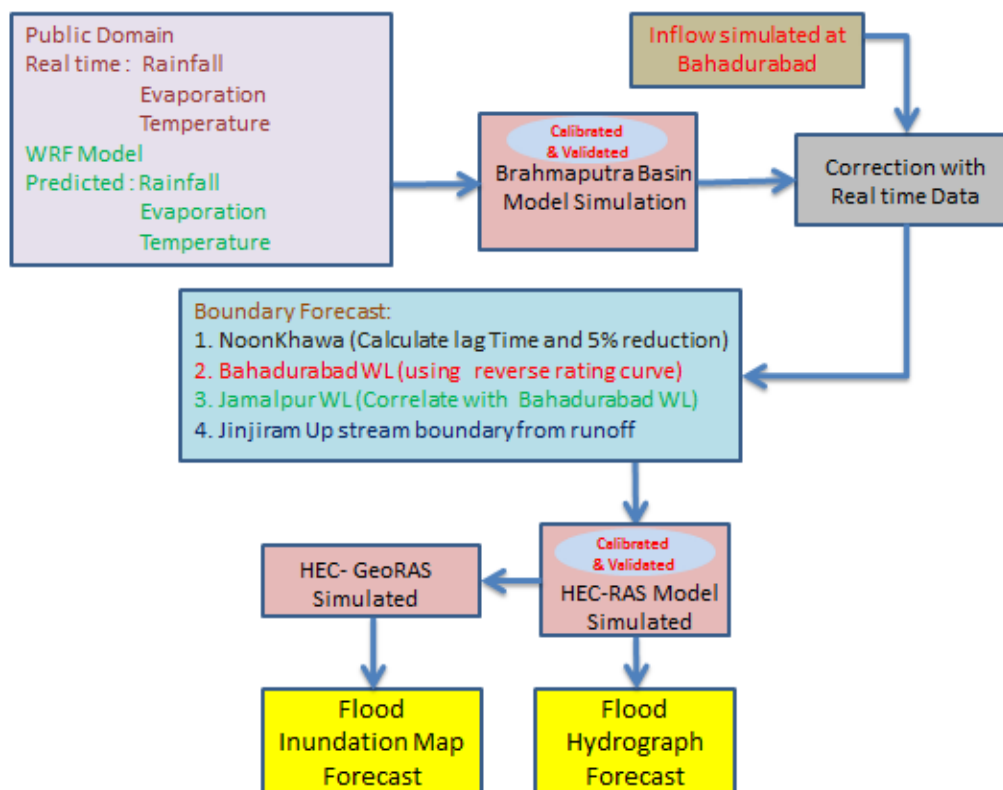


**Figure 4.11** Sequence of activities for flood forecast system in study area

### ***Step-I: Rainfall Prediction***

A WRF model customized for the GBM basin is simulated for producing rainfall prediction with lead time of five days. The WRF itself needs boundary inputs, which is available in the public domain. The Environmental Modeling Center (EMC) of National Centers for Environmental Prediction (NCEP) provides a wide variety of national and international weather guidance products. One of the products of EMC is Weather Prediction (domestic, global out to 15 days). The Global Forecast System GFS model product is updated in every 6 hours, and that updated at 00 UTC with spatial resolution of  $0.5^{\circ} \times 0.5^{\circ}$  is used as boundary input for simulation of WRF model of the GBM basin. The WRF model is recommended to run every day at very early morning (at 04:00 AM of BST). Rainfall prediction for next 5 days could be available at 10:00 AM (Bangladesh Standard Time, BST).

### ***Step-II: Cross border Inflow Forecast***

The Brahmaputra basin model is then simulated of the time period starting from previous 2 years up to the date of forecast using real time rainfall and WRF model computed forecasted rainfall. Thus, the Brahmaputra basin model produces discharge at Bahadurabad forecast with lead time of 5 days (from 06:00 AM of BST to next 120 hours). The model generated inflow forecast is finally corrected applying the disagreement observed between measured and simulated values at the date of forecast.

### ***Step-III: Generate Boundary for HEC-RAS Model***

At this step, Bhadurabad station rating curve (Collected from IWM) has been used to generate forecast water level boundary at Bahadurabad station. Noonkhawa forecast inflow boundary has been generated 12 hours lag and 5% reduction of Bahadurabad forecast inflow that's produced by HEC-HMS. Jamalpur forecast water level has been generated with respect to Bahadurabad to compare both station hydrograph, shown the relation in table 4.5. Other boundary has been generated associate catchment runoff with this river.

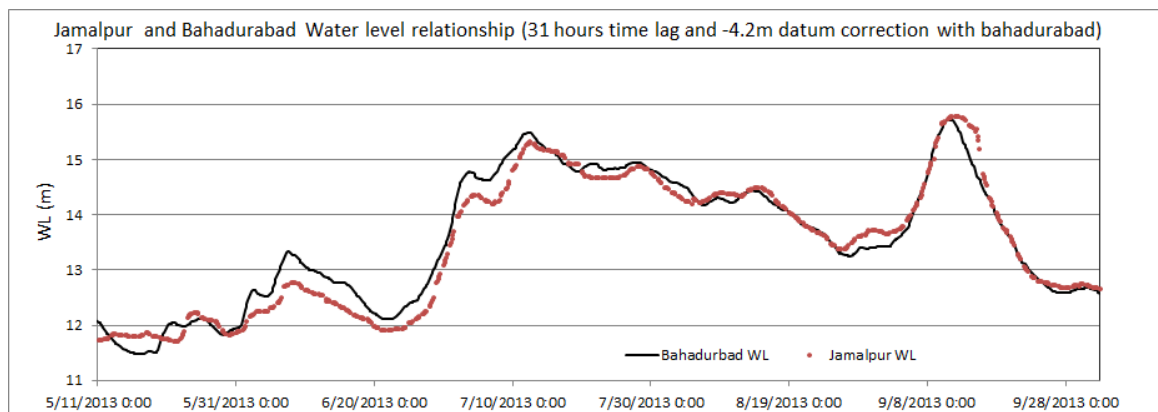
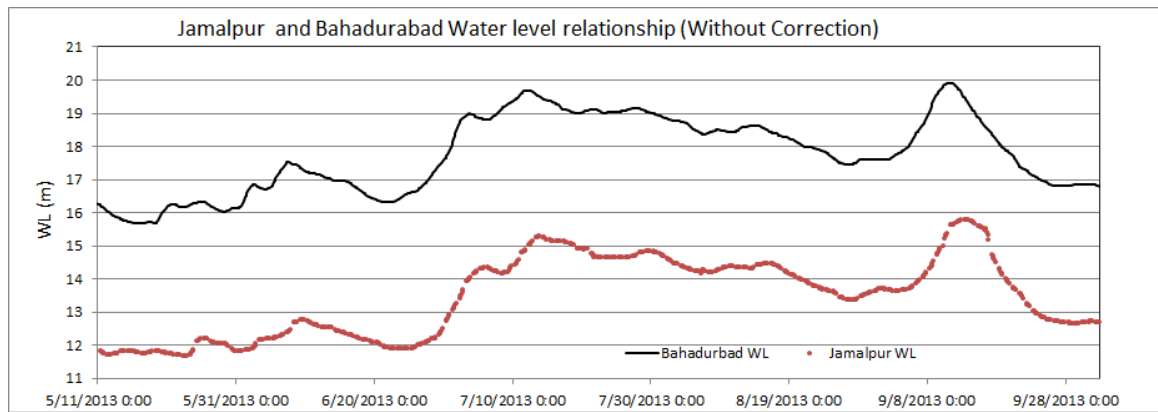


**Figure 4.12** Forecast WL generation at Jamalpur with respect to Bahadurabad

**Table 4.5** Summary of Forecast Boundary generation

Boundary Name	River Name	Expression for Interpolation
		$WL = (Q/25.4)^{1/2.92}$ , when $Q < 17909 \text{ m}^3/\text{s}$
Bahadurabad	Brahmaputra	$WL = (Q/540)^{1/1.992}$ , when $17909 \text{ m}^3/\text{s} \leq Q < 34841 \text{ m}^3/\text{s}$
		$WL = (Q/980)^{1/2.73}$ , when $Q \geq 34841$
Noonkhawa	Old Brahmaputra	$Q = Q_{\text{Bahadurabad}} - 5\% Q_{\text{Bahadurabad}}$ and 12 hours lag
Jamalpur	Old Brahmaputra	$WL = WL_{\text{Bahadurabad}} - 4.2\text{m}$ and 31 hours lag
Dharla Outfall	Brahmaputra	Runoff of Dharla associtae cathment
Tessta Outfall	Brahmaputra	Runoff of Teesta associtae cathment
Jinjiram	Jinjiram	Runoff of Jinjiram associtae cathment



#### Step-IV: Flood Forecast in Study area

The HEC-RAS Model of the study area is also simulated for 12 days as specified earlier using boundary inputs available from observed data. The model produces flood forecast in all significant channels and flood plains in the target areas with 5 days lead time. Flood forecast generated on the channels are then transferred/extrapolated to nearest object/places: Union Parishad Offices, Schools, Madrasa, Mosques, Village Markets, and any other desired places that is identified as crucial to the local community.

#### 4.8 Inundation Mapping

After complete the forecast system, using HEC-GeoRAS extension has used to process the model data for Arc-GIS format. This data has contained water elevation with location coordinate.

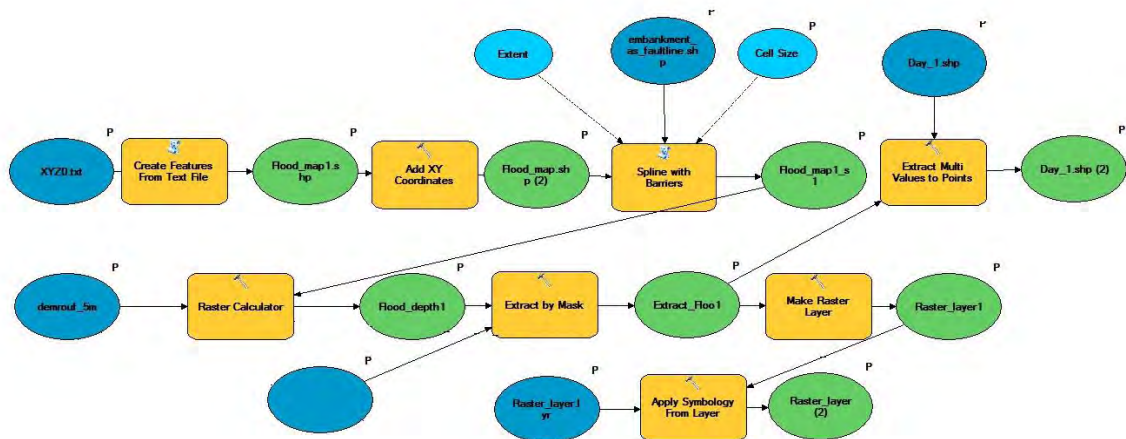


**Figure 4.13** Developed Arc-GIS model builder layout for forecasting inundation mapping.

## CHAPTER 5

### RESULTS AND DISCUSSIONS

#### 5.1 Calibration of HEC-HMS Model

HEC-HMS has the capabilities to process automated calibration in order to minimize a specific objective function, such as sum of the absolute error, sum of the squared error, percent error in peak, and peak-weighted root mean square error. However, in many cases, the resulted automated parameters are not reasonable and practical. In this study, manual calibrated method was adopted to determine a practical range of the parameter values preserving the hydrograph shape, minimum error in peak discharges and volumes. The whole 12 parameters needed for the SMA (Soil Moisture Accounting model) were taken into consideration in this simulation (HEC, 2000). The maximum infiltration rate and the maximum soil depth as well as the percolation rates and groundwater components had significant influence on the simulated flow discharges. The remaining parameters were adjusted to match the simulated and observed peak flows, volumes, time to peaks and hydrograph shape. The 12 parameters needed for the SMA were estimated as shown in Table (5.1).

**Table 5.1** SMA parameters for Brahmaputra Basin simulation

PARAMETER	VALUE
Canopy Storage Capacity	1 mm
Surface Storage Capacity	20 mm
Soil Storage Capacity	400 mm
Soil Tension Storage Capacity	150 mm
Soil Maximum Infiltration Rate	2 mm/hr
Soil Maximum Percolation Rate	0.3 mm/hr
Groundwater 1 Storage Capacity	150 mm
Groundwater 1 Max. Percolation Rate	0.3 mm/hr
Groundwater 1 Storage Coefficient	50 mm
Groundwater 2 Storage Capacity	50 mm
Groundwater 2 Max. Percolation	0.3 mm
Groundwater 2 Storage Coefficient	50 mm

While adjusting parameter values during model calibration, the wet period of the year were weighted more heavily, ensuring that the model would accurately simulate, to some

extent, the high flooding period in each simulated year. The evaporation model used in conjunction with the SMA algorithm takes into account evaporation and transpiration. To model transpiration, the rooting depth was determined to be the maximum depth of the soil profile.

Excess rainfall was transformed to direct runoff using the Clark unit hydrograph technique. In this method, the processes of translation and attenuation of excess rainfall dominate the movement of flow through a watershed. Translation is the movement of flow down gradient through the watershed in response to gravity. Attenuation results from the frictional forces and channel-storage effects that resist the flow, (Straub et al., 2000). The translation of flow throughout the watershed is based on time -area curve, which expresses the curve of the fraction of watershed area contributing runoff to the watershed outlet as a function of time since the start of excess rainfall. The time-area curve is bounded in time by the watershed time of concentration. On the other hand, attenuation of flow can be represented with a simple, linear reservoir for which storage is related to outflow. The two parameters HMS/Clark parameters are the time of concentration and the storage coefficient and are set for the Brahmaputra basin as 150 and 150 hours, respectively(IWM, 2014).

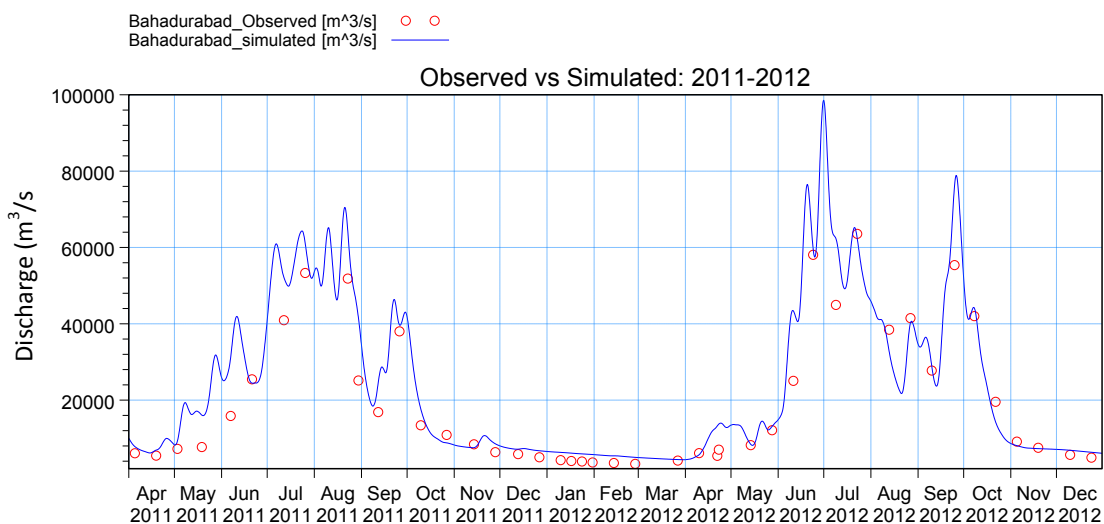


**Figure 5.1** Observed and Simulated discharge at the outlet of the Brahmaputra basin.

The simulated flow discharges as an output of the HMS based on the above-mentioned parameters are compared to the observed ones for the calibration period is shown in figure 5.1 and figure 5.2 illustrates the scatter of the observed and simulated discharges testing the accuracy of the simulated flow discharges.

It can be pointed out that the model produced relatively reasonable results taking into consideration averaged (time invariant) parameters were used for the whole calibrated period 2011-2012 and lumped parameters values for the whole area of the Brahmaputra Basin. From Figure 5.1, it can be noticed out that the model succeeded to produce a relatively similar hydrograph shape. However, the Nash-Sutcliffe coefficient of efficiency (NSE) was used to judge the model performance. The estimated NSE value for the calibration period is 0.85 which may be satisfactory to judge on the similarity and consistency between the observed and simulated hydrograph shape.

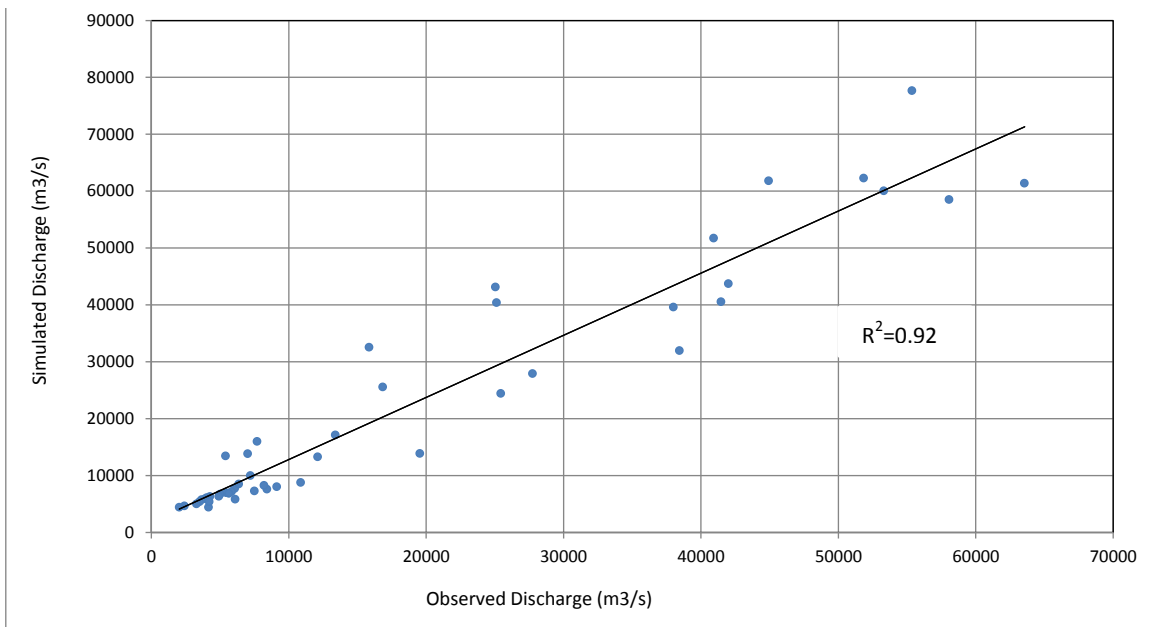


**Figure 5.2** Scatter plots for Observed and simulated data comparison

As depicted from Figure 5.2 it is clear that the model produced slightly over estimated results due to the fact that the periods of high flows were given much consideration and weight during the calibration phase. It should be mentioned that, in the calibration stage, one set of parameters are applied to the whole period which comprised different levels of flooding year cases. Accordingly, the model performance differed from one year to another.

**Table 5.2** Statistical analysis for calibration period at Bahadurabad

STATS PARAMETER	CALIBRATION PERIOD (2011-2012)
Correlation Co-efficient $R^2$	0.92
Nash-Sutcliffe Efficiency Co-eff. (NSE)	0.85
Mean Absolute Error (MAE)	4467.86

## 5.2 Validation of HEC-HMS Model

Model validation demonstrates the capability of the model to produce accurate predictions for periods outside the calibration period, (Refsgaard and Knudsen, 1996). Model validation for this study was used to determine the effectiveness of the calibrated parameters in predicting the flow discharges at Bahadurabad of Brahmaputra River for the period 2013-2014. Figure 5.3 shows the simulated and observed flow discharges for the validation period. Figure 5.4 shows demonstrate the scatter of the observed and simulated discharges for the validation stage. It can be noticed that the simulated discharges values are higher than the observed ones. The estimated NSE value for the validation period is 0.82 which is relatively small value. Similar to the calibration stage, the model produced rather slightly over simulated flows in the case of low flooding year.

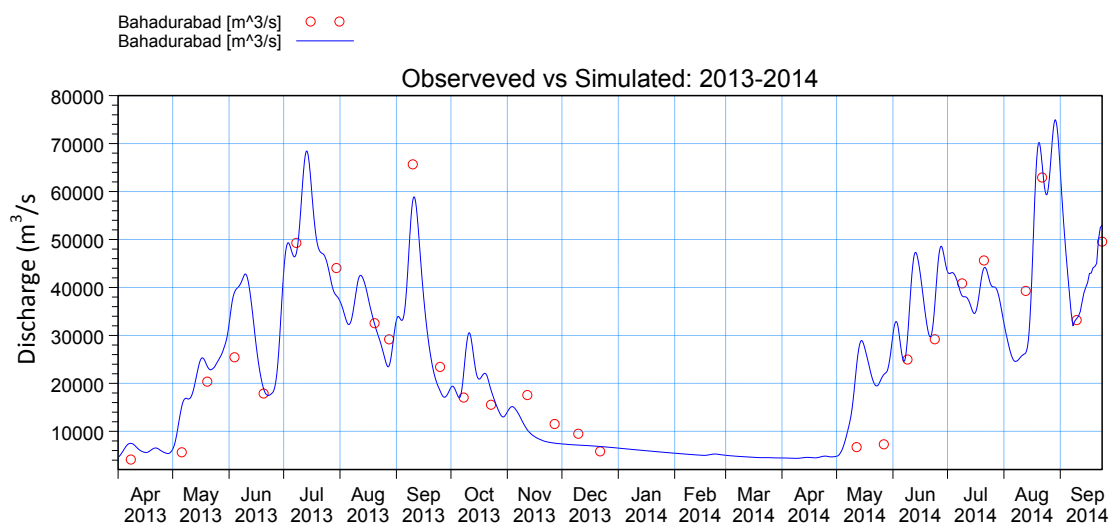


**Figure 5.3** Observed and Simulated discharge at the outlet of the Brahmaputra basin for validation period.

Although, the model produced acceptable results for the low flow period of year 2013, unfortunately, it did not respond well to the considerable high rainfall occurred in the beginning of this year which occurred after dry period, i.e. high rainfall on dry condition.

**Table 5.3** Statistical analysis for Validation period at Bahadurabad

STATS PARAMETER	Validation Period (2013-2014)
Correlation Co-efficient $R^2$	0.83
Nash–Sutcliffe Efficiency Co-eff. (NSE)	0.82
Mean Absolute Error (MAE)	5572.07

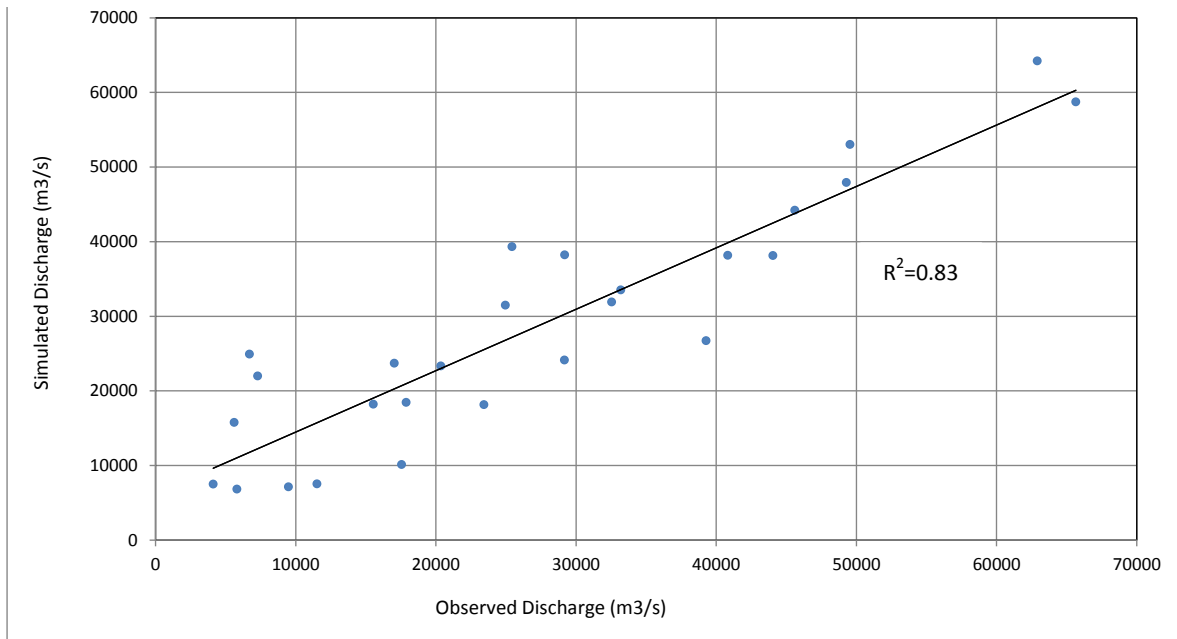


**Figure 5.4** Scatter plots for Observed and simulated data comparison for validation period

This may be ascribed to the effect of the linear structure of the SMA algorithm in simulating the rainfall-runoff process which is a non-linear process. Finally, it may be noted out that seasonality (wet and dry seasons), spatial distribution of rainfall and the expected soil and land cover heterogeneity may be source of errors in the hydrological modeling in a large scale watershed such as Brahmaputra (5, 83,000 sq.km). This may lead to the importance of developing a seasonal parameterization approach where each simulated year is divided into two simulation periods (wet and dry seasons) and accordingly one parameter set is obtained for each period. A Geographic Information System (GIS) based data can also improve the model performance.

### 5.3 Sensitivity Analysis of HEC-HMS Model

Sensitivity analysis is a method to determine which parameters of the model have the greatest impact on the model results. It ranks model parameters based on their contribution to overall error in model predictions. Sensitivity analysis can be local and global (Haan, 2002). In the local sensitivity analysis, the effect of each input parameter is determined separately by keeping other model parameters constant. The result is a set of sensitivity functions, one for each model parameter. In the global sensitivity analysis all

model inputs are allowed to vary over their ranges at the same time. Global sensitivity is based on the use of probabilistic characteristics of the input random variables.

A local sensitivity analysis was adopted for evaluating the parameters of the continuous HEC-HMS model. The final set of the parameters of the calibrated model was considered as a baseline/nominal parameter set. After getting the optimized parameters, their sensitivity is also observed. Among the optimized parameters are Surface Storage Capacity, Initial Surface Storage, Maximum Soil Infiltration Rate and Tension Zone Storage Capacity shows the higher sensitive. The model was run repeatedly with the baseline value for each parameter increased 10%, 20% and 30%, while keeping all other parameters constant at their nominal starting values. For that change, the total volume of runoff observed.

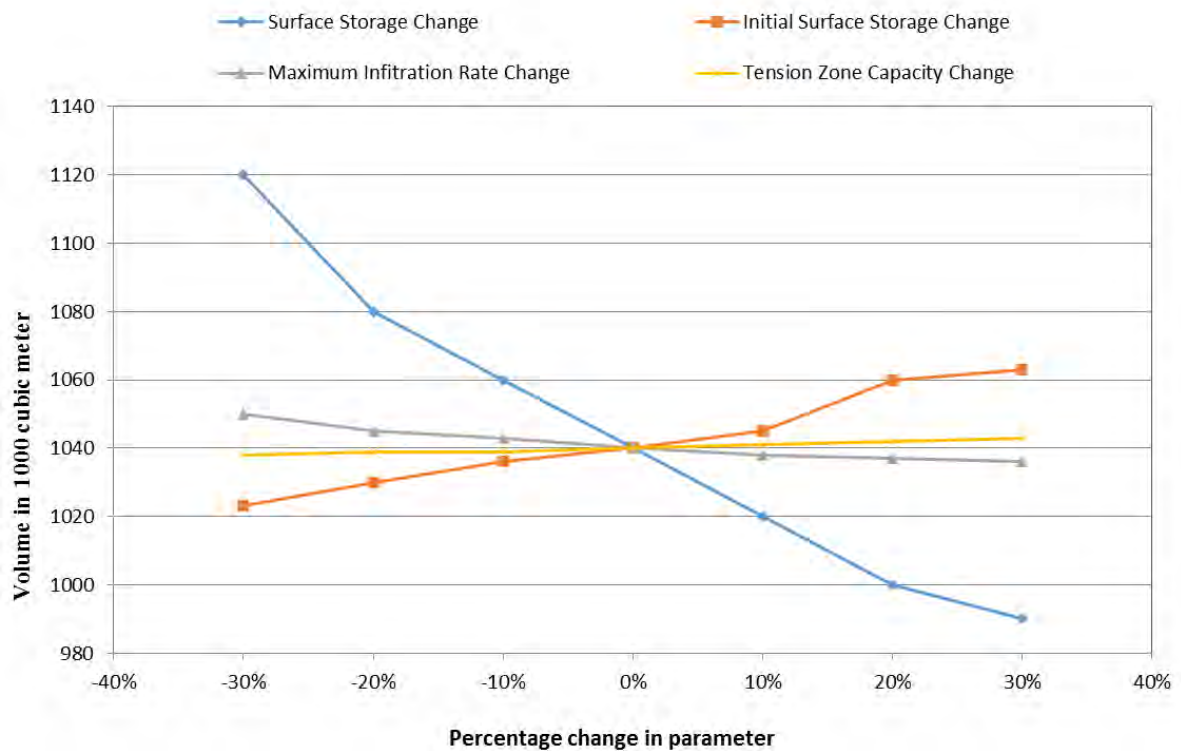


**Figure 5.5** Sensitivity scenarios of the change in the continuous model parameters.

#### 5.4 Calibration of HEC-RAS Model

The Manning's roughness coefficient ( $n$ ) and the coefficient of expansion/contraction ( $k$ ) were set as key HEC-RAS parameters to calibrate. Figure 5.6 shows an example of a sensitivity analysis for calibration of roughness for the Brahmaputra River. It can be observed that simulated water stage converges to the observed water stage with a

systematic selection of the n-value, showing that model calibration of roughness can improve the accuracy of model simulation significantly.

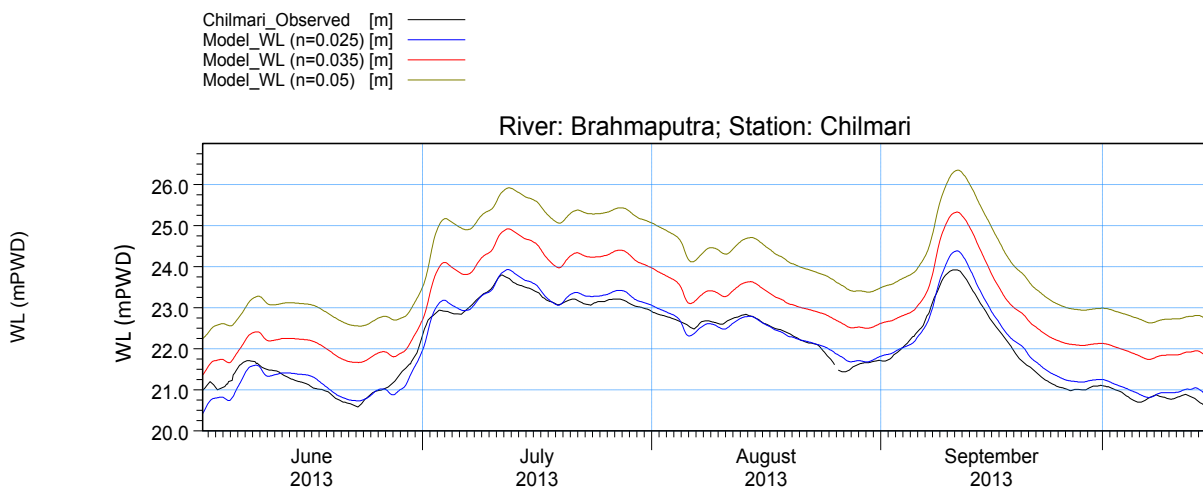


**Figure 5.6** Sensitivity analysis of n-value at Brahmaputra river with respect to observed and simulated water data data.

Based on such sensitivity analysis, calibrated n-values were selected for each schematized river section. Values of 0.10 and 0.30 were kept as universal coefficient of contraction and expansion losses, respectively, for the entire HEC-RAS modeling domain. According to the HEC-RAS Hydraulic Reference Manual these values are very typical for large rivers (Siddique-E-Akbor et al., 2011).

**Table 5.4** Calibrated Manning's n-value for schematized rivers in HEC RAS.

SL	River	n Value		
		Left Bank	Channel	Right Bank
1	Brahmaputra	0.026	0.025	0.026
2	Old_Brahmaputra	0.025	0.025	0.025
3	Jinjiram	0.035	0.035	0.036

The output of the HEC-RAS model is shown against observed water level data in Figure 5.7 at Chilhari and Noonkhawa, where river water level measurement gaged is using ground instrumentation of BWDB for the year 2013. For the Brahmaputra River, the HEC-RAS model simulated water level was in close agreement with the observed data, with slight overestimation of the flood waves. Overall,  $R^2$  and NSE against observed water level data was found to be around 1 (table 5.5).



**Table 5.5** Statistical analysis for calibration period at Noonkhwa and Chilmari station on Brahmaputra River.

STATS PARAMETER	Noonkhawa	Chilmari
Correlation Co-efficient $R^2$	0.93	0.94
Nash–Sutcliffe Efficiency Co-eff. (NSE)	0.96	0.93
Mean Absolute Error (MAE)	0.18	0.21
Mean Square Error (MSE)	1.46	4.14
Root Mean Square Error (RMSE)	1.21	2.04

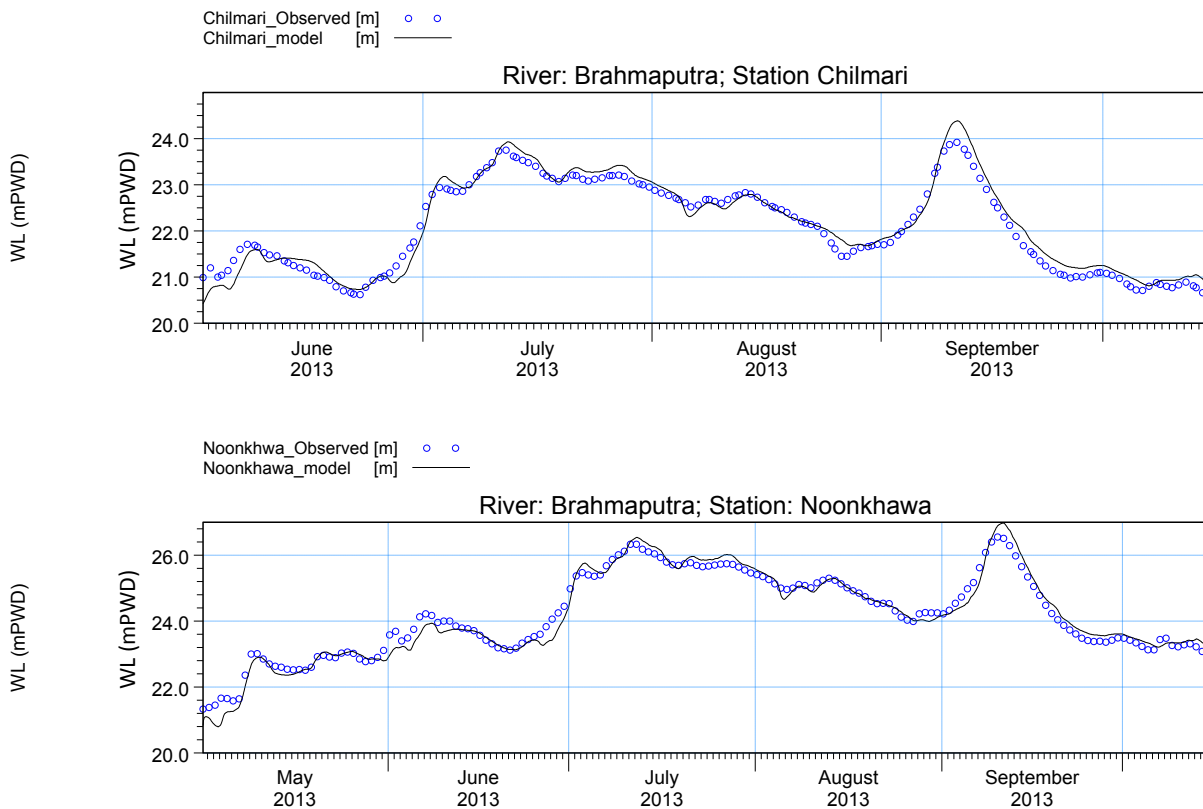


**Figure 5.7** Observed and Simulated WL at Chilmari and Noonkhwa on the Brahmaputra River.

## 5.5 Validation of HEC-RAS Model

Model validation demonstrates the capability of the model to produce accurate predictions for periods outside the calibration period, (Refsgaard and Knudsen, 1996). Model validation for this study was used to determine the effectiveness of the calibrated parameters in predicting the water level at different location of Brahmaputra River and Jinjiram River for the period 2014. Figure 5.8 shows the simulated and observed water level for the validation period. It can be noticed that the simulated water level are higher than the observed ones specifically peak point, HEC-RAS had a tendency to slightly overestimate the peaks (Siddique-E-Akbor et al., 2011). Similar to the calibration stage, the model produced rather slightly over simulated water level in peak stage.

**Table 5.6** Statistical analysis for validation period at different station on Brahmaputra River and Jinjiram River.

STATS PARAMETER	Noonkhawa	Dhonarchar	Chilmari	Lalkura
Correlation Co-efficient $R^2$	0.95	0.97	0.92	0.94
Nash–Sutcliffe Efficiency Co-eff. (NSE)	0.91	0.96	0.88	0.93
Mean Absolute Error (MAE)	0.39	0.15	0.35	0.16
Mean Square Error (MSE)	27.83	0.61	76.15	0.69
Root Mean Square Error (RMSE)	5.28	0.78	8.73	0.83

Also, the HEC-RAS model performance during validation period in terms of statistical analysis (table 5.6) and visually (figure 5, 8) is good.

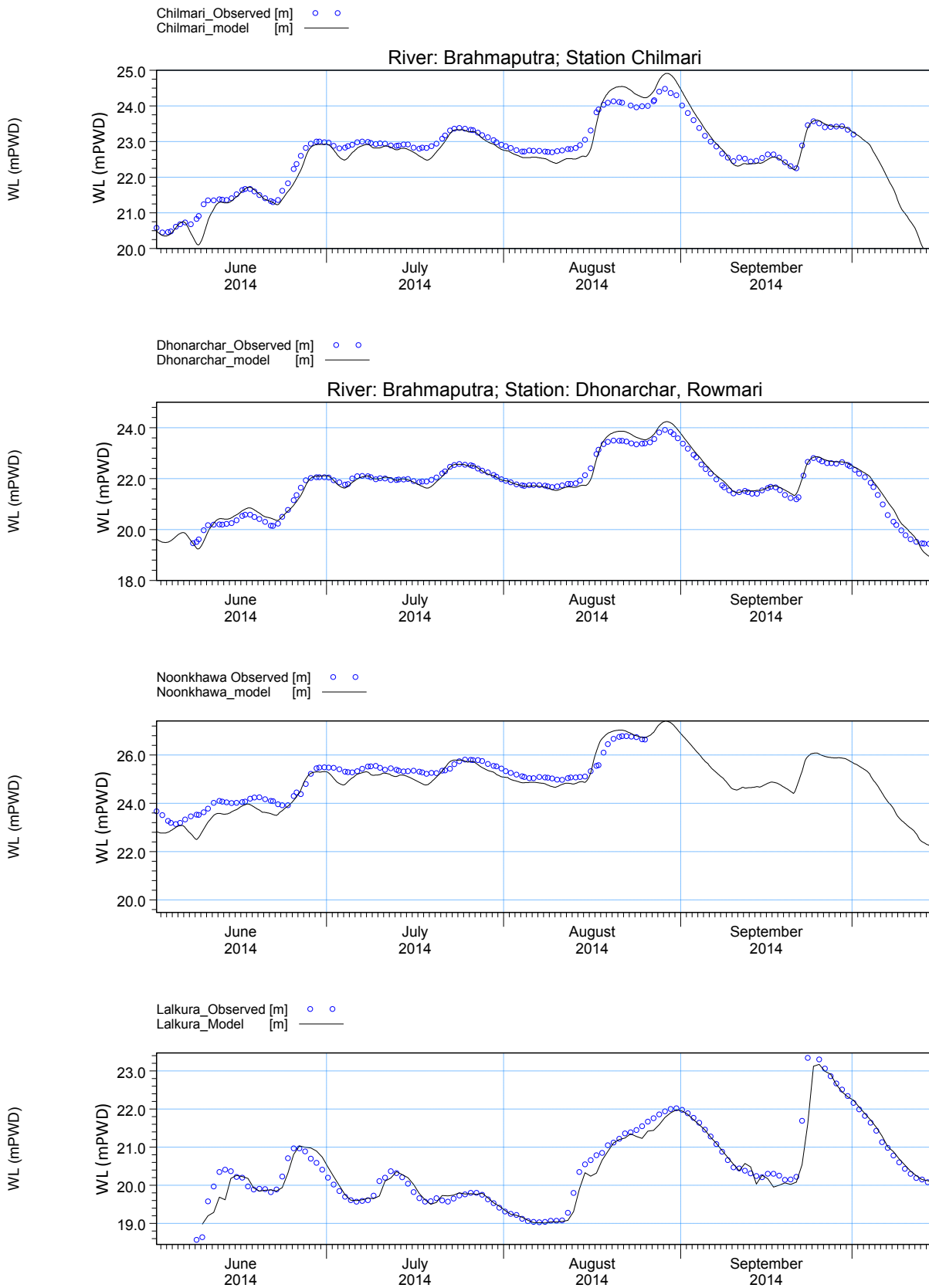


**Figure 5.8** Observed and Simulated WL at Chilmari, Dhonarchar and Noonkhawa on the Brahmaputra River and Lalkura on Jinjiram river.

## 5.6 Flood Forecast System

The HEC-RAS Model generates flood forecast with lead time of five days in the target areas at the desired locations or objects. It needs boundary inputs both for real time and forecast period. Two different models: WRF model and HEC-HMS basin model work together to produce boundary inputs of the HEC-RAS model. The details of activities for generation of flood forecast are described as below, and the sequence of the works done is shown in Flow Figure 5.9.

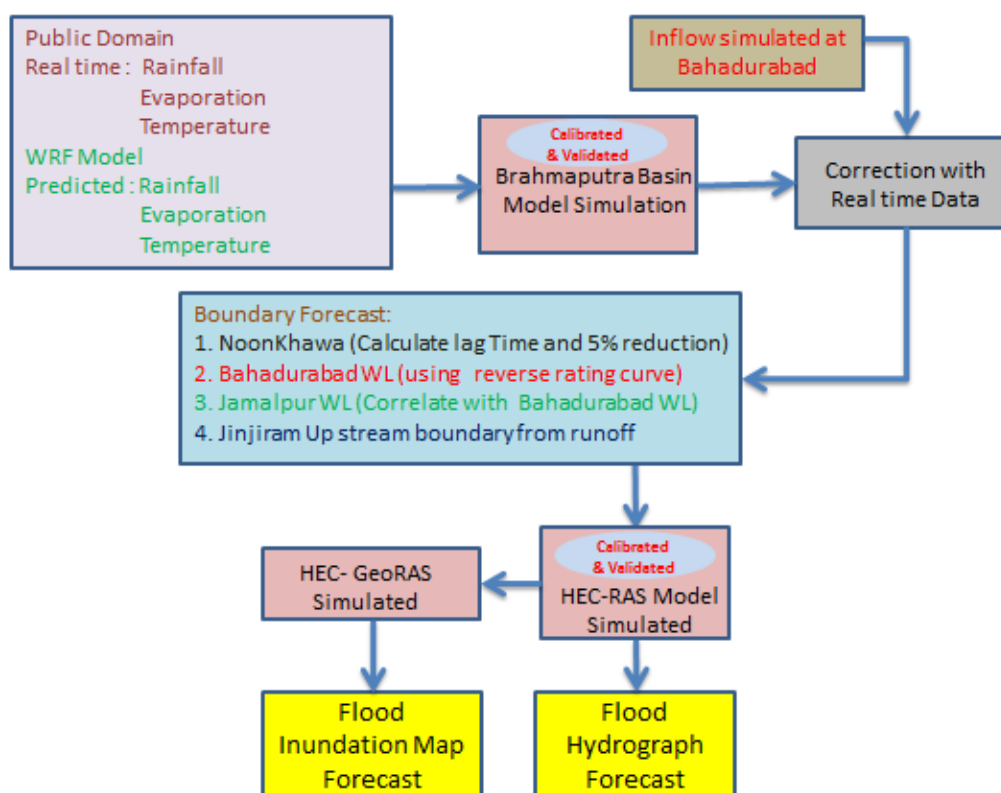


**Figure 5.9** Flood Forecasting System

The WRF model is simulated for producing rainfall prediction for five days on forecast date. The WRF model is run every day at very early morning during 1<sup>st</sup> June to 15 October, 2015 and rainfall prediction for next 5 days. The HEC-RAS Model of is also simulated for 12 days as specified earlier 7 days using boundary inputs available from observed and next 5 days using forecast boundary. The model produces flood forecast in all significant channels and flood plains in the study areas with 5 days lead time. Flood forecast generated on the channels and flood plain are then transferred/extrapolated to nearest object/places using HEC-GeoRAS.

The flood forecast are usually generated in two forms: flood hydrographs at stations and flood inundation maps.

### 5.7 Forecast Hydrograph

Flood forecast in the study area have also been generated by plotting hydrographs at 2 stations, one is Dhanarchar its located Brahmaputra side and other one is Lalkura, its located Jinjiram river side. The forecast hydrographs comprise flood level of 12 days where 7 days before the date of forecast (hind cast) and five days after date of forecast. Some typical flood forecast hydrographs made on 19 September 2014 at Dhonarchar and Lalkura at Rowmari Upazilla are given in following Figures 6.2.

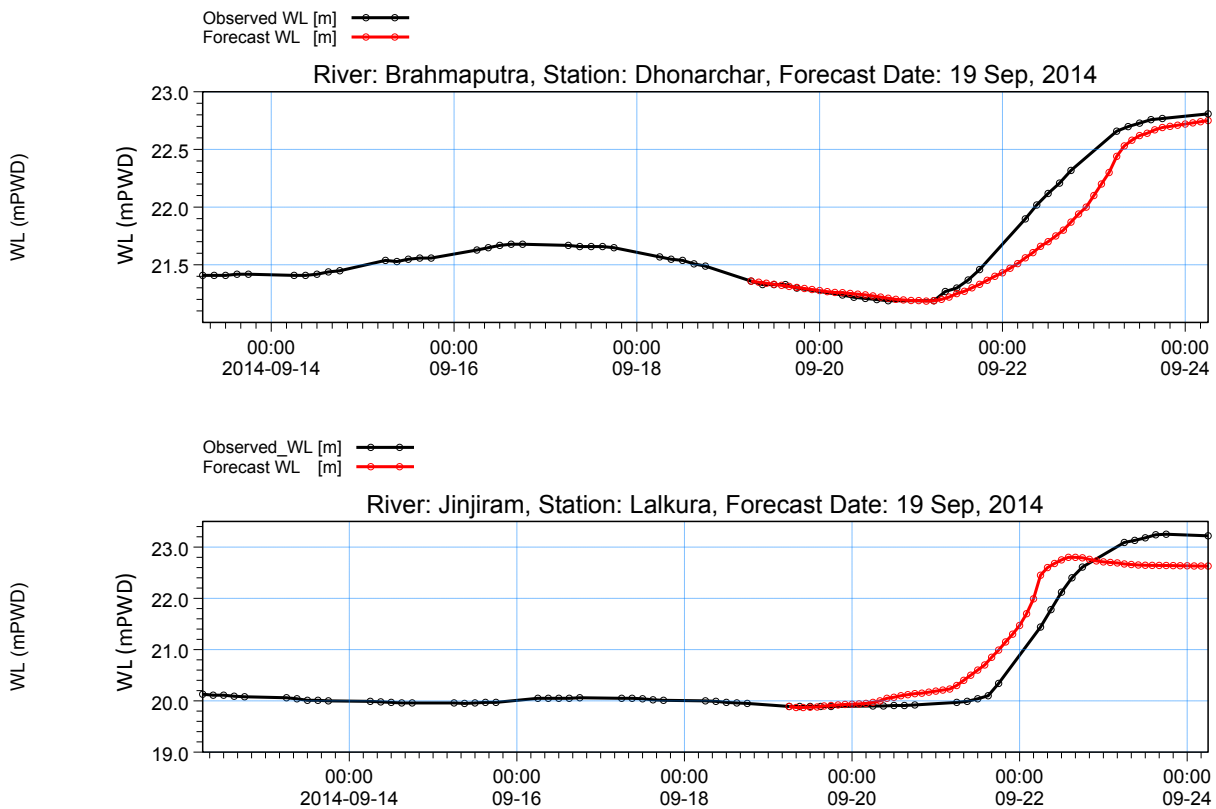


**Figure 5.10** Sample plot of flood forecast as hydrographs, Forecast date: 19 Sep, 2014

## **5.8 Forecast Inundation Map**

Flood inundation map in the study areas have been generated. Six flood inundation maps have been generated for study area comprising flood inundation at the date of forecast and next five forecast days. Flood inundation are classified through gradually varied color with five different range of flood depth: F0 (0-0.30 m), F1 (0.30-0.90 m), F2 (0.90-1.80 m), F3 (1.80-3.60 m), F4 (>3.60 m). Real time and forecasted flood inundation maps prepared on 19 September 2014 study area are given figure 5.11, 5.12, 5.13, 5.14, 5.15, 5.16 as a sample.

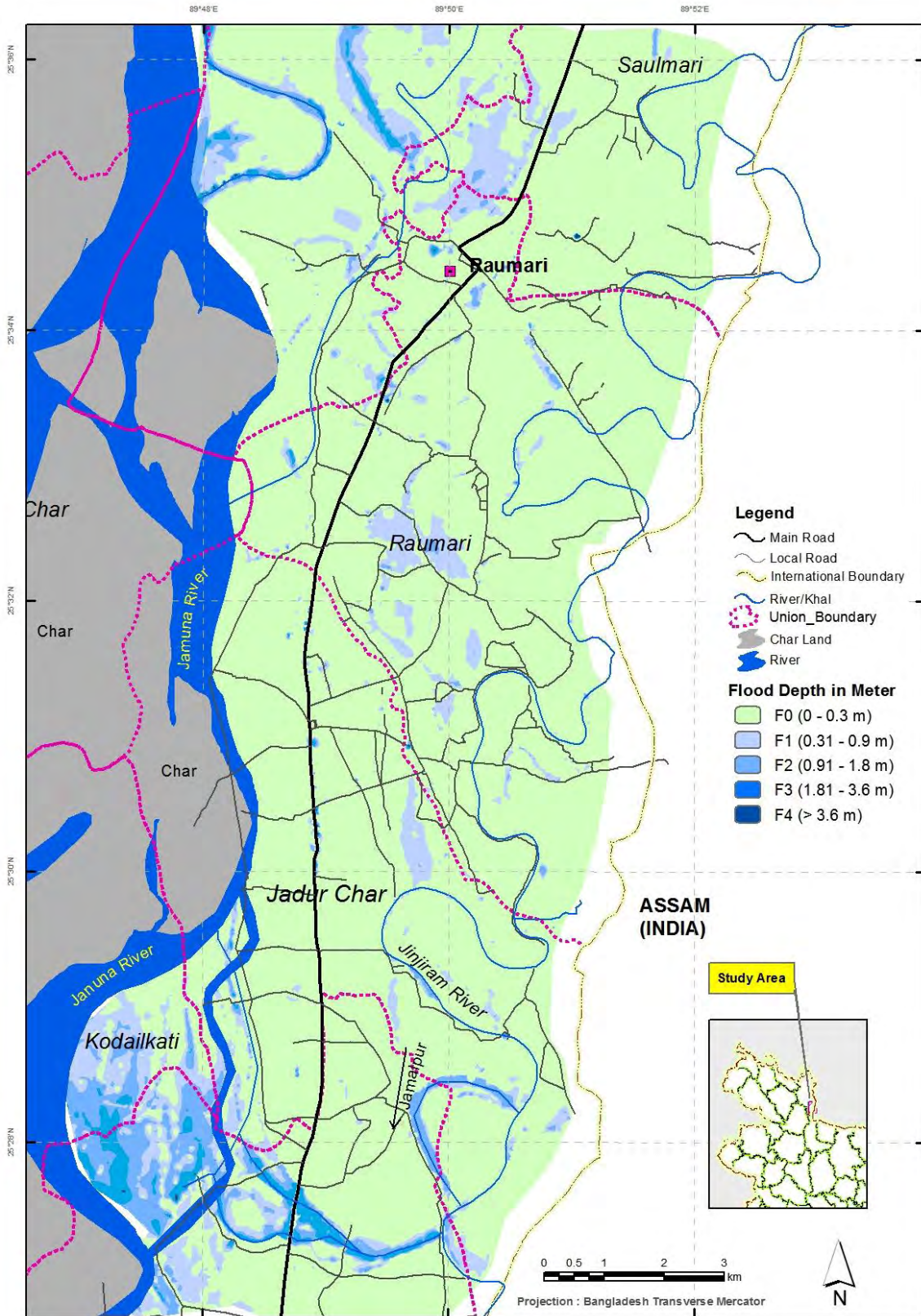


**Figure 5.11** Real time inundation map prepared on 19 September, 2014



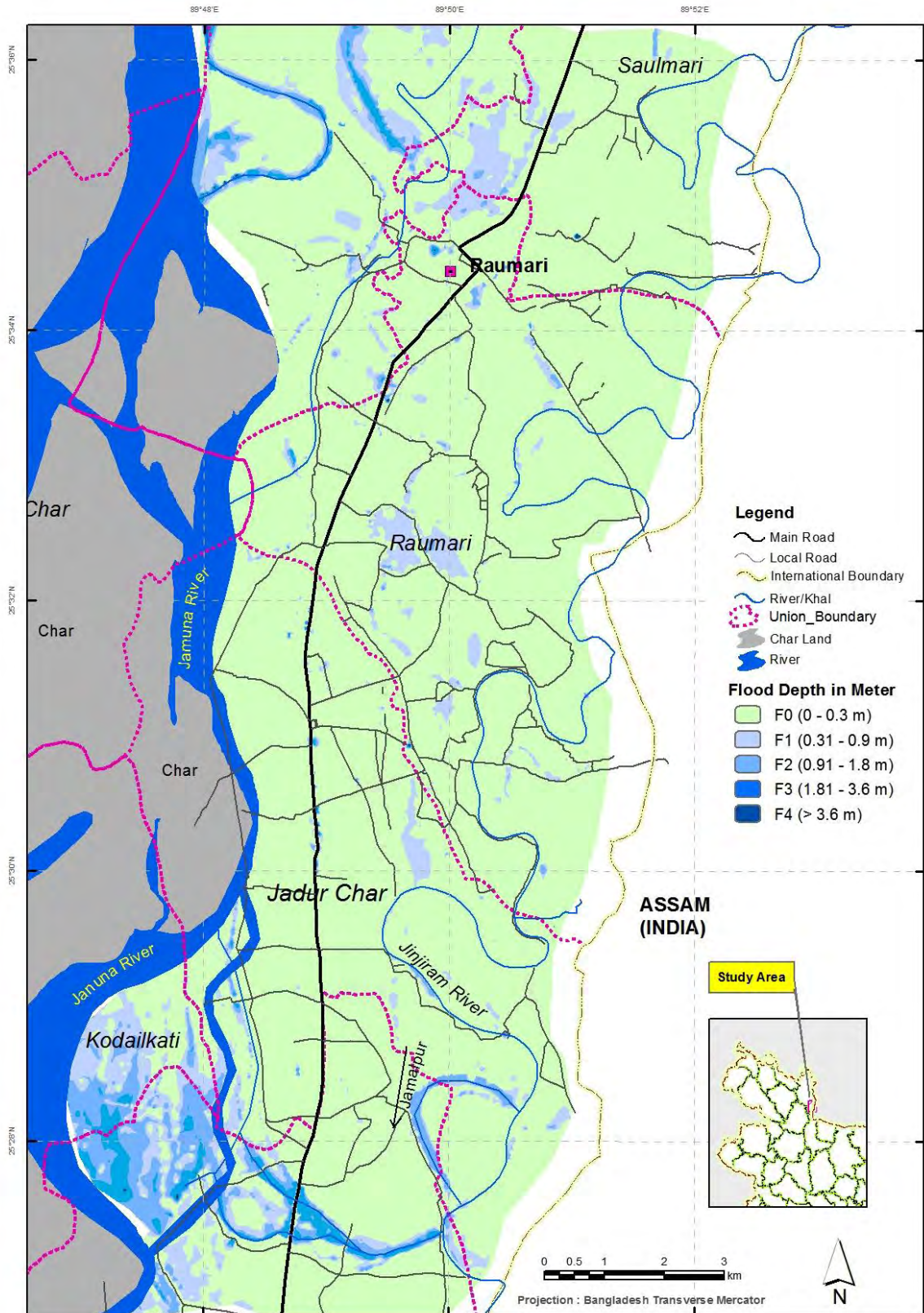


**Figure 5.12** 1<sup>st</sup> day (20 Sep, 2014) forecast inundation map prepared on 19 September, 2014



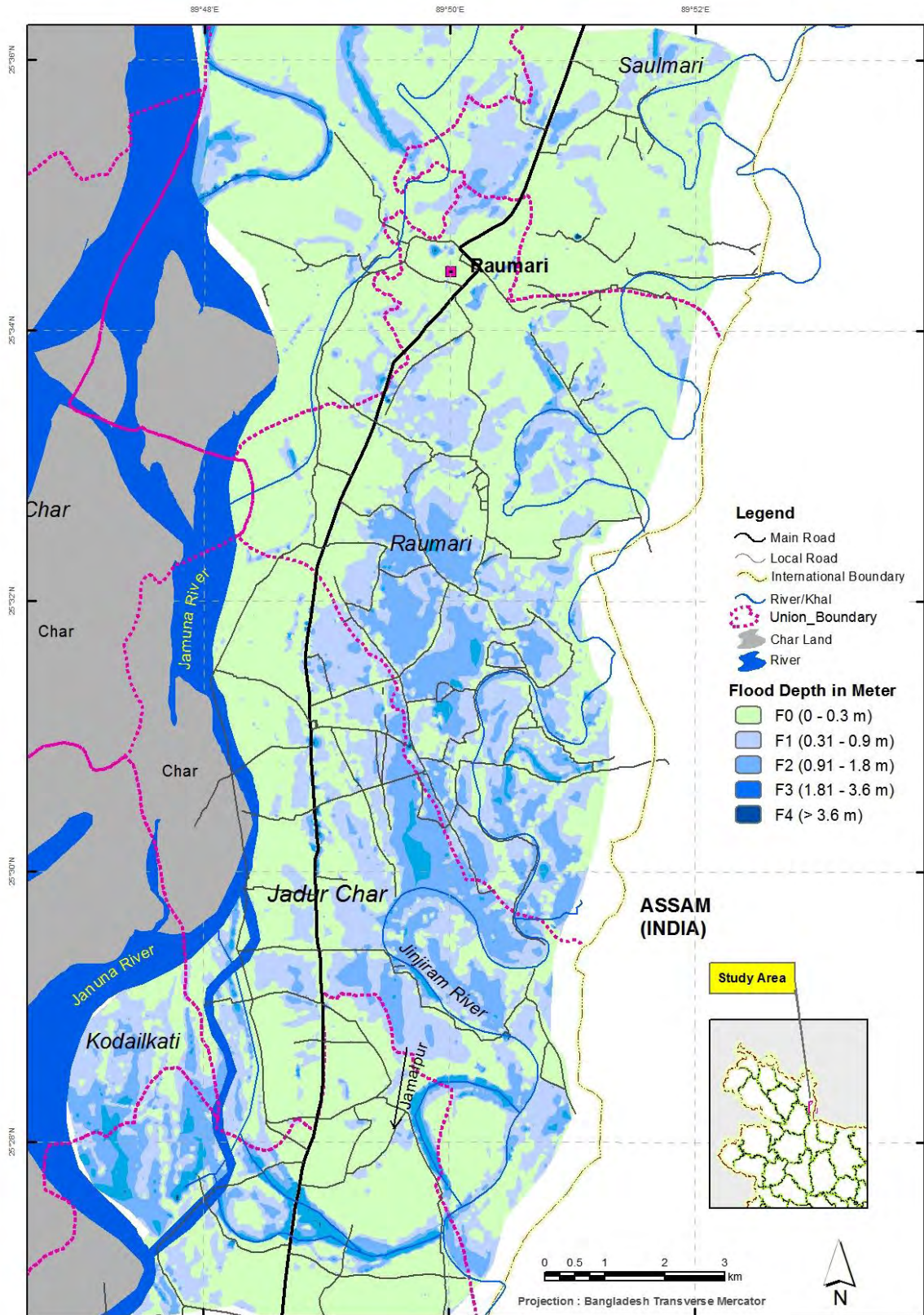


**Figure 5.13** 2<sup>nd</sup> day (21 Sep, 2014) forecast inundation map prepared on 19 September, 2014



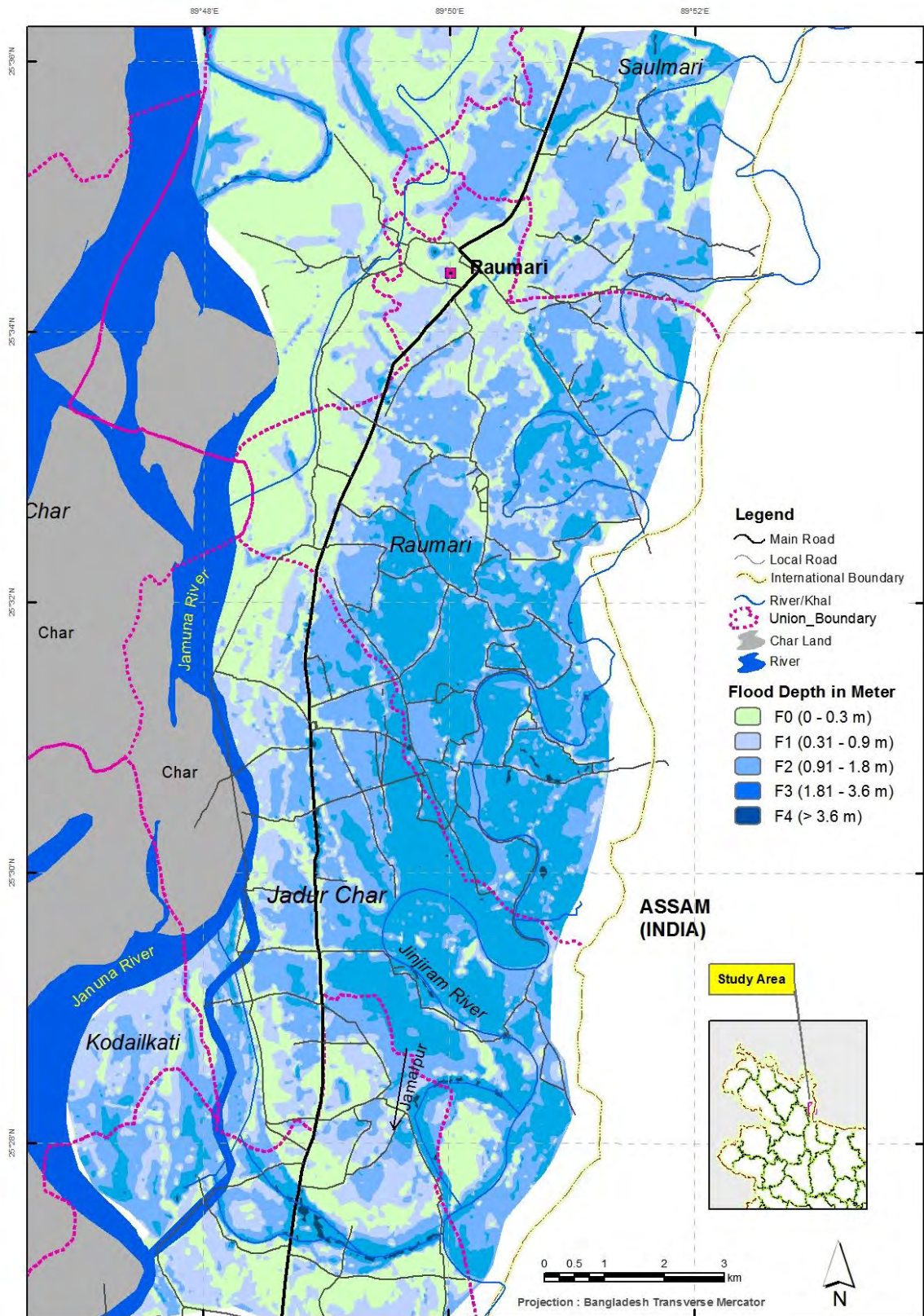


**Figure 5.14** 3<sup>rd</sup> day (22 Sep, 2014) forecast inundation map prepared on 19 September, 2014



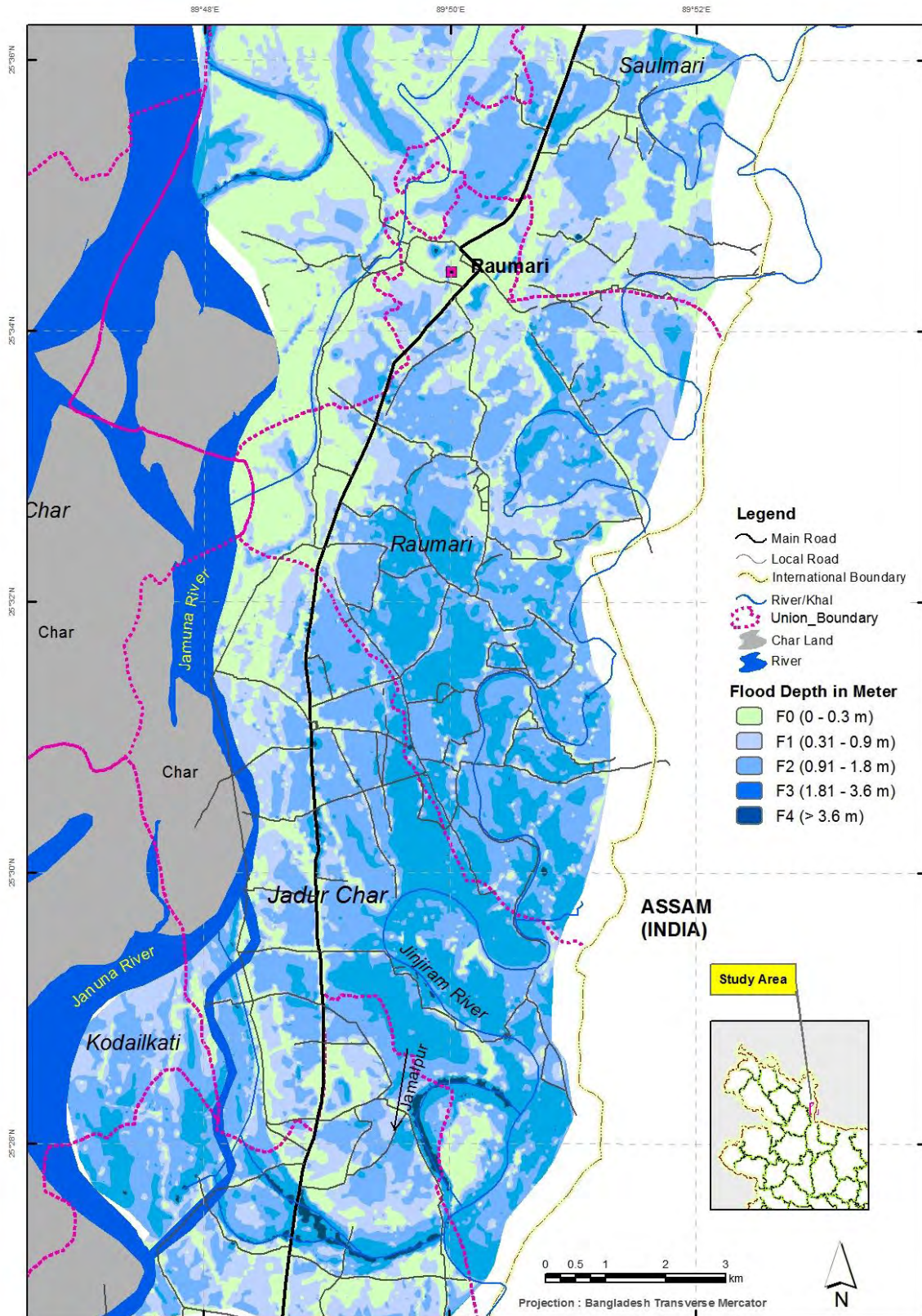


**Figure 5.15** 4<sup>th</sup> day (23 Sep, 2014) forecast inundation map prepared on 19 September, 2014



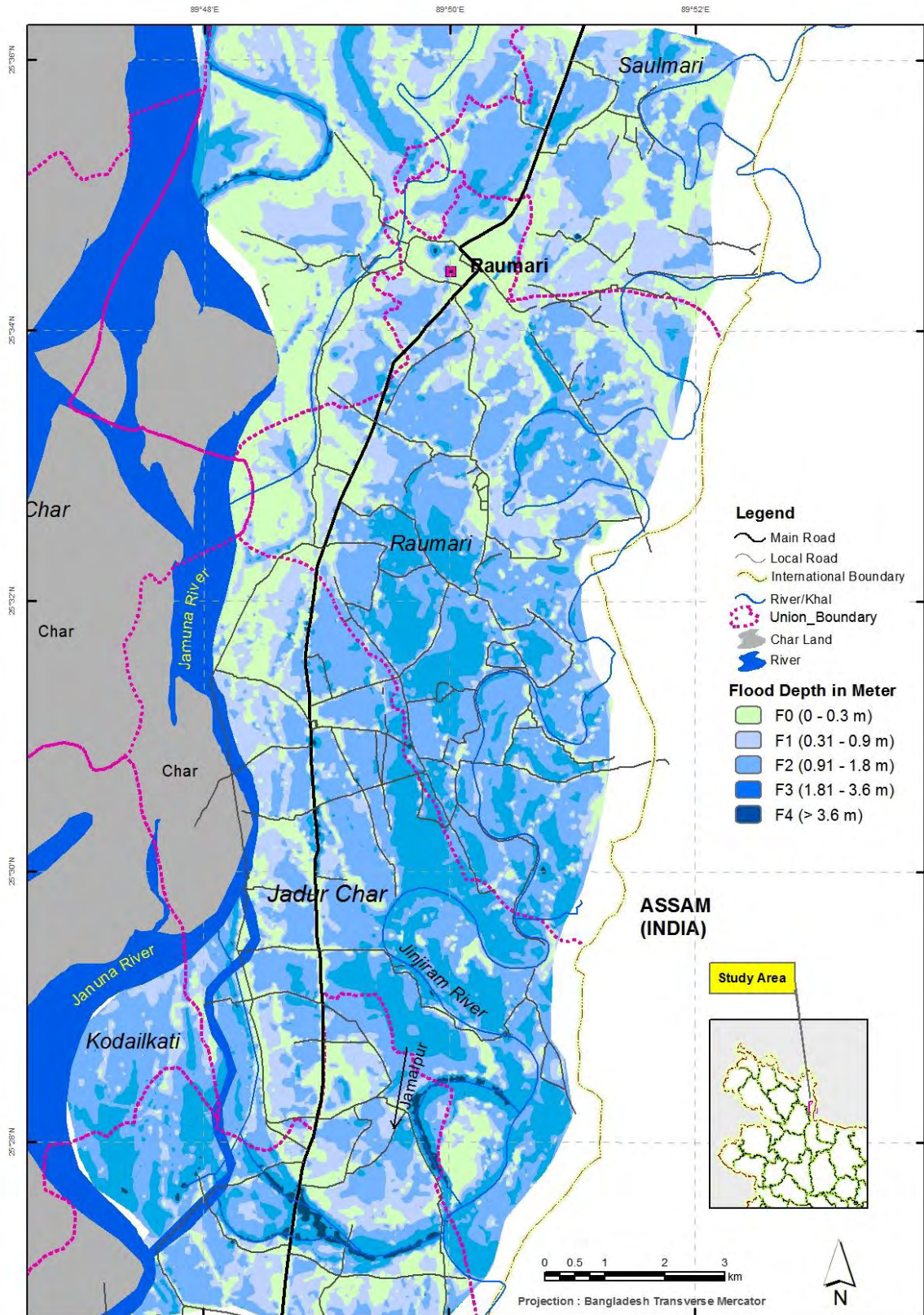


**Figure 5.16** 5<sup>th</sup> day (24 Sep, 2014) forecast inundation map prepared on 19 September, 2014

## 5.9 Forecast Performance

Flood forecast performance at two locations in study area has been assessed through computation of three different statistical parameters: Coefficient of Determination ( $R^2$ ), Mean Absolute Error (MAE) and Nash–Sutcliffe Efficiency Co-eff. (NSE)) observed in the monsoon in 2014. The parameters have been computed by comparing the model forecast against real time measured water levels. The computed parameters are given in Table 5.7. Based on the values of parameters, the performance of the model has been classified as defined by following five levels of scales (FFWC, 2013).

**Table 5.6** Model forecast performance based on statistical parameter

Sl. No.	Scale	Value
1	Good	MAE $\leq$ 0.15 meter & $r^2 \geq 0.9$
2	Average	MAE $\leq$ 0.2 meter & $>0.15$ meter and $r^2 \geq 0.7$ & $<0.9$
3	Not satisfactory	MAE $\leq$ 0.3 meter & $>0.2$ meter and $r^2 \geq 0.4$ & $<0.7$
4	Poor	MAE $\leq$ 0.4 meter & $>0.3$ meter and $r^2 \geq 0.3$ & $<0.4$
5	Very Poor	MAE $>$ 0.4 meter or $r^2 < 0.3$

Source: FFWC, 2013

5 days performance hydrograph and scatter plot are given in the figure 5.17 to 5.26 and the values of parameters observed in between forecast water level and observed water level are given in Table 5.7 in Dhonarchar station (Brahmaputra side) at Rowmari

**Table 5.7** Statistical analysis for five days forecast flood water level at Dhonarchar, Rowmari

STATS PARAMETER	1-Day	2-Day	3-Day	4-Day	5-Day
Correlation Co-efficient $R^2$	0.99	0.95	0.90	0.81	0.72
Nash–Sutcliffe Efficiency Co-eff. (NSE)	0.99	0.95	0.89	0.78	0.62
Mean Absolute Error (MAE)	0.07	0.17	0.25	0.35	0.46
Mean Square Error (MSE)	0.02	0.36	1.62	6.18	18.59
Root Mean Square Error (RMSE)	0.13	0.60	1.27	2.49	4.31
Performance	Good	Good	Good	Below Average	Poor

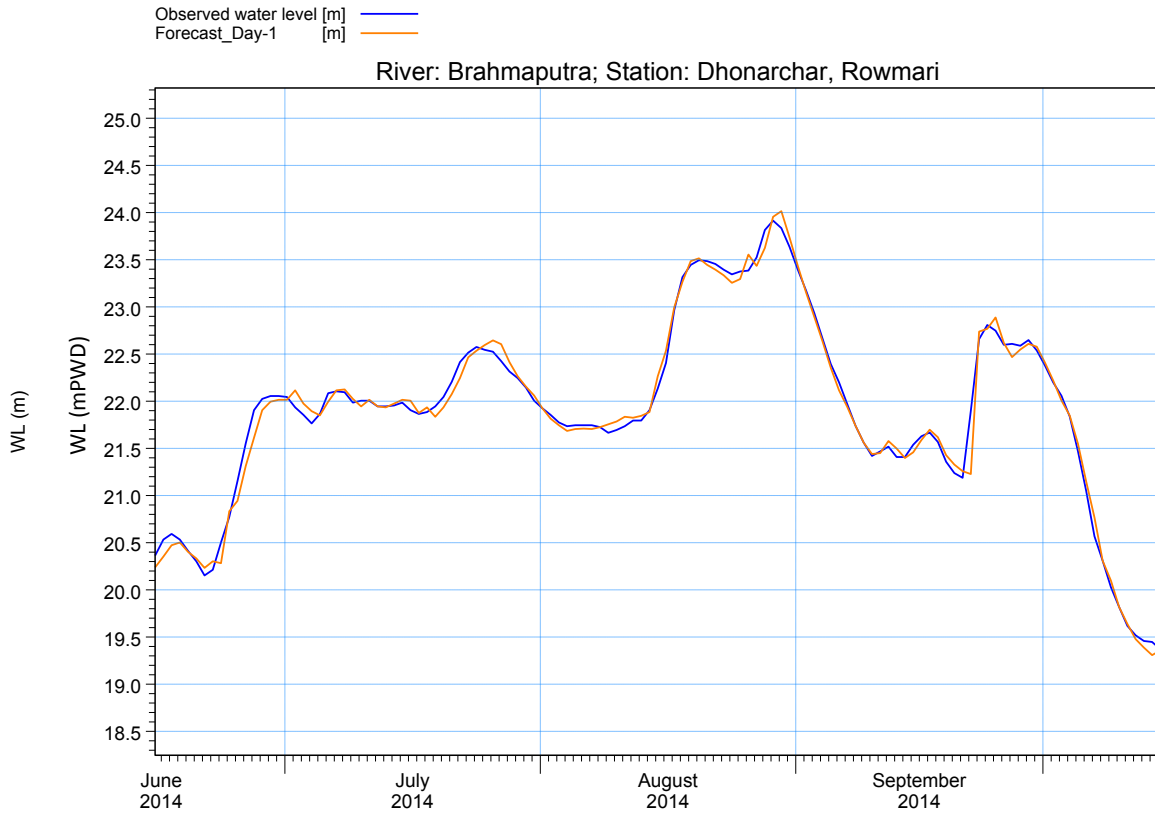


Figure 5.17 1<sup>st</sup> day forecast water level and observed WL comparison at Dhonarchar

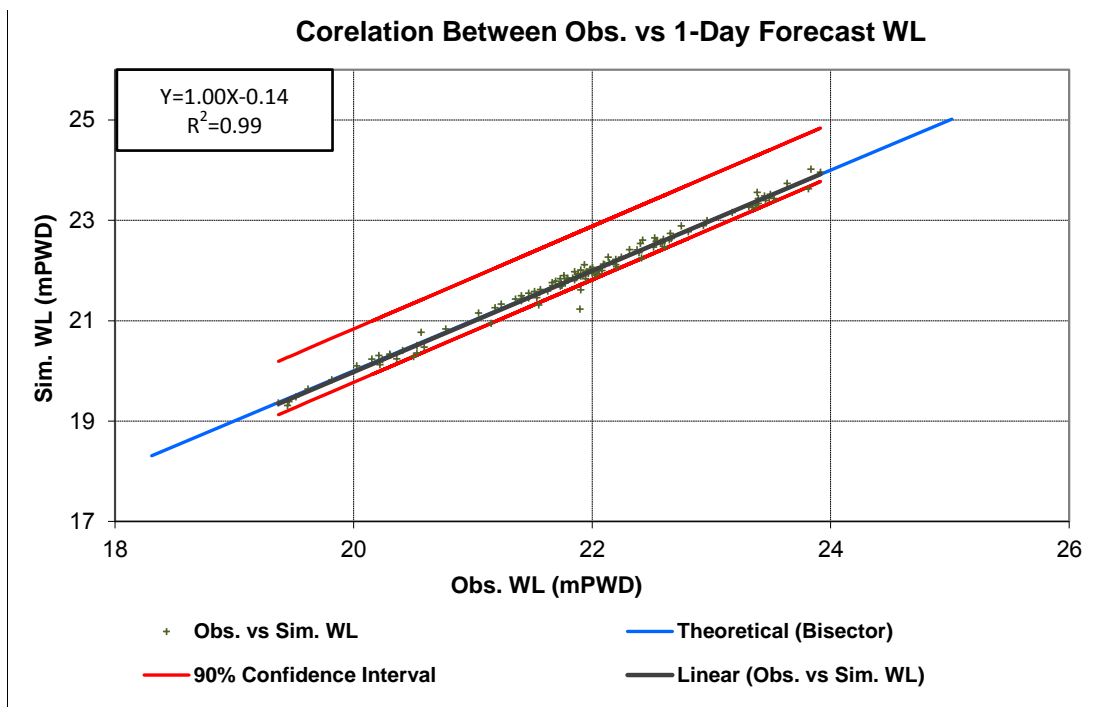


Figure 5.18 Scatter plots for 1<sup>st</sup> day forecast WL and observed comparison at Dhonarchar

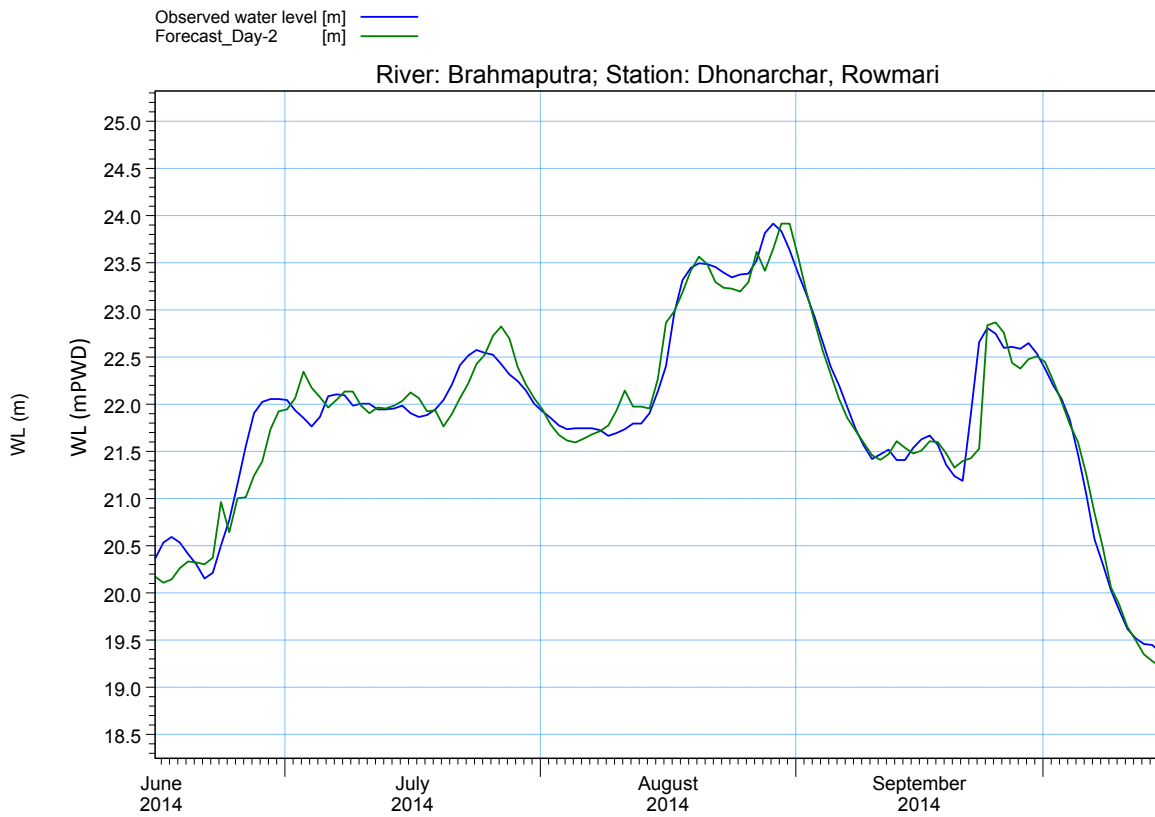


Figure 5.19 2<sup>nd</sup> day forecast water level and observed WL comparison at Dhonarchar

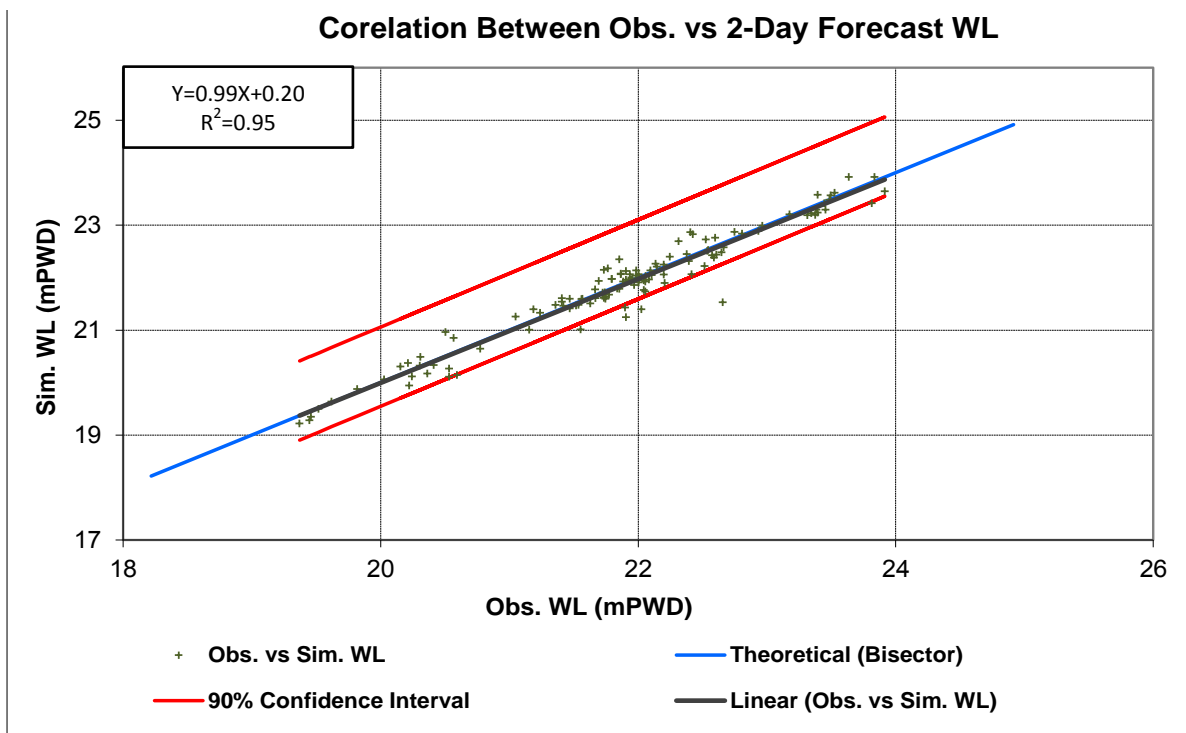


Figure 5.20 Scatter plots for 2<sup>nd</sup> day forecast WL and observed comparison at Dhonarchar

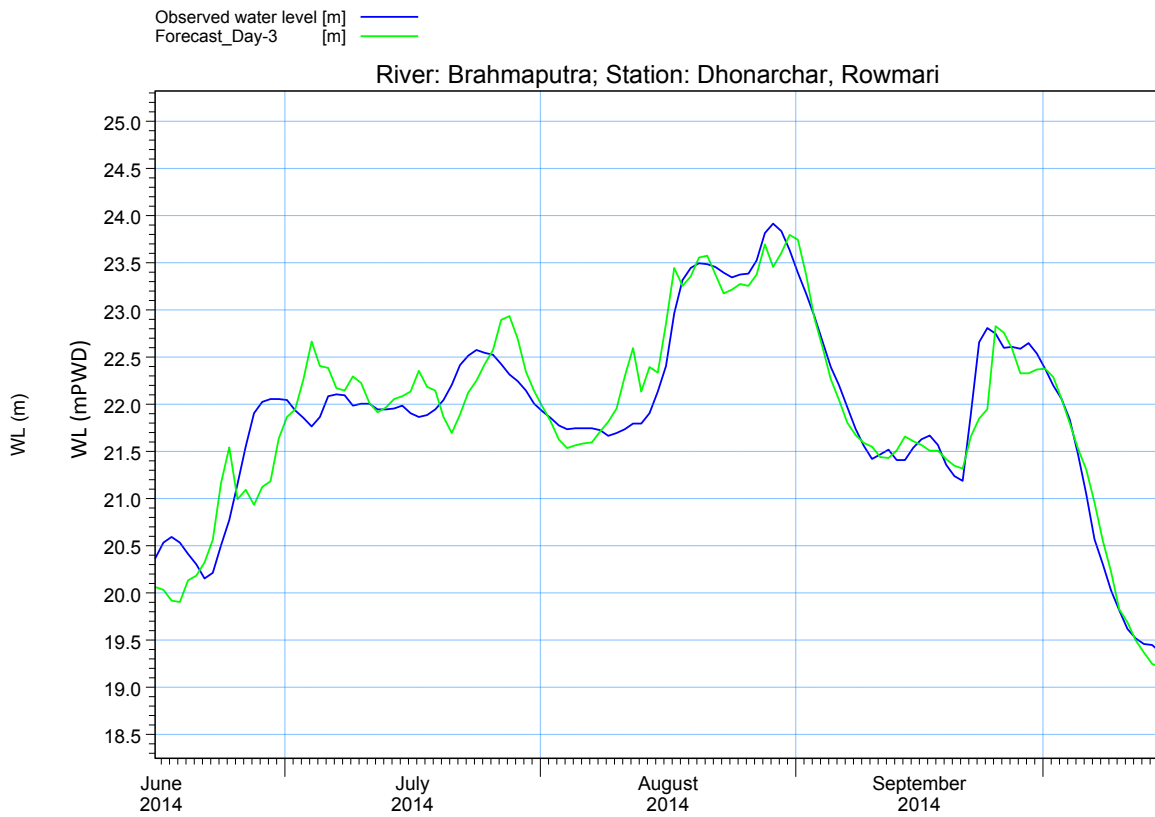


Figure 5.21 3<sup>rd</sup> day forecast water level and observed WL comparison at Dhonarchar

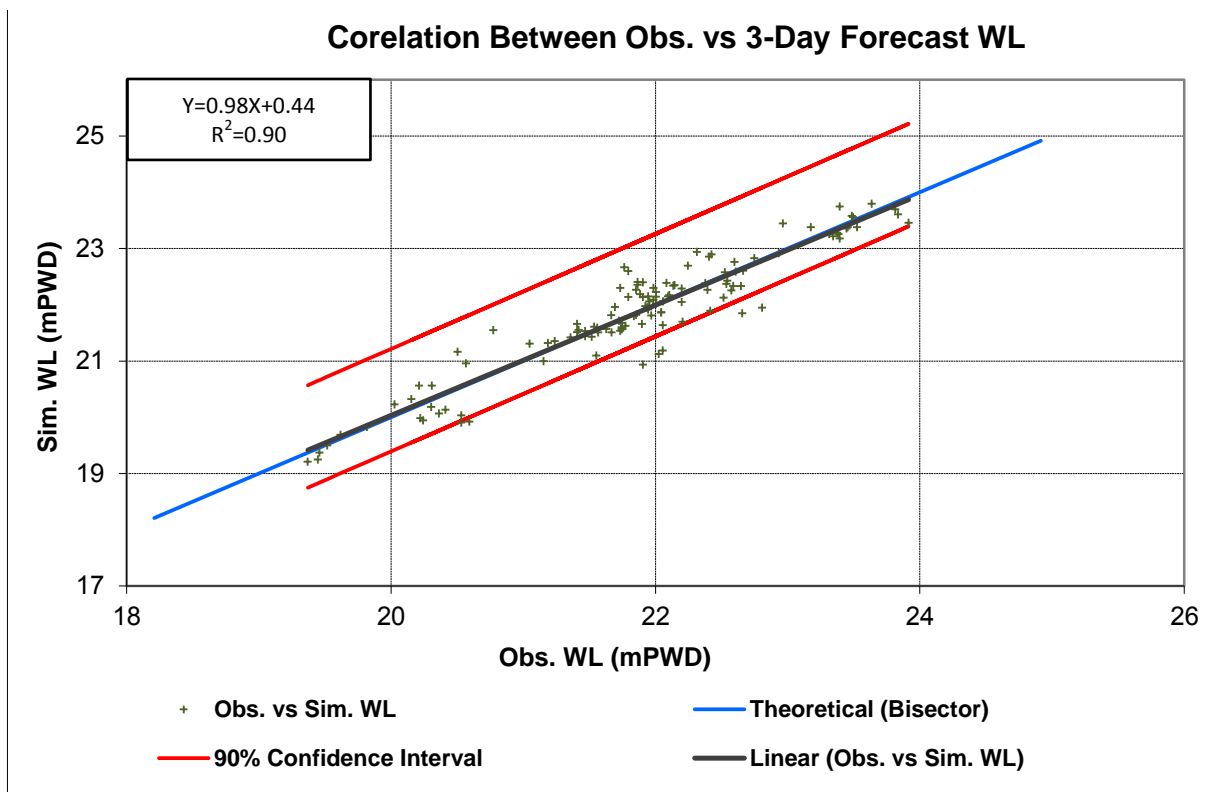


Figure 5.22 Scatter plots for 3<sup>rd</sup> day forecast WL and observed comparison at Dhonarchar



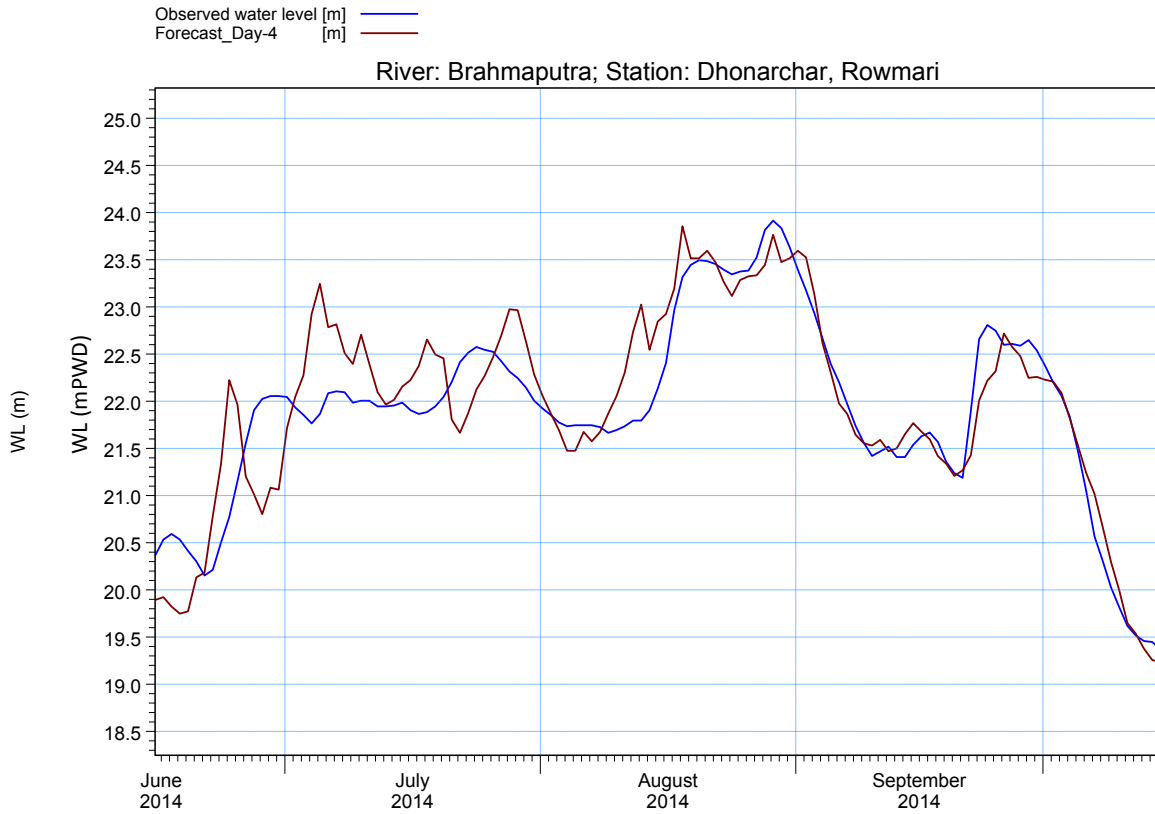


Figure 5.23 4<sup>th</sup> day forecast water level and observed WL comparison at Dhonarchar

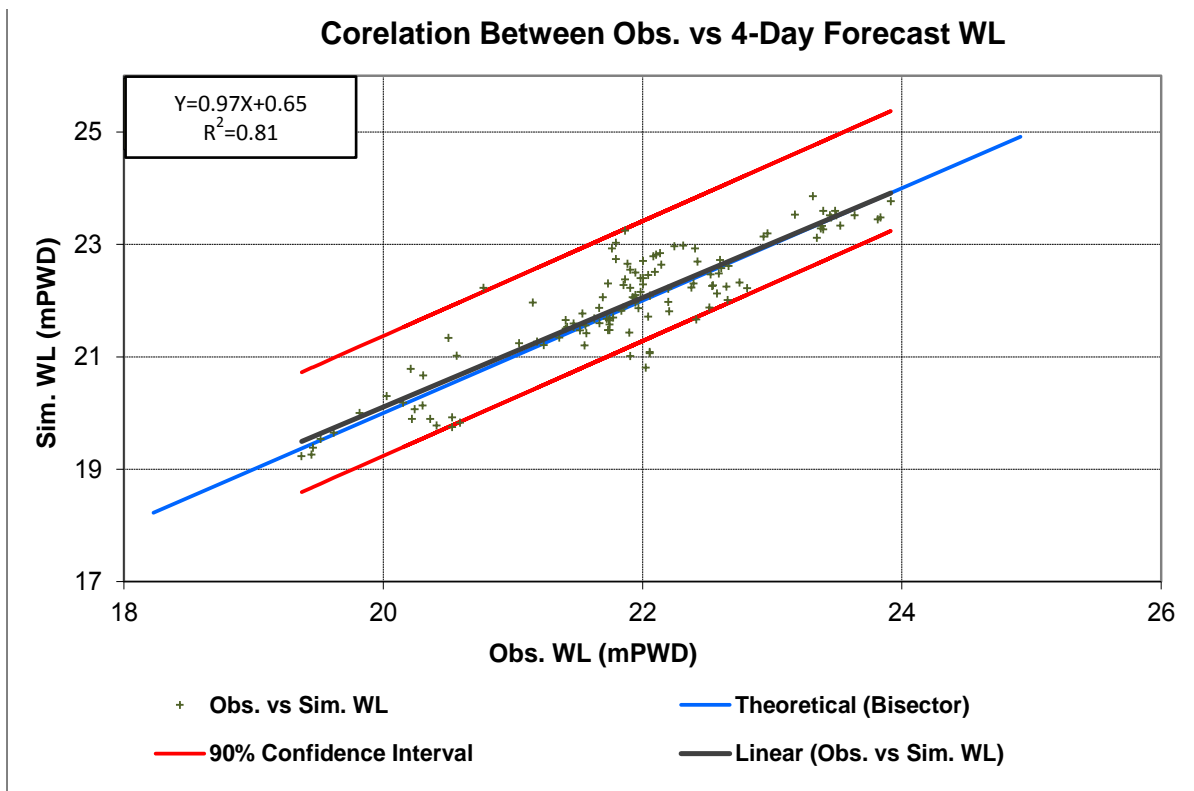


Figure 5.24 Scatter plots for 4<sup>th</sup> day forecast WL and observed comparison at Dhonarchar

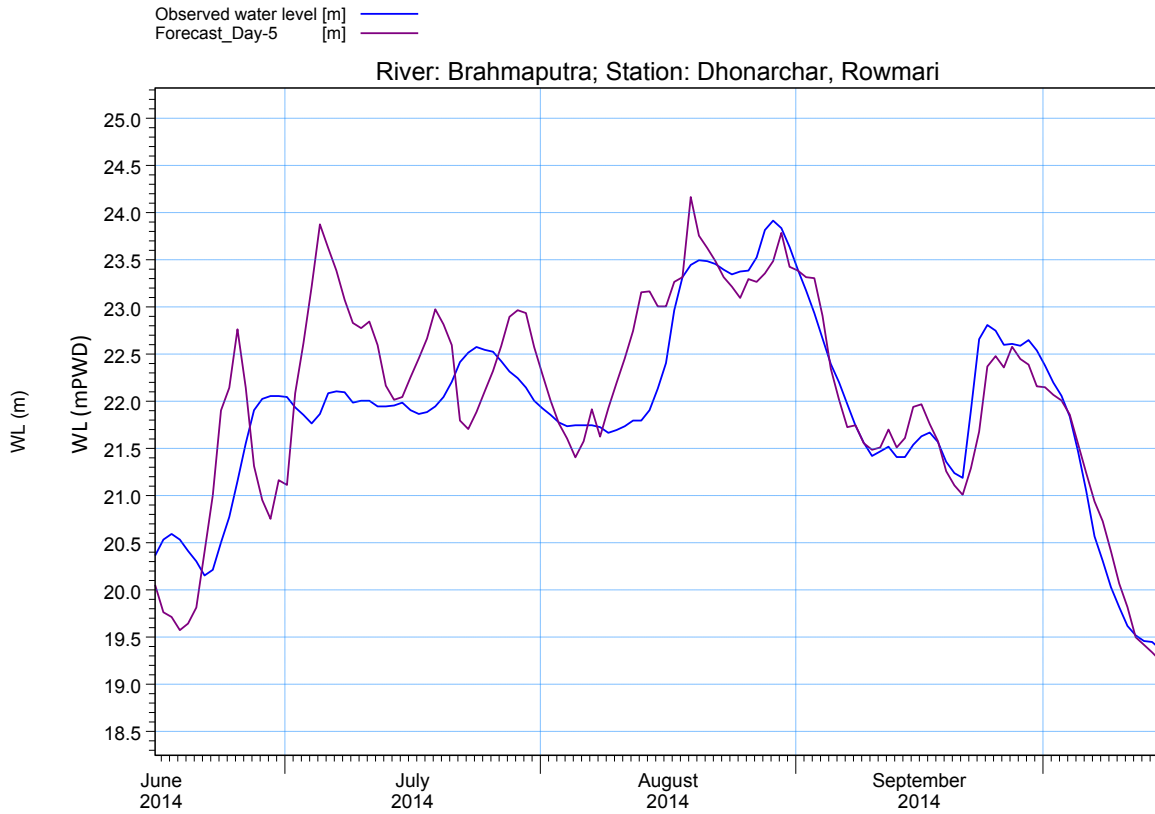


Figure 5.25 5<sup>th</sup> day forecast water level and observed WL comparison at Dhonarchar

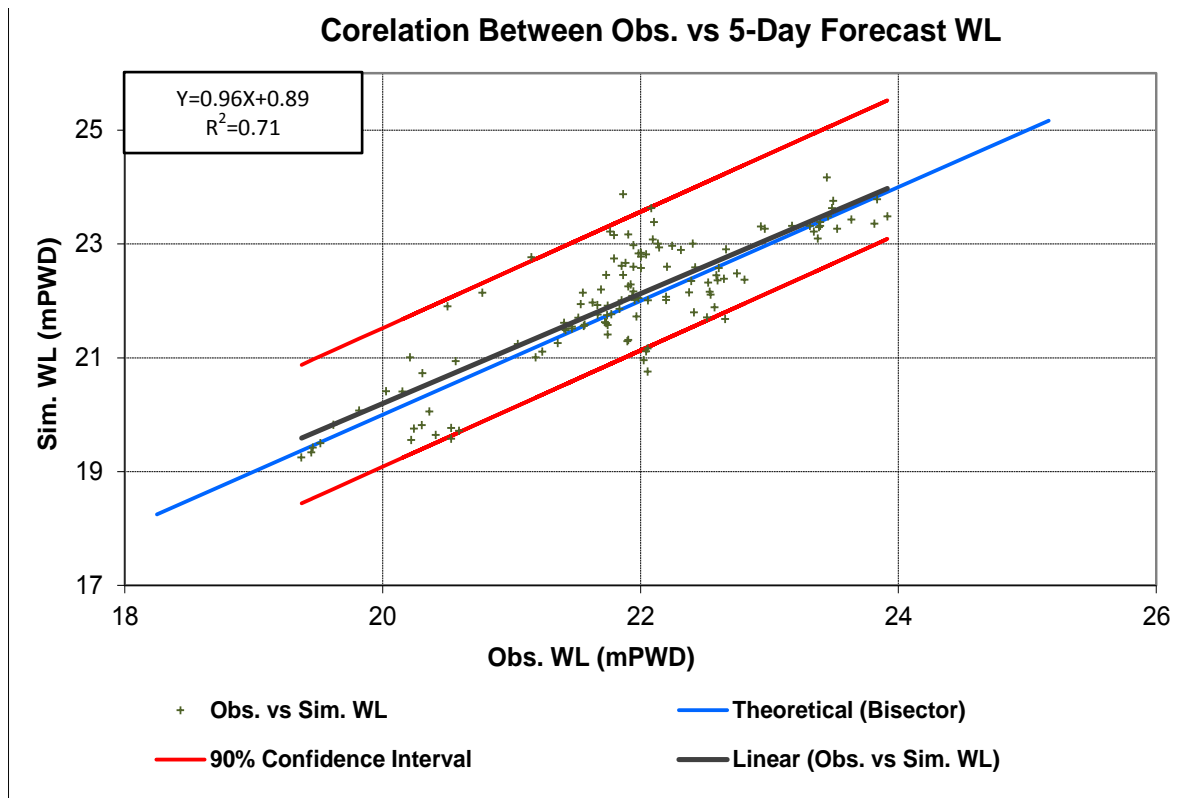
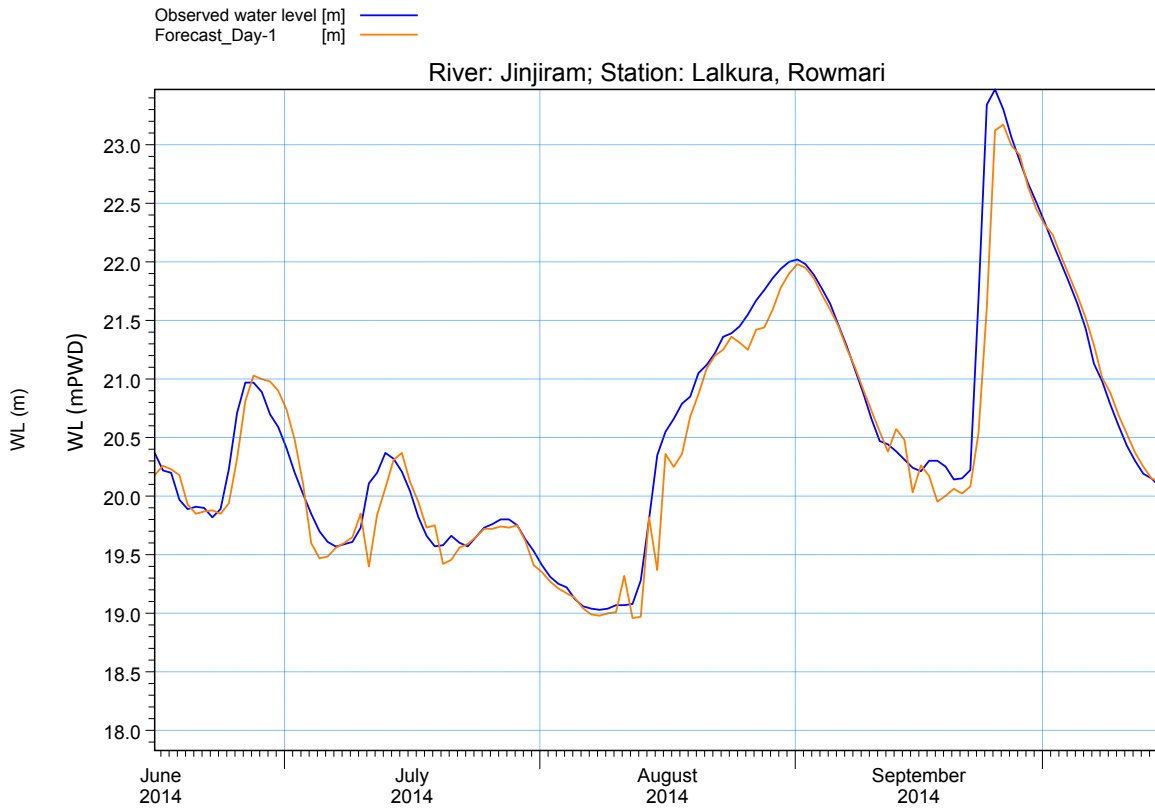


Figure 5.26 Scatter plots for 3<sup>rd</sup> day forecast WL and observed comparison at Dhonarchar

5 days performance hydrograph and scatter plot are given in the figure 5.27 to 5.36 and the values of parameters observed in between forecast water level and observed water level are given in Table 5.8 in Lalkura station (Jinjiram river side) at Rowmari

**Table 5.8** Statistical analysis for five days forecast flood water level at lalkura, Rowmari

STATS PARAMETER	1-Day	2-Day	3-Day	4-Day	5-Day
Correlation Co-efficient $R^2$	0.93	0.89	0.73	0.58	0.44
Nash–Sutcliffe Efficiency Co-eff. (NSE)	0.93	0.89	0.72	0.54	0.36
Mean Absolute Error (MAE)	0.16	0.24	0.34	0.44	0.55
Mean Square Error (MSE)	0.71	1.68	10.77	28.98	55.42
Root Mean Square Error (RMSE)	0.84	1.30	3.28	5.38	7.44
Performance	Good	Good	Average	Poor	Poor



**Figure 5.27** 1<sup>st</sup> day forecast water level and observed WL comparison at Lalkura

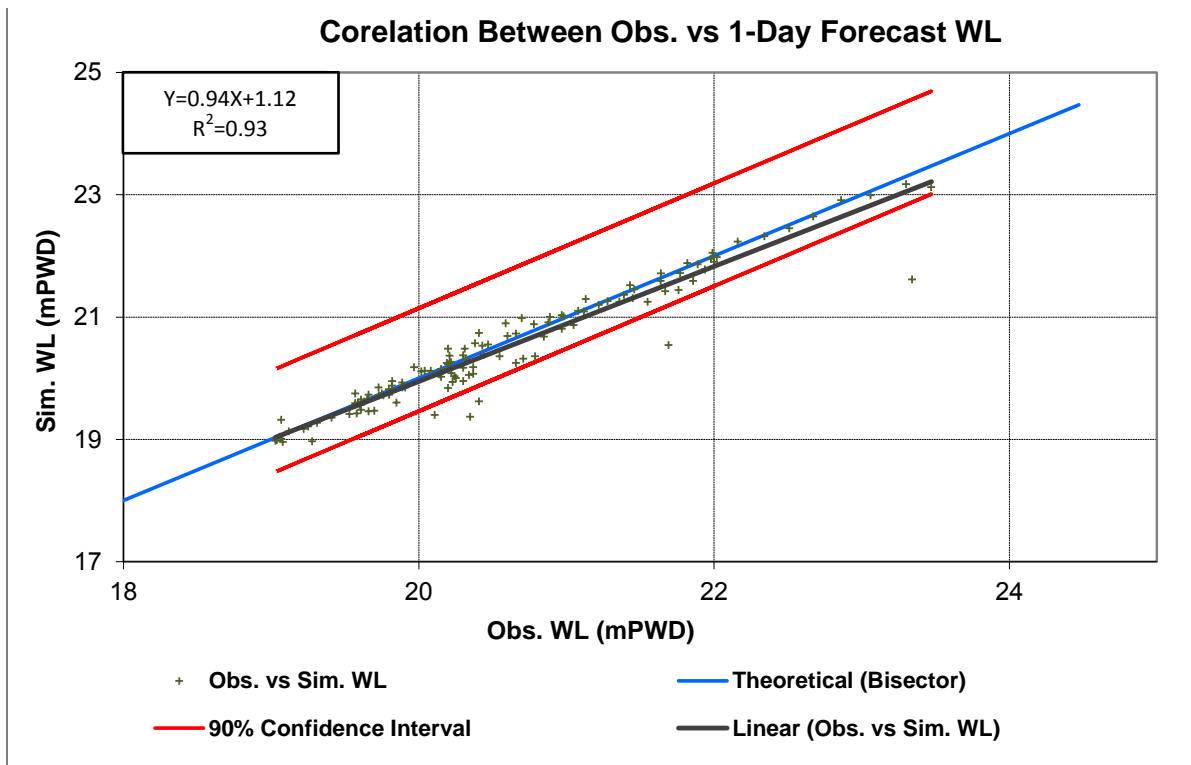


**Figure 5.28** Scatter plots for 1<sup>st</sup> day forecast WL and observed comparison at Lalkura

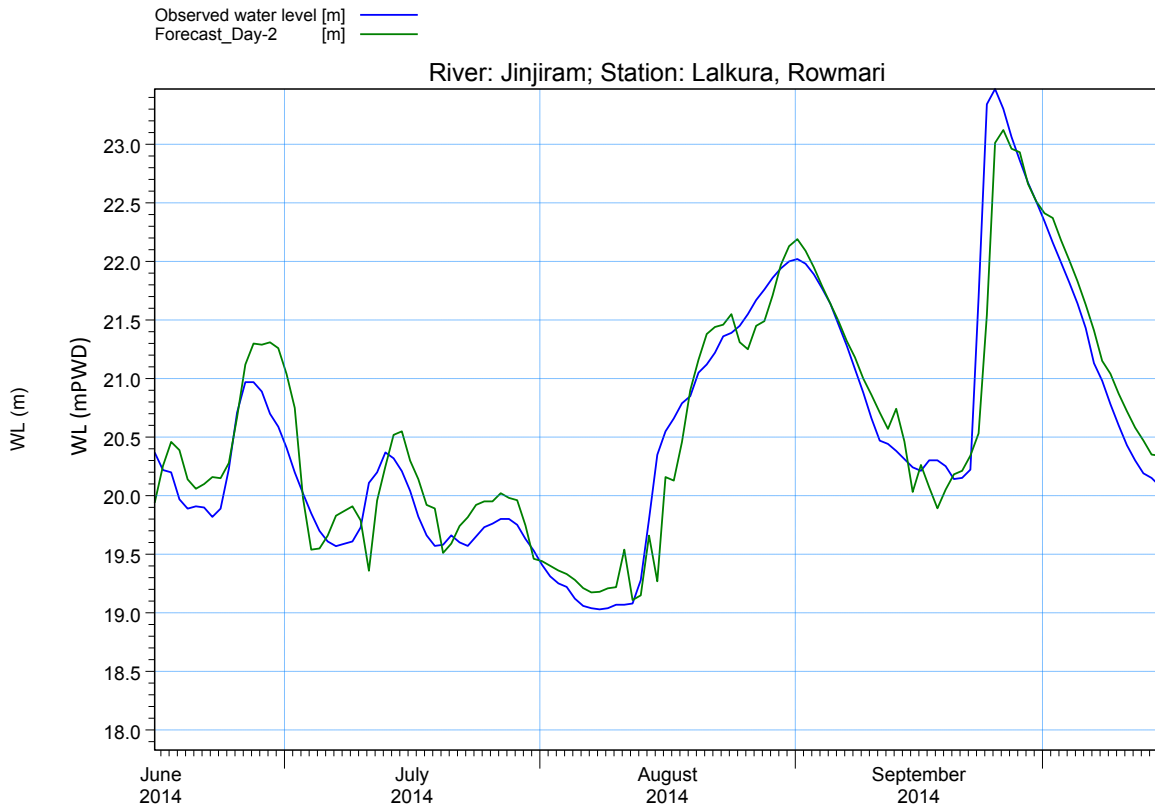


Figure 5.29 2<sup>nd</sup> day forecast water level and observed WL comparison at Lalkura

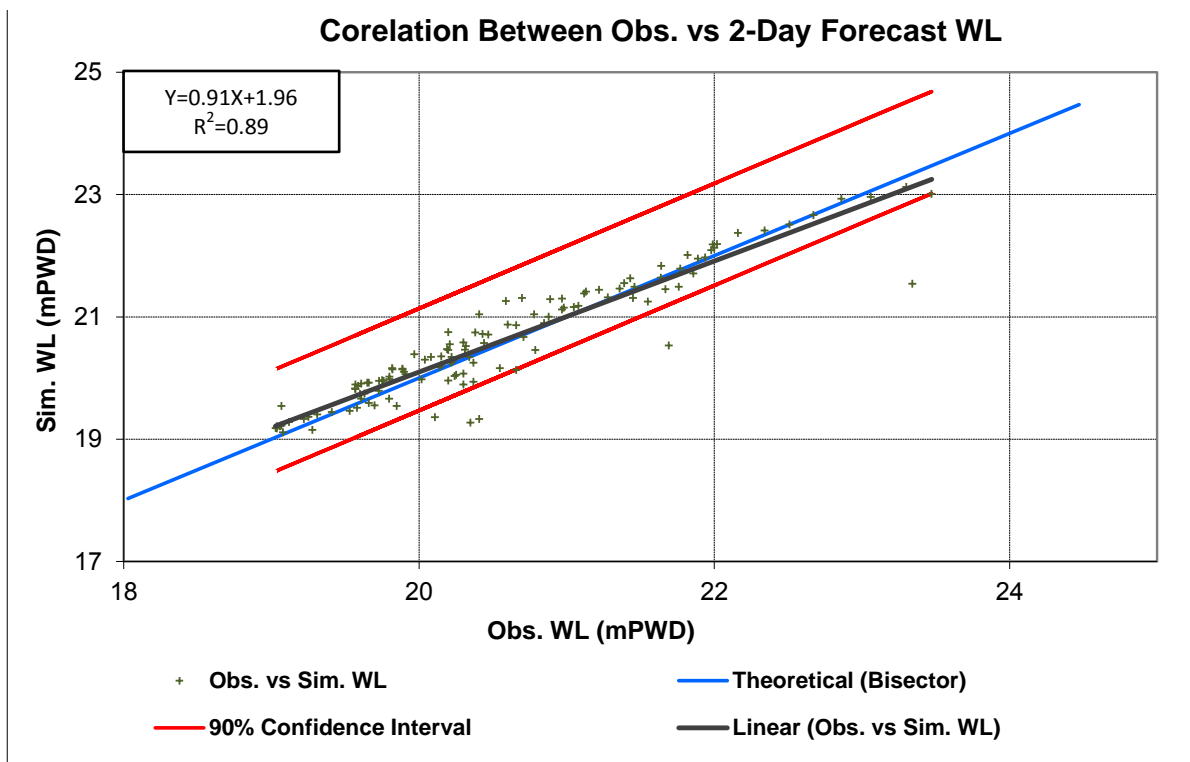


Figure 5.30 Scatter plots for 2<sup>nd</sup> day forecast WL and observed comparison at Lalkura

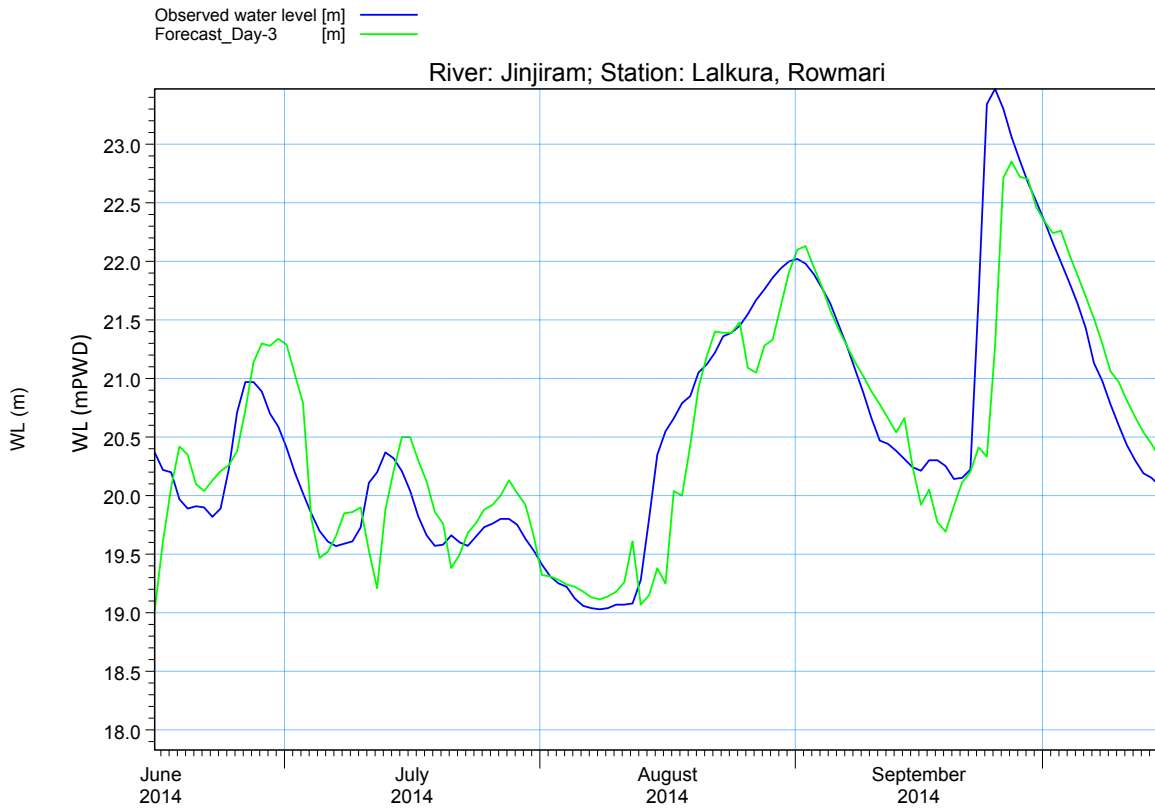


Figure 5.31 3<sup>rd</sup> day forecast water level and observed WL comparison at Lalkura

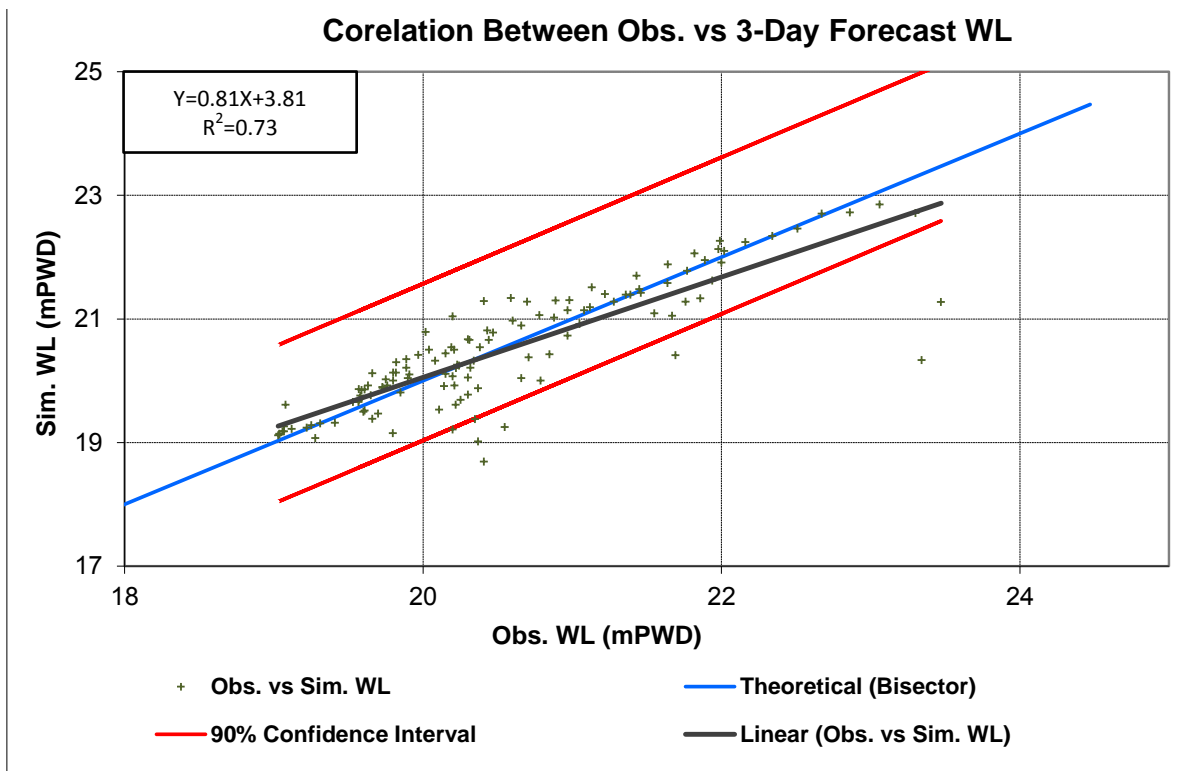


Figure 5.32 Scatter plots for 3<sup>rd</sup> day forecast WL and observed comparison at Lalkura

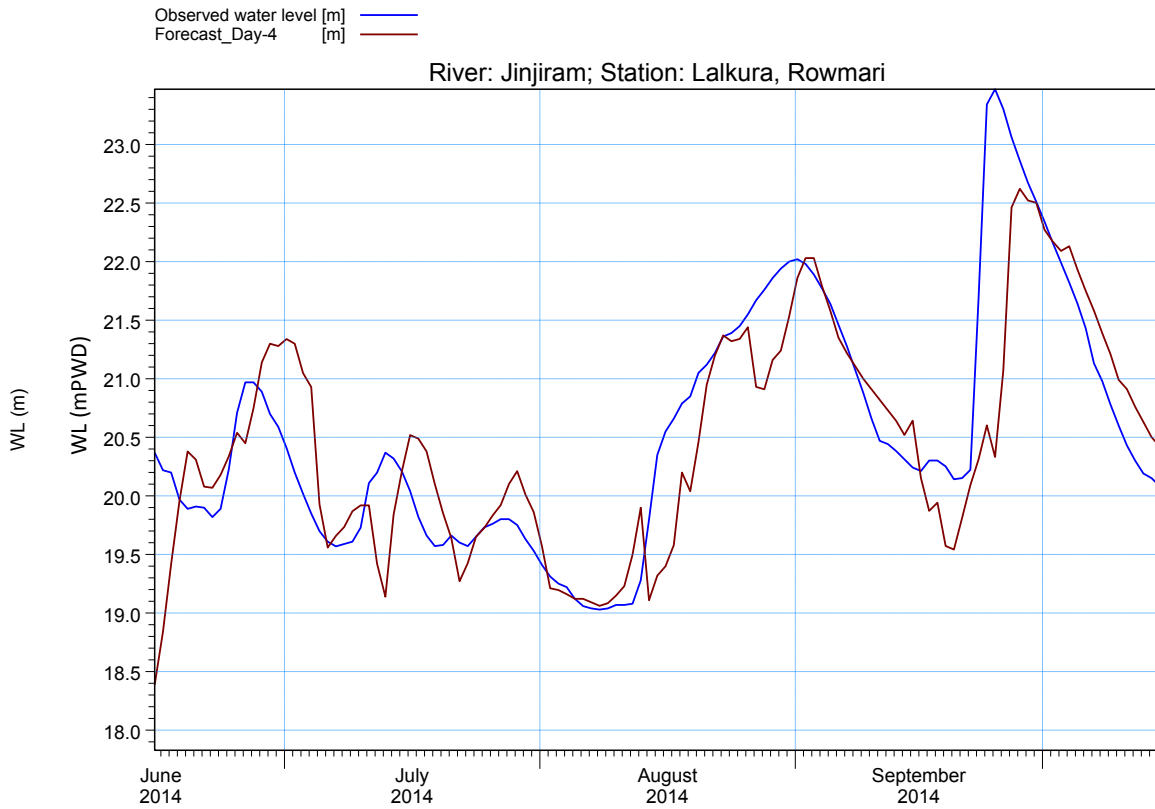


Figure 5.33 4<sup>th</sup> day forecast water level and observed WL comparison at Lalkura

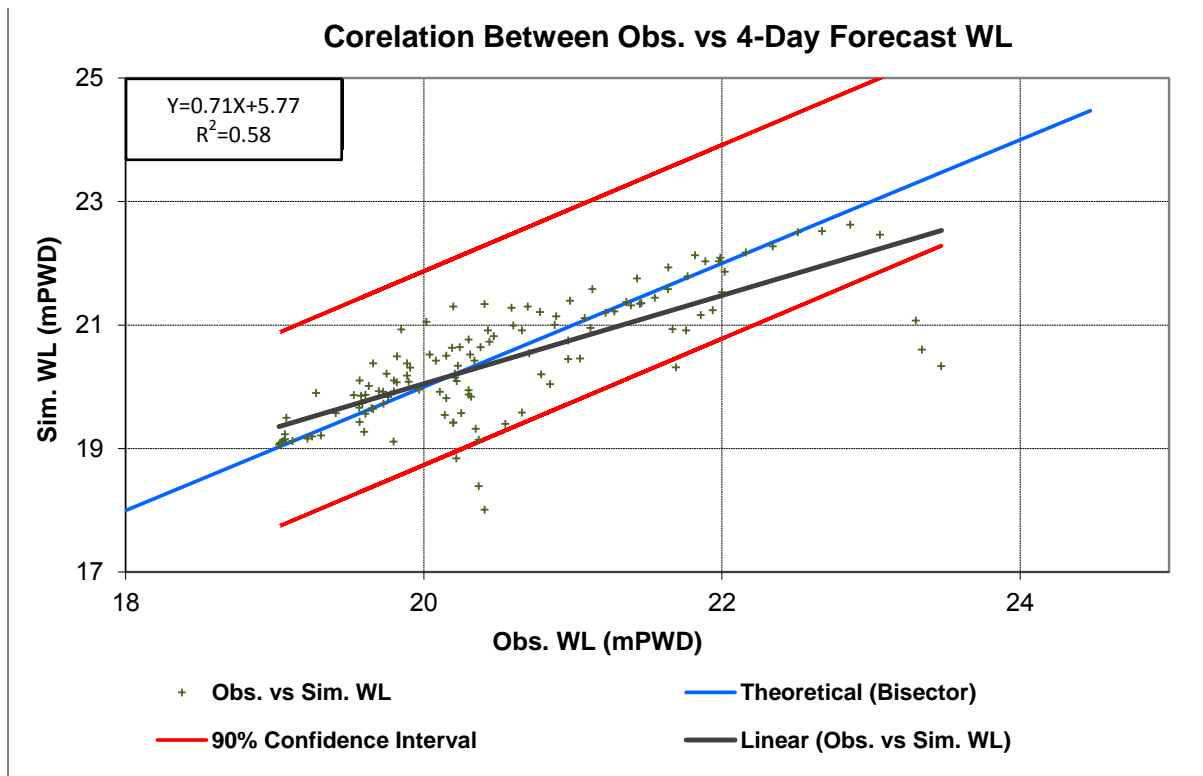


Figure 5.34 Scatter plots for 4<sup>th</sup> day forecast WL and observed comparison at Lalkura

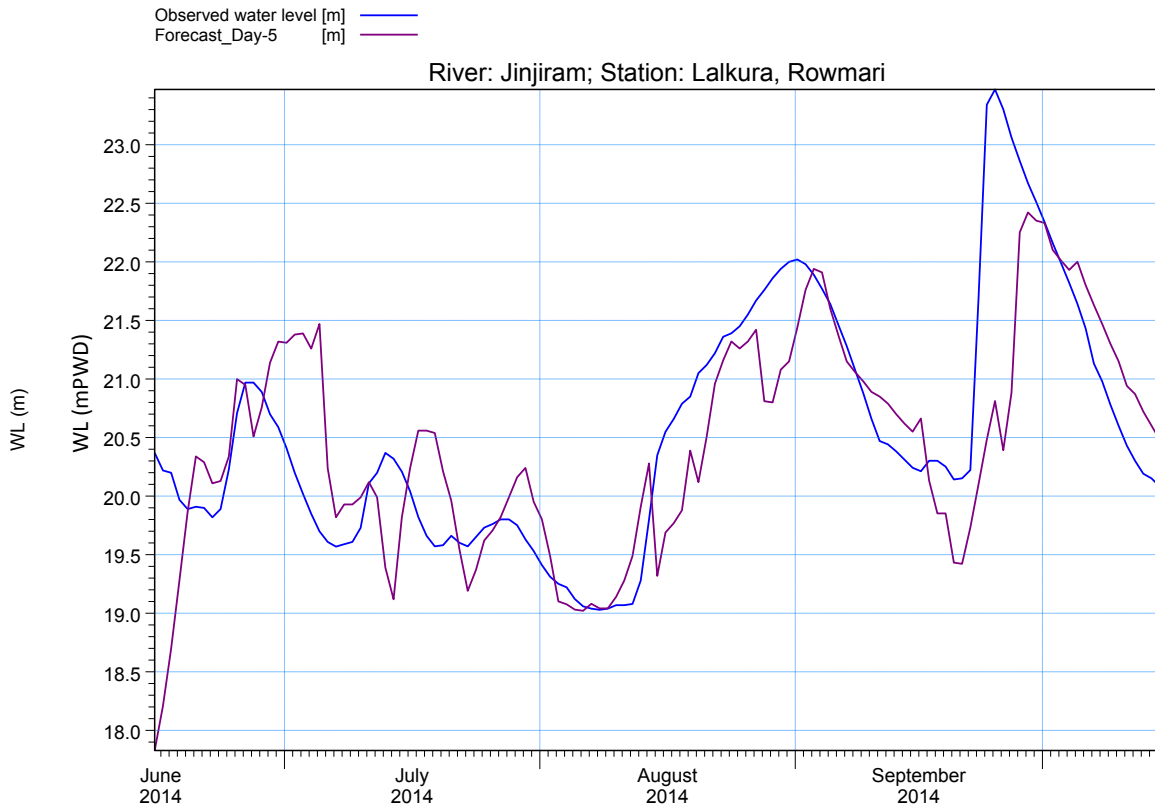


Figure 5.35 5<sup>th</sup> day forecast water level and observed WL comparison at Lalkura

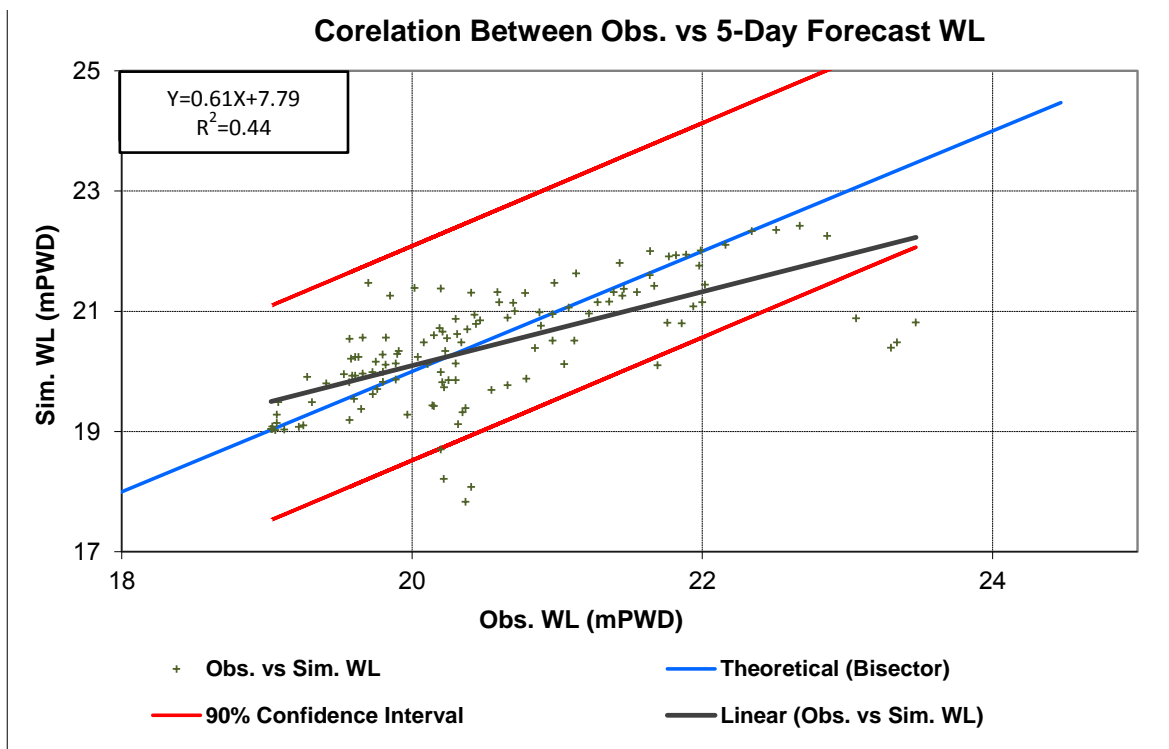


Figure 5.36 Scatter plots for 5<sup>th</sup> day forecast WL and observed comparison at Lalkura



The hydrodynamic model has been calibrated year 2013 and validated year 2014. As a data scarcity in the study region, flood forecast performance has done the same validation hydrological event. The forecast duration of the study is only one year which is very short and insufficient to develop and testing of the local level flood forecasting model and warning system. Therefore, this model system statistically has given first 3days good performance. The study has been carried out based on real time data available at BWDB and IWM and forecast simulation using WRF predicted rainfall.

The Assam range of hills gradually rise in height eastward from 300 m in the Garo hills to about 3,000 m in the Naga hills. The low clouds brought in by the south-west monsoon get interrupted on the southern face of the Khasi and Jaintia hills by a 1,830 m high ridge and cause extremely heavy rainfall along the Cherrapunji-Mawphlang-Pynursla belt. This is generally of the order of 11,000 mm per annum, the highest in the world. The clouds that pass over this 1,830 m ridge along this belt precipitate in the Brahmaputra valley, their intensity increasing towards the foothills of the Himalayas. The rainfall in the Brahmaputra valley ranges from 2,125 mm in Kamrup to about 4,142 mm in Tirap Division of the Arunachal (23). This huge rainfall has created flood mainly in the Brahmaputra basin. WRF geo-data base is updated by Himalaya's elevation and land use data and predicated rainfall more accurately within short range forecast but its deviate in long period gradually. So, this study has given better forecast in Brahmaputra River.

On other hand Jinjiram River originated from Tura hill-bottom and it behave like flashy river. WRF geo-data base is not updated by Tura's elevation and land use data that why predicated rainfall is not match actual rainfall and sometimes its fail to catch sudden rainfall event. If WRF geo-data base update by actual land elevation of Tura hill and landuse data, it would be better perform. Also this study flood warning system would has given better performance in Jinjiram River first 3 days.

The study area is located in the floodplains of the Brahmaputra river and Jinjiram river but different in hydrological characteristic. There is a north-south elongated road in the Roumari area. The western part of the road is fully exposed to flood of the Brahmaputra River while the eastern part is protected from the Brahmaputra river but exposed to flood of the jinjiram river and experience only flash flood coming from adjacent eastern hilly areas in India.

## CHAPTER 6

# CONCLUSIONS AND RECOMMENDATIONS

### 6.1 General

Bangladesh is one of the most flood prone countries in the world. Around 20% of the country is affected by flooding of different depths even in an average hydrological event, and that may be raised up to 70% under higher hydrological storm like 100 years return period. Every flood causes widespread damage in rural and urban areas and set back the country's efforts to alleviate poverty. Protecting the agricultural lands from the flood, structural measures like implementation of flood control and drainage (FCD) projects was started in the country since early sixties. Flood forecasting and warning system can be instrumental for awareness building of local communities and assessment of associated hazards. The main objective of this study is to develop flood forecasting system by coupling hydrological model for Brahmaputra basin and one dimensional hydrodynamic model using WRF predicted rainfall. This system is capable to forecast inundation map and flood hydrograph at renowned places for 5 days lead time during any monsoon season. The results obtained from the present study can be summarized as the following conclusions.

### 6.2 Conclusions

The following conclusions can be drawn after summarizing the present study-

- I. An HEC-HMS continuous hydrologic simulation model is developed for the Brahmaputra basin based on Soil Moisture Accounting (SMA) algorithm and excess rainfall was transformed to direct runoff using the Clark unit hydrograph technique. Muskingum-cunge and kinematic wave theory are used in channel routing and all parameters are calculated from geographic data. The HMS application produced satisfactory performance taking into consideration lumped parameters and real time rainfall station data used. Also, among the optimized parameters; Surface Storage Capacity, Initial Surface Storage, Maximum Soil Infiltration Rate and Tension Zone Storage Capacity show the higher sensitive. The estimated NSE value for the calibration period and validation period is 0.85

and 0.82 respectively, which may be satisfactory to judge on the similarity and consistency between the observed and simulated hydrograph shape.

- II. The hydrodynamic model (HEC-RAS) of the study area has been developed along with the mighty Brahmaputra River and Jinjiram River. This model simulate for 2013 and 2014 monsoon season. Main Upazilla road Char Rajibur to Rowamari behaves like flood barrier as a result flood pattern of the Brahmaputra side of the study area and Jinjiram side are different. Also Flood hydrograph indicates western side of the study area flood by Brahmaputra River and eastern side of the study area is flooded by Jinjiram River. HEC-RAS model performance during calibration and validation period in terms of  $R^2$  and NSE against observed water level data is found to nearly 1. The Manning's roughness coefficient ( $n$ ) and the coefficient of expansion/contraction ( $k$ ) are key parameters to calibrate of HEC-RAS model.
- III. In this study a weather model (WRF) is coupled with a hydrologic model (HEC-HMS) and a hydraulic model (HEC-RAS) for forecasting flood hydrograph and flood inundation map in Rowmari Upazilla at Kurigram district. WRF 3.2 weather model was used to predict rainfall over the Brahmaputra basin with lead time of 5 days. Then output of the weather model (WRF model) was coupled with calibrated hydrologic model. WRF is simulated every day for 1st June-2014 to 15th October 2014; and these predicted rainfalls incorporate to HEC-HMS and the generated forecast boundary condition for hydrodynamic model (HEC-RAS) with specific correction. Then forecast boundary condition ingested to the HEC-RAS 4.1.0 (Hydrologic Engineering Center-River Analysis System) hydraulic model for water profile computations along the river and water level in every grid point of the study area.
- IV. Noonkhawa forecast inflow boundary for hydrodynamic model has been generated 12 hours lag and 5% reduction of Bahadurabad forecast inflow that's produced by HEC-HMS. Jamalpur forecast water level has been generated with respect to Bahadurabad to compare both station hydrograph. Other boundary has been generated associate catchment runoff with this river.

- V. Difference between water level interpolation surface from hydrodynamic model and land elevation surfaces is considered as depth of inundation for forecast date and next 5 days. Output of HEC-RAS was exported to ArcMap 10.1 where it was visualized as a flood inundation map with the use of the extension of HEC-GeoRAS. In this study flood inundation maps for Rowmari Upazilla at Kurigram district is prepared using IWM surveyed 5m x 5m resolutions DEM. So this inundation map has house level information and flood area are defined into five qualitative classes viz. F0 (0 - 0.3 m), F1 (0.31 - 0.9 m), F2 (0.91 - 1.8 m), F3 (1.81 - 3.6 m), F4 (> 3.6 m) based on the inundation depth. Every flood map shows Brahmaputra side of Rowmari and Jinjirim side of Rowmari flood pattern are different and water level is also different. Jinjiram River behaves like flashy river.
- VI. Flood forecast performance at two locations in study area has been assessed through computation of three different statistical parameters: Coefficient of Determination ( $R^2$ ), Mean Absolute Error (MAE), and Maximum Peak Error (MPE) observed in the monsoon in 2014. The performance of flood forecast at Dhonarchar on Brahmaputra varies from very good to poor for lead time of one to five days. First 3 days forecast performance is visually and statistically impressive according to BWDB guideline. The forecast performance at Lalkura on Jinjiram River first 2days is impressive and after 3days its performance gradually deteriorates.
- VII. Early warning is important for saving lives and property from natural disasters in general and for providing information to facilitate evacuation from floodplains in particular. By giving sufficient advance notice in a clear and informative manner, the damage from disasters can be mitigated considerably. Co-operation among governments, national meteorological and hydrological services and local communities is necessary. Raising awareness and improving preparedness are essential factors in making non-structural measures more efficient. This study is invented forecast flood hydrograph that indicate the next 5days water level trend and Flood inundation mapping in a low lying area based on excess water level in conjunction with digital elevation model (DEM) analysis in the GIS atmosphere can be effectively accomplished. The responsible authorities use this product as a

flood warning system are provided to local people what will happen next 5days and it will be an excellent tool to manage disasters well in advance from this kind of study.

### **6.3 Recommendations**

Floods are among the most frequently-occurring and deadly of natural phenomena, affecting an average 520 million people a year. In recent decades, almost half the people killed as a result of natural disasters have been victims of floods, which also account for about one-third of economic losses from these disasters worldwide (APFM, 2013). In this study, a hydrologic and hydrodynamic model coupling with WRF model is used to produce flood map and flood hydrograph. Some actions can be recommended for the improvement of this study for future prediction:

- The development of model parameterization methodology using geographic information systems is highly recommended for HEC-HMS model. More hydrological data and satellite images are highly needed to take into account the climatic, hydrological and soil characteristics spatial variability in such large basin for better and accurate modeling of the hydrological processes in the catchment.
- Internal khal/creek plays vital role to local flood and inundation map. It is recommended to incorporate the internal khal to the hydrodynamic model (HEC-RAS Model)
- For the comprehensive study of local structure like that bridge, culvert, regulator or any kind of intervention should be consider for actual scenario of local flood.
- In this study, for forecasting part to use WRF predicted rainfall, here WRF predicated rainfall data is not calibrated. For better performance should be used calibrated WRF rainfall data.
- Brahmaputra Basin is large watershed area. In this study, only forty-nine rainfall stations are used in this area. It is not represent the actual rainfall pattern. For better performance incorporate more real-time rainfall station.

- First 2 days forecast performance is impressive but after 2days forecast deteriorates. For better forecast performance should be update WRF higher version, its geo-data base are more fine and precise.

## References:

Adams, T. et al. 2008, "The Ohio River Community HEC-RAS model", NOAA, Silver Spring.

Alho P, Roberts MJ, Käyhkö J., 2007, "Estimating the inundation area of a massive, hypothetical jökulhlaup from northwest Vatnajökull, Iceland", *J. Nat. Hazards*. 41(1): 21-42.

APFM, 2013, "flood forecasting and early warning" World Meteorological Organization, Integrated Flood Management Tools Series No.19, page no 3.

Bangladesh Bureau of Statistics (BBS), 2002, Ministry of Planning, Bangladesh.  
Bangladesh Water Development Board, (BWDB), 2000-2001, Annual Report, Dhaka

Barkau, Robert L. 1996, "UNET: One-Dimensional Unsteady Flow Through a Full Network of Open Channels", User's Manual. Army Corp of Engineers, Hydrologic Engineering Center, July. Report Number A486513.

Bedient, Philip B., Wayne Charles Huber, Baxter E. Vieux., 2008, "Hydrology and floodplain analysis", Prentice Hall.

Bennett, T.H., 1998, "Development and application of a continuous soil moisture accounting algorithm for the Hydrologic Engineering Center Hydrologic Modeling System (HEC-HMS)", MS thesis, Dept. of Civil and Environmental Engineering, University of California, Davis.

Bhuiyan, M.S., 2006, "Flood Forecasting, Warning and Response System", Workshop on Options for Flood Risk and Damage Reduction in Bangladesh.

Dooge, J.C.I., 1959, "A general theory of the unit hydrograph." *Journal of Geophysical Research*, 64(2), 241 -256.

Erich J. Plate, 2002, "Early Warning System For The Mekong River", *Journal of Hydro-environment Research*, Page 80 – 94.

FFWC, 2005, "Consolidation and strengthening of flood forecasting and warning services" Final Report, Volume II –Monitoring and evaluation, Bangladesh Water Development Board, Dhaka.

FFWC, 2005, "Consolidation and strengthening of flood forecasting and warning services", Final Report, Volume II – Monitoring and evaluation, Bangladesh Water Development Board, Dhaka.

Fread, D.L., 1988, "The NWS DAMBRK Model: Theoretical Background/User Documentation. Office of Hydrology", National Weather Service (NWS), Maryland, U.S.A.

Haan, C.T., 2002, “Statistical methods in hydrology”, Second Edition, Iowa State Press, 496 p.

HEC, 2000, “Hydrologic Modeling System: Technical Reference Manual”, ver. 4.0, US Army Corps of Engineers Hydrologic Engineering Center.

HEC, 2005, “HEC-RAS river analysis system. Hydraulic Reference Manual”, ver. 4.1, U.S. Army Corps of Engineering.

Hicks, F.E., P.M. Steffler, 1990, “Finite Element Modelling of Open Channel Flow”, Water Resources Engineering Report No. 90-6, Department of Civil Engineering, University of Alberta, Edmonton, AB.

Hopson, T.M. and Webster, P.J., 2009, “A 1–10-Day Ensemble Forecasting Scheme for the Major River Basins of Bangladesh: Forecasting Severe Floods of 2003–07”, Journal of Hydrometeorology, Boston, v.II, pp 618.

Hossain, A.N.H. Akhtar, 2004, “Flood Management: Issues and Options”, Presented in the International Conference organized by Institute of Engineers, Bangladesh.

Hossain, F. et al., 2013, “Can a Radar Altimetry Satellite Deliver on the Promise of an Operational and Real-Time Transboundary Flood Forecasting System for Flood-prone Bangladesh?” International Journal of Remote Sensing.

Hossain, M.A., 2006, “Weather Forecasting for Flood Disaster Mitigation”, Workshop on Options for Flood Risk and Damage Reduction in Bangladesh.

Islam, S.R., Dhar, S.C., 2000, “Bangladesh Floods of 1998: Role of Flood Forecasting & Warning Centre”, BWDB, Dhaka.

Ismail Yucel et al, 2015, “Calibration and Evaluation of a Flood Forecasting System: Utility of Numerical Weather Prediction Model, Data Assimilation and Satellite-based Rainfall”, Geophysical Research, Vol. 17, EGU2015-10261.

IWM, 2006, “Local Level Flood Forecasting Applying Remote Sensing Technology in River Basin Management”, Prepared for BWDB.

IWM, 2006, “Research and Prediction Modelling Through Upgrading of Flood Forecasting System by Increasing Lead Time and Introducing Location Specific Flood Warning”, Prepared for BWDB.

IWM, 2014, “Local Level Flood Forecasting Applying Remote Sensing Technology in River Basin Management”, Prepared for BWDB, 2014.

IWM, 2014, “Water Availability, Demand And Adaptation Option Assessment Of The Brahmaputra River Basin Under Climate Change”, Prepared for ICIMOD, 2014.

Laprise R., 1992, “The Euler Equations of motion with hydrostatic pressure as an independent variable”, Mon. Wea. Rev., 120, 197–207.



M. M. G. T. De Silva, S. B. Weerakoon, Srikantha Herath, 2013, “Modeling of event and continuous flow hydrographs with HEC–HMS; A case study in the Kelani River basin Sri Lanka” *Journal of Hydrologic Engineering*.

Mirza M.M.Q, Dixit A., Nishat A., 2003, “Flood Problem and Management in South Asia”, Springer Science+Business Media Dordrecht.

Moges, S., 2007, “Flood Forecasting and Early Warning System (FFEWS) an Alternative Technology for Flood Management System and Damage Reduction in Ethiopia”, FWU Water Resources Publications, Volume No: 06.

Moustafa S. EL-Sammany, 2010, “Forecasting of Flash Floods Over Wadi Watier – Sinai Peninsula Using the Weather Research and Forecasting (WRF) Model”, *Nile Basin Water Science& Engineering Journal*, Vol.3, Issue2.

Ooyama K. V., 1990, “A thermodynamic foundation for modeling the moist atmosphere”, *J.Atmos. Sci.*, 47, 2580–2593.

Practical Action, (2009), “Early warning Saving Lives” Practical Action/ European Commission.

Rabi Gyawali, et al, 2013, “Continuous Hydrologic Modeling of SnowAffected Watersheds in the Great Lakes Basin Using HEC-HMS” *Journal Of Hydrologic Engineering*.

Rahman M.M. et al, 2014, “An Analytical Study of Flood Management in Bangladesh”, *IOSR Journal of Engineering (IOSRJEN)*, ISSN (e): 2250-3021, ISSN (p): 2278-8719, Vol. 04, Issue 01, V7, PP 01-06.

Refsgaard, J. C., Knudsen, J., 1996, “Operational validation and intercomparison of different types of hydrologic models”, *Water Resources Research*, 32, 2189–2202.

Reshma T, Venkata Reddy K, Deva Pratap, 2013, “Simulation of Event Based Runoff Using HEC-HMS Model for an Experimental Watershed”, *International Journal of Hydraulic Engineering* 2013, 2(2): 28-33.

Rimes, 2014, "Community Response to Early Warning System for Flood-2014" Prepared for BWDB, 2014.

Sammany, M.S., 2010, “Forecasting of Flash Floods over Wadi Watier – Sinai Peninsula Using the Weather Research and Forecasting (WRF) Model”, *Nile Basin Water Science& Engineering Journal*, Vol.3, pp 88.

Siddique-E-Akbor, A. H., F. Hossain , H. Lee , C. K. Shum., 2011, “Inter-comparison Study of Water Level Estimates Derived from Hydrodynamic-Hydrologic Model and Satellite Altimetry for a Complex Deltaic Environment. Remote Sensing of Environment”, vol. 115, pp. 1522-1531 (doi:10.1016/j.rse.2011.02.011).

Straub, T. D., Melching, C. S., Kocher, K. E., 2000, "Equations for Estimating Clark Unit-Hydrograph Parameters for Small Rural Watersheds in Illinois", Water-Resources Investigations Report 00-4184m, U.S. Department Of The Interior U.S. Geological Survey In cooperation with the Illinois Department of Natural Resources, Office of Water Resources.

Tingsanchali T, Karim M., 2005, "Flood hazard and risk analysis in the southwest region", *Hydrol Process* 2005; 19: 2055-69.

V. Thiemi, B. Bisselink, F. Pappenberger, J. Thielen, 2014, "A pan-African Flood Forecasting System", *Hydrol. Earth Syst. Sci. Discuss.*, 11, 5559-5597, doi: 10.5194/hessd-11-5559-2014.

Wardah, T. et al. 2011, "Quantitative Precipitation Forecast using MM5 and WRF models for Kelantan River Basin", *World Academy of Science, Engineering and Technology International Journal of Environmental, Earth Science and Engineering* Vol:5 No:11.

WARPO, 2004, "National Water Management Plan (NWMP)." Ministry of Water Resources, Bangladesh, Dhaka.

WRF, 2012, "Advanced Research WRF (ARW) Modeling System" Version 3.2.

Xuefeng Chu, A.M.ASCE, Alan Steinman, 2009, "Event and Continuous Hydrologic Modeling with HEC-HMS" *Journal of Irrigation and Drainage Engineering*, Vol. 135, No. 1.

Yang J, Townsend RD, Daneshfar B., 2006, "Applying the HEC-RAS model and GIS techniques in river network floodplain delineation", *Canadian. J. Civil. Eng.* 33(1): 19-28.

Chuan T, Jing Z (2006). Torrent risk zonation in the Upstream Red River Basin based on GIS, *J. Geogr. Sci.* 16(4): 479-486.

Zhang, H. L. et al., 2013, "The effect of watershed scale on HEC-HMS calibrated parameters: a case study in the Clear Creek watershed in Iowa, USA" *Hydrology and Earth System Sciences Discussions*.